Hunter, Central and Lower North Coast
Regional Climate Change Project 2009

REPORT 3

# Climatic Change Impact for the Hunter, Lower North Coast and Central Coast Region of NSW

An initiative of the Hunter & Central Coast Regional Environmental Management Strategy

The Hunter & Central Coast Regional Environmental Management Strategy – a program of the Environment Division of Hunter Councils

Authors: Karen L. Blackmore (Earth Sciences, School of Environmental and Life Sciences, University of Newcastle) and Ian D. Goodwin, Climate Risk CORE, Macquarie University

Publisher
HCCREMS (Hunter Councils Inc. as legal agent)
PO Box 137
THORNTON NSW 2322
Phone: 02 4978 4020
Fax: 4966 2188
Email: envirodirector@huntercouncils.com.au

ISBN: 978-1-920859-39-8

Suggested Bibliographic Citation:
Blackmore. K.L. & Goodwin, I.D (2009). Report 3: Climatic Change Impact for the Hunter, Lower North Coast and Central Coast Region of NSW. A report prepared for the Hunter and Central Coast Regional Environmental Management Strategy, NSW.

Acknowledgements

New South Wales Government

Funding has been provided by the New South Wales Government through its Climate Action Grants Program; Valuable support & assistance have been provided by the Tom Farrell Institute & Newcastle Innovation (The University of Newcastle) and Climate Risk CORE (Macquarie University)
Cover photograph: Hugh Cross

# Executive Summary

This report provides the results of Stages 3 and 4 of a four stage project to identify the potential impacts of climate change in the Hunter, Central and Lower North Coast region of New South Wales. In order to identify the potential impacts of climate change on the region, HCCREMS commissioned the University of Newcastle to conduct the scientific research required for the project. This research has been carried out over a number of stages (four in total). These stages involved:

- Stage 1: identification of the key synoptic patterns relevant to the study region;
- Stage 2: analysis of how the synoptic patterns drive climate and climate-related variability in the region;
- Stage 3: downscaling CSIRO global climate model (GCM) predictions for New South Wales (NSW) to the study region; and,
- Stage 4: determination of the potential climate change impacts on the region based on the statistical downscaling.

Regional climate impacts have been resolved throughout this study using a statistical downscaling approach, based principally on the projected monthly representation of the sea-level pressure field output from the CSIRO Mk3.5 GCM. A process known as self-organising mapping (SOM) was selected to derive the key synoptic types (STs) from monthly sea level pressure (SLP) data. A total of twelve (12) STs were selected as drivers of climate variability in the region. The statistical downscaling approach involved the determination of relationships between each of the twelve STs and recorded values for key climate variables obtained from the Bureau of Meteorology. Projected changes in climate were then obtained by analysing shifts or changes in the frequency of occurrence of STs.

The process of deriving STs from the GCM output data and analysing the projected shifts in STs is a unique approach to downscaling GCM outputs to derive sub-regional projections. This is because it utilises the relationship between synoptic types derived from GCM output and actual climate data to understand and inform the downscaling process. GCM outputs for key climate variables such as temperature and precipitation are generally used for climate change projections. The approach adopted in this research seeks to identify changes in the “drivers” of these key climate variables and thus infer their change. Additionally, the scale of GCM outputs is generally quite coarse and would not have provided information at the regional and sub regional scale required by the project.

The results of the analysis are reported as general key climate change impacts for the Hunter, Central and Lower North Coast region and as specific climate change impacts

through four case studies. These case studies focus on climate change impacts for:

- the viticulture industry;
- human health concerns related to extreme heat events;
- bushfire weather; and,
- coastal impacts of extreme events.

Climate change impacts for the region and each of the four case studies are summarised below.

## OVERVIEW OF KEY CLIMATE CHANGE IMPACTS FOR THE HUNTER, CENTRAL AND LOWER NORTH COAST REGION

*Precipitation, Evaporation and Water Balance*

- Some seasonal and zonal changes in precipitation are projected. Although no overall increase in precipitation outside historical boundaries of natural variability is projected for the period from 2020-2080, a return to precipitation patterns similar to those experienced during the 1948-1976 IPO period (La Nina like –ve phase) is projected. Some seasonal shifts are also projected with moderate to high confidence, with decreases of approximately 12.5% for the coastal and central zones during winter, and increases of approximately 13% in these zones during spring. A significant 33% increase in autumn rainfall in the western zone is also projected.

- A statistically significant decrease in water balance in the western zone is projected for the period from 2020-2080. Seasonal shifts in water balance in the coastal and central zones balance out to produce no change in annual projections. Projections (2020-2080) for summer are for increases in average daily water balance of ~1.3mm in the central zone and ~0.5mm in the western zone relative to the 1970-2007 period. Water balance in the coastal zone remains relatively unchanged. A significant decrease of ~1.9mm in average daily water balance for autumn is projected in the central zone. Decreases of ~0.9mm and ~0.3mm per day are expected in autumn in the coastal and western zones respectively. Increases in the coastal and western zones are projected for winter; ~0.7mm per day in the coastal zone and ~0.2mm per day in the western zone. A decrease of ~0.5mm per day is projected in the central zone during winter. Spring projections are for increased average daily water balance in all zones; ~1.8mm per day in the coastal zone, ~1.3mm per day in the central zone and ~1.4mm per day in the western zone.

*Air Temperature*

- Minimum temperatures will generally be warmer, particularly in the west of the region. Projections (2020-2080) in the coastal and central zones for summer are for

decreases in average minimum temperature of ~0.8°C relative to the 1970-2007 period. A significant increase of ~4.2°C in average minimum temperature for summer is projected in the western zone. Increases in all three zones are projected for autumn; ~1.4°C in the coastal and central zones and again a significant ~4.8°C in the western zone. Winter projections are for warmer average minimum temperatures in the coastal and central zones (~1.3°C and ~1.2°C respectively) and lower temperatures in the western zone (~0.8°C). The study region is likely to experience lower average spring minimum temperatures with a decrease of ~0.2°C projected for the coastal and central zones, and ~1.2°C in the western zone.

- The most significant changes in average maximum temperatures are projected to occur during autumn and winter in the region. Projections (2020-2080) in the coastal and western zones for summer are for decreases in average maximum temperature of ~0.2°C relative to the 1970-2007 period. No change for summer is projected in the central zone. Increases in all three zones are projected for autumn; ~1.2°C in the coastal zone, ~1.8°C in the central zone and ~2.0°C in the western zone. Winter projections are for warmer average maximum temperatures, ~1.3°C in the coastal zone, ~1.6°C in the central zone and ~1.8°C in the western zone. The study region is likely to experience lower spring average maximum temperatures with a decrease of ~0.7°C projected for the coastal zone, and ~1.3°C in the central and western zones.

*Extreme Events*

- The frequency of weather patterns responsible for extreme storm events along the NSW coast suggest an increase in the mean circulation pattern (ST1) during autumn/winter, and accordingly there is a higher probability of east coast low (ECL) formation.

- Projected changes in the frequency of occurrence of STs associated with high rainfall events are likely to impact the region. An increase in the frequency of occurrence of high rainfall events in summer and autumn are projected in all zones. A corresponding decrease in extreme rainfall events during winter and spring is also projected.

- Projected increases in ST12 during summer and autumn are likely to result in increased frequency of extreme heat days (EHDs) in the region during the period from 2020-2080.

- No change in winter frost events is projected, however increases in autumn and spring are projected for the western and central parts of the region.

OVERVIEW OF CLIMATE CHANGE IMPACT CASE STUDIES

*Potential Impacts of Climate Change on the Hunter Valley Wine Industry*

Historic records indicate some statistically significant trends in key climate variables (Table 1). Heat degree days (summation), winter minimum temperatures, and average annual 3pm humidity have recorded increases since 1973. Decreases in annual frost days and daily pan evaporation in winter and spring are also evident.

| Climate Variable/Indicator | Historic Trend | Amount |
|---|---|---|
| Heat degree days (summation) | Increasing | ~3$^{o}$C per annum from 1958-2008 |
| Winter minimum temperature | Increasing | ~1.7$^{o}$C from 1957-2007 |
| Annual frost days* | Decreasing | ~24 days between 1957-2007 |
| Daily Pan Evaporation (winter and spring) | Decreasing | ~1mm/24hr for winter, ~0.8mm/24hr for spring from 1970-2007 |
| Average annual 3pm humidity | Increasing | ~5.5% from 1973-2007 |

Table 1 - Statistically significant trends in historic data from key climate variables/indicators

* Although a statistically significant decreasing linear trend is evident, two distinct cycles are present. The average frost days per annum for the period from 1957-1971 is ~26 whereas the latter period from 1972-2007 records only ~7 frost days per annum.

Changes in key climate variables are projected for the climate zones covering the Hunter Valley wine growing region (Table 2). A return to precipitation patterns similar to those experienced during the 1948-2007 period indicates increasing variability and thus high rainfall events are also likely to increase. Overall increases in minimum and maximum temperatures are projected however some seasonal decreases are also likely.

| Climate Variable | Projected Change |
|---|---|
| **Precipitation** | No trend however a return to precipitation patterns experienced during the 1948-1976 period is projected |
| **High rainfall events** | Increases during summer, autumn and winter. Decrease during spring. |

| | |
|---|---|
| **Minimum temperature** | Increases during summer, autumn and winter and a decrease during spring in the western zone<br><br>Increases during autumn and winter and decreases during summer and spring in the central zone |
| **Maximum temperature** | Decrease during summer and spring and increases during winter and autumn |

Table 2 - Summary of projected climate changes

The changes in key climate variables, together with the projected changes in indices relevant to the viticulture industry, provide the basis for the assessment of risks and opportunities for the industry. This information may then subsequently provide the input for the development of adaption plans and strategies for climate change.

*Potential Impacts of Climate Change on Extreme Heat Events Affecting Public Health in the Hunter, Lower North Coast and Central Coast Region*

Identified are the key historical and projected changes likely to influence the region, the natures of which are detailed in the tables below. Historic records show statistically significant increases in the level of yearly worst 3-day heat events. There are no statistically significant trends in either 1-day or 3-day extreme heat events over the period analysed.

| Heat Stress Indicators | Historic Trend |
|---|---|
| Yearly worst 3-day heat events | Increases of 2.2$^{o}$C at Jerrys Plains and 1.75$^{o}$C at Murrurundi |

Table 3 - Historic trends in heat stress indicators

Despite projected decreases in average maximum temperature and average temperature during summer and spring, the frequency of occurrence of extreme heat events in the region is projected to increase. This may occur as a result of a projected lowering of extreme heat threshold values.

| Key Climate Variable | Projected Change |
|---|---|
| Maximum Temperature | Decreases in the coastal and western zones for summer of ~0.2$^{o}$C. No change for summer is projected in the central zone. Decreases during spring of ~0.7$^{o}$C projected for the |

| | |
|---|---|
| | coastal zone, and ~1.3°C in the central and western zones. |
| Extreme Heat Events | Overall, an increase of approximately 7% is projected during summer with no change projected for spring. |
| Average Temperature | Slight decreases during summer and spring are projected (~0.5°C during summer and spring decreases of ~0.4°C in the coastal zone, and ~0.8-0.9°C in the central and western zones). |

Table 4 - Summary of projected changes to key climate variables

Due to the relationship between a location's average temperature and extreme heat threshold for that location, projected decreases in average temperature are thus likely to lower existing heat stress thresholds in the community. It is also noted that changes to average minimum temperatures are likely and may also impact on heat stress thresholds. Further research is recommended to analyse the impact of minimum temperatures on heat stress and the relationship between minimum temperatures and threshold values.

*Potential Impacts of Climate Change on Bushfire Risk in the Hunter, Lower North Coast and Central Coast Region*

Changes in key climate variables that drive fire weather are projected for the period from 2020-2080 AD (Table 5). Based on estimates for the projected period, the most significant changes to bushfire related climate variables in the region are projected to occur during autumn. Increases in average wind speed and maximum temperature in this season, combined with projected decreases in relative humidity are likely to result in increases in the number of days classified using fire danger indices as high or extreme. No changes in these variables are projected for summer, and summer rainfall is projected to return to a similar pattern to that experienced during the period from 1948-1976 (i.e. higher rainfall than that experienced in the last 30 years). This period was a historically wetter period than that experienced in the more recent 30 years (i.e. 1977-2007) and thus is likely to result in higher fuel moisture content.

| Climate Variable | Projected Change |
|---|---|
| **Average wind speed** | Increases in average wind speed of approximately 1km/hr are projected for autumn. These increases are offset by a similiar decrease projected to occur during spring. |

| | |
|---|---|
| **Maximum temperature** | Decrease during summer and spring and increases during winter and autumn |
| **Relative humidity** | Decreases during autumn and winter. Increase during spring. |
| **Precipitation** | No trend however a return to precipitation patterns experienced during the 1948-1976 period is projected (i.e. higher rainfall than that experienced in the last 30 years) |

Table 5 - Summary of projected climate changes

These projected impacts for the Hunter, Central and Lower North coast provide a different perspective to that published in the recent CSIRO reports on climate change impacts on bush fire (Hennessey, et al. 2005 and Lucas, et al. 2007). Two key differences in the analysis approaches result in some variations in results. Firstly, temperature projections used in the CSIRO analysis are based on the annual global mean warming (Hennessey, et al. 2005 pg.16) whereas the approach adopted in this case study relies on projected seasonal differences. That is, projected increases in temperature are not applied uniformly to all months. Secondly, this case study has focused explicitly on the Hunter, Central and Lower North Coast region of NSW whereas the CSIRO research considers the south-east region of Australia. As such, the weather data (i.e. actual temperature, wind, rainfall and humidity records from the BOM) used to downscale output from the GCM to the region differs and this may account for some variability in results. Despite this, projected autumn increases in key climate variables suggest agreement with the CSIRO position that fire danger in autumn would also likely increase, pushing suitable times for prescribed burning into winter.

*Potential Impacts of Climate Change on Extreme Events in the Coastal Zone of the Hunter, Lower North Coast and Central Coast Region*

Changes in key climate variables associated with extreme weather events are projected for the period from 2020-2100 AD (Table 6). The most significant changes in key climate variables are projected to occur during autumn and spring, with some possible localised impacts (especially in Newcastle). Storm frequency is projected to increase during autumn and winter with an associated increase in extreme sea levels. Adjusted sea-level rise levels for 2050 and 2100 AD is also provided.

| Climate Variable | Projected Change |
|---|---|
| **Extreme Rainfall Events** | Increase in summer, decrease in autumn, no change for winter (except slight increase in Newcastle) and slight increase during spring. |
| **Wind gusts** | No change for summer, increase for autumn and spring, decrease in winter. |
| **Storm Frequency and Wave Climate** | Increase in storm frequency during autumn and winter.<br><br>A slight increase in wave height for summer to 2030-2040 followed by a decrease, slight decrease in wave height during autumn, decrease in significant wave height during winter. No trends in mean wave direction. |
| **Sea-Level rise and Extreme Sea Level** | Sea-level rise of +0.4 m and +0.9 m above the 1990 sea-level by 2050 and 2100 AD respectively (Draft Sea-Level Rise Policy, 2008) adjusted to +0.37m and +0.845m due to regional impacts.<br><br>Increase in storm frequency during autumn and winter. |

Table 6 - Summary of projected climate changes

During the period from 1948 to 2007, the coastal areas of the Hunter, Central and Lower North Coast region have seen significant changes in extreme weather behaviour including:

- the number of daily rainfall events greater than or equal to 50mm occurring throughout the region's coastal zone per annum has increased;
- the number of rainfall events with three consecutive days each averaging 50mm or more have increased during spring; and,
- potentially damaging wind gusts (>= 65km/hr) have decreased during autumn.

Climate projections for this region align with these historical trends, and thus continuation of these trends is likely.

LIMITATIONS

We have approached the problem of sensitivity and predictive skill testing by training the methods on a calibration period from 1968 to 1990. This period spans a natural shift in the mean state of the climate, between a La Nina-like and an El Nino-like state, referred to as the Interdecadal Pacific Oscillation (IPO). The GCM's do not fully capture the range and shift in frequency of the key ST's determined from the analysis of the observed or instrumental sea-level pressure data (NCEP-NCAR Reanalysis data). Hence the GCM's do not fully capture the inherent interdecadal variability in the natural climate system that produces the climate shift and extremes that society, agriculture and the natural environment respond to.

Generally, the climate change projections for the 2020-2040, 2040-2060 and 2060-2080 are comparable, and do not display the interdecadal variability observed in the historical record. Hence, the projected climate variables should be interpreted as indicative of the shifts in climate relative to the specific historic period (i.e. +ve or –ve IPO phase). For example, if the shift is towards the interdecadal mean values experienced in the 1948-1976 period of persistent La Nina-like climate, then environmental management, planning and policy decisions should draw on the historical impacts during this period, when drafting responses to future climate change during this century. We interpret all statistically significant trends in this study as being of moderate to high confidence, and accordingly, all non statistically significant trends as being indicative of low confidence projections.

The climate change projections reported in this study provide the next order of detail and insight over the previous CSIRO (2007) projections for the region, and it is now possible to assess the sensitivity and associated climate change risks for the sub-regional zones: coastal; central; and, western. It is important to note that the science of climate change impact projection will advance with the next generation of GCM's.

# Table of Contents

# List of Figures

## List of Tables

## Appendices

# Glossary

| | |
|---|---|
| *20C3M* | *Simulations of the 20th century* |
| *BMU* | *Best Matching Unit* |
| *CSIRO* | *Commonwealth Scientific and Industrial Research Organisation* |
| *ECL* | *East Coast Low* |
| *EHD* | *Extreme Heat Day* |
| *GCM* | *Global Climate Model / General Circulation Model* |
| *HCCREMS* | *Hunter Central Coast Regional Environmental Management Strategy* |
| *IPCC* | *Intergovernmental Panel on Climate Change* |
| *IPO* | *Interdecadel Pacific Oscillation* |
| *NCEP* | *National Centers for Environmental Protection (US)* |
| *NCAR* | *National Center for Atmospheric Research (US)* |
| *NNR* | *NCEP/NCAR* |
| *SLP* | *Sea Level Pressure* |
| *SOM* | *Self Organised Mapping* |
| *SRES* | *Special Report on Emissions Scenarios* |
| *SST* | *Sea Surface Temperature* |
| *ST* | *Synoptic Type* |

# 1 Introduction

This report has been developed for the Hunter and Central Coast Regional Environmental Management Strategy (HCCREMS) and represents a core element of a regional climate change research and adaptation project being implemented by HCCREMS and its 14 member councils. The key objectives of this project include:

1. to identify the potential regional and sub regional impacts of climate change in the Hunter, Central and Lower North Coast region of New South Wales;
2. to use this information to raise awareness and understanding by local governments, industry and community in the region of the potential impacts of climate change on their activities; and
3. to improve the awareness and capacity of these groups to accurately assess climate risk and to develop and implement appropriate adaptation strategies in response.

In order to identify the potential impacts of climate change on the region, HCCREMS commissioned the University of Newcastle (via Newcastle Innovation) to conduct the scientific research required for the project. This research has been carried out over a number of stages (four in total). These stages involved:

(1) identification of the key synoptic patterns relevant to the study region;
(2) analysis of how the synoptic patterns drive climate and climate-related variability in the region;
(3) downscaling CSIRO global climate model (GCM) predictions for New South Wales (NSW) to the study region; and,
(4) determination of the potential climate change impacts on the region based on the statistical downscaling.

This report primarily summarises the work undertaken and results generated during Stages 3 and 4 of this research.

The process of deriving Synoptic Types from the GCM output data and analysing the projected shifts in STs is a unique approach to downscaling GCM outputs to derive sub-regional projections. This is because it utilises the relationship between synoptic types derived from GCM output and actual climate data to understand and inform the downscaling process. GCM outputs for key climate variables such as temperature and precipitation are generally used for climate change projections. The approach adopted in this research seeks to identify changes in the “drivers” of these key climate variables and thus infer their change. Additionally, the scale of GCM outputs is generally quite coarse and would not have provided information at the regional and sub regional scale required by the

project.

Stage 1 of the research focused on the identification and collation of regionally specific climate data for use in Stages 2, 3 and 4. The study region encompasses 14 local government areas of the Hunter, Central and Lower North Coast region of NSW. A detailed quality assurance procedure was implemented to identify data sets that are of a suitable nature for use in the project. The data includes: Australian daily precipitation; Australian daily maximum and minimum temperatures; Australian hourly temperature, humidity and pressure; Australian daily evaporation; Australian daily wind data; Australian hourly wind data; Daily cloudiness, visibility and sunshine hours data for Bureau of Meteorology (BOM) districts 60, 61 and 62; Six minute pluvial data for districts 60, 61 and 62, NSW monthly ocean wave height, period and direction data, and monthly ocean tide gauge data on sea-level.

Additionally, an important component of Stage 1 of the project was to define the key synoptic patterns that drive the climate variability of the region for use in the downscaling of the Global Climate Model (GCM) output to a regional scale. A process known as self-organising mapping (SOM) was selected to derive the key synoptic types (STs) from monthly sea level pressure (SLP) data from January 1948 to December 2007. Data from the US National Centre for Environmental Prediction (NCEP)/National Centre for Atmospheric Research (NCAR) known as NCEP/NCAR reanalysis data were used for this process. This data will be referred to as NNR throughout this document. An initial 35 key STs were selected during Stage 1 of the project. These STs and the selected key climate data sets provided input to the analysis conducted in Stage 2 of the project.

Stage 2 of the project provided an analysis of climate variability, and of how synoptic patterns drive climate and climate-related variability in the region. The key outcome of Stage 2 was a comprehensive analysis of sub-regional climate distributions, including seasonal, interannual and interdecadal variability of key climate variables and extreme events. Additionally, the drivers of climate variability in the region were analysed. This incorporated an analysis of key synoptic patterns and their influence on sub-regional climate distributions. The 35 STs, derived using the SOM process in Stage 1, were evaluated as drivers of climate variability in the region. Analysis revealed that the large number of types made isolating specific type “signatures”, in terms of unique climate characteristics, difficult. As such, the SOM process was repeated to derive 6, 9, 12, 15 and 20 types. These STs were then evaluated for their ability to explain climate variability in the region. A SOM consisting of 12 STs (3x4) was found to be optimal.

In Stage 3 of the project, the outputs of a number of GCMs were evaluated and the output from the CSIRO Mk3.5 GCM was downscaled to provide sub-regional scale projections for the study region. During the planning phase of this project, the CSIRO Mk3.5 global GCM

was identified for use in downscaling projections to the study region. However, recent research has identified that a number of GCMs may provide useful outputs for the Australian continent (i.e. Perkins, et al. (2007)) and thus Stage 3 was expanded to include a full analysis of all relevant GCMs. This review concluded that the CSIRO Mk3.5 model remained the most suitable for use on the project.

Following the final selection of the CSIRO Mk3.5 model, the downscaling process was completed. Results from this process are reported in terms of projected changes in key climate variables (i.e. precipitation, maximum and minimum temperatures, average temperature and the diurnal cycle, humidity, evaporation, average wind speed, wind gusts, sea level rise and extreme sea levels, wave climate and extreme events). These projected changes are derived from analysing the projected shifts in STs. As identified in Stage 2 of this project, STs are able to be used to explain climate variability in the region. Understanding the projected shifts in STs provides not only a means to assess changes in key climate variables, but provides a rich understanding of the changing mechanisms driving climate variability in the region.

Utilising the results from Stage 3, Stage 4 of the project then involved the determination of the potential climate change impacts on the region based on the statistical downscaling. The results of this process are included in this report in the section entitled 'Analysis of Key Climate Variables by Synoptic Type'. More detailed analysis of projected climate change in relation to four specific sectors is also provided as four independent cases studies. These case studies focus on the regional impacts of climate change for the viticulture industry, human health as a result of extreme heat events, bushfires, and extreme events affecting the coastal region.

# 2 Project Methodology

The overall methodological approach adopted for this research project relies on the identification of synoptic patterns that drive climate variability in the region and their relationship to key climate variables (Figure 1). The relationships between these synoptic types (STs) and measurements for key climate variables obtained from BOM stations are used to derive sub-regional projections. That is, each ST is related to a mean regional spatial pattern for each key climate variable, and changes in the frequency of occurrence of STs are used to determine the associated change in key climate variables. For example, if a ST associated with high coastal rainfall is determined to increase in frequency over the projected period, an estimate of the likely associated increase in coastal rainfall as a result of this change in frequency can be made.

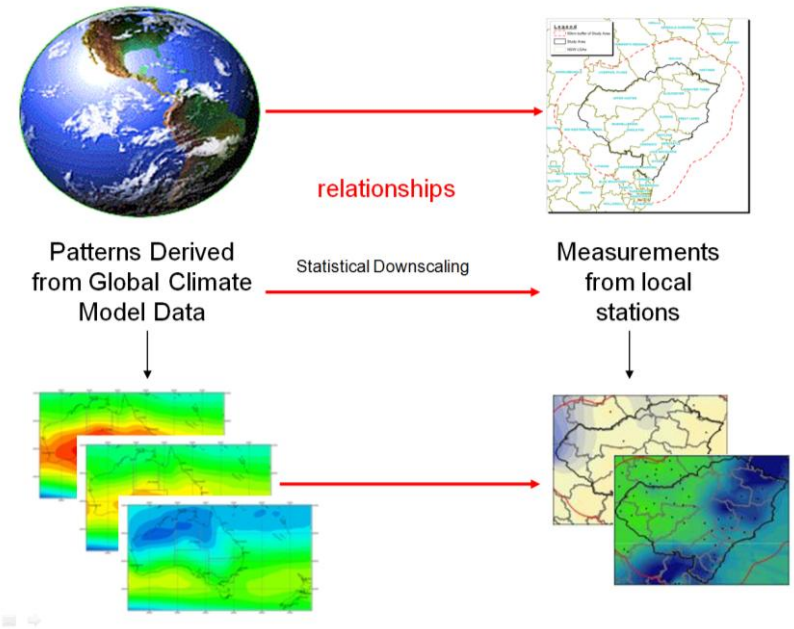


Figure 1 – Simple overview of project methodology

In Stages 1 and 2 of the project, synoptic patterns were derived using the self-organising mapping (SOM) process using NNR data from 1948 to 2007. This process was initially used to cluster global reanalysis monthly sea-level pressure (SLP) data for the region into twelve (12) STs. These types allow the subtle discrimination of regional climate patterns on key climate parameters such as rainfall, evaporation and temperature. In Stage 2, the 12 STs generated were shown to capture a range of significant synoptic features that are known to

influence the weather of the region, including the clear seasonal trends in the location and intensity of the subtropical anticyclone, the monsoonal trough, the circumpolar trough, and the longwave features in the Pacific and Indian Ocean sectors. Each month from January 1948 through to December 2007 has been classified according to the 12 synoptic patterns, resulting in a monthly time series of synoptic types. A description of each of these STs is included as Appendix A.

The following sections (2.1 to 2.3) describe the methodology used in Stages 3 and 4 of the project. The primary work undertaken and presented in this report includes:

- evaluating the match between the 12 STs derived from the NNR data and the CSIRO Mk3.5 output and/or synoptic types derived from the CSIRO Mk3.5 output;
- determining the relationship between STs and key climate variables using statistical downscaling; and,
- assessing the impacts of projected changes in the frequency of occurrence of STs on the region's climate zones.

## 2.1 Calibration and Evaluation of Global Climate Models

Initially, only the output from Australia's CSIRO Mk3.5 was proposed for use in this research. A preliminary evaluation of the suitability of CSIRO Mk3.5 model output data was conducted. This involved assessing the synoptic types (STs) produced from the CSIRO model sea level pressure (SLP) output data for the calibration period (January 1968 to December 1996) against those derived from the NNR data for the same time period. This preliminary analysis identified issues with matching the STs produced from the NNR data with those derived from the output from the CSIRO Mk3.5 model (i.e. low percentage match between the two data sets). In order to address this issue, a literature review was conducted to identify other potential GCMs or combinations of GCMs that may provide a greater level of matching.

An analysis of GCMs relevant to this project was presented by Perkins, et al. (2007). The authors of this article provide an analysis of the performance of 16 models in terms of simulated maximum temperature, minimum temperature and precipitation over 12 regions of Australia. Results of their analysis are presented as a ranking of model performance, in terms of the selected parameters, over all of Australia. From these rankings, four additional models (to the CSIRO model) were selected for use in the Stage 3 analysis. The selected models are listed in the Table 7. The rank order of the model, as provided by Perkins et al, is shown in brackets beside the model name.

| Model Name | Institution, sponsoring agency, country |
|---|---|
| CSIRO-Mk3.5 (2) | CSIRO, Australia |
| ECHO-G (3) | Meteorological Institute of the University of Bonn (Germany), Institute of KMA (Korea), and Model and Data Group |
| IPSL-CM4 (4) | Institut Pierre Simon Laplace, France |
| MIROC 3.2 (1) | Center for Climate System Research, University of Tokyo, National Institute for Environmental Studies, Frontier Research Center for Global Change, Japan Agency for Marine-Earth Science and Technology (JAMSTEC) |
| MRI-CGCM2.3.2 (5) | Meteorological Research Institute, Japan Meteorological Agency, Japan |

Table 7 - Summary of models used in the analysis

In addition to the five selected models, three ensembles were evaluated. The use of an ensemble is a method that has been successfully employed in other studies (Teng et al. 2006). An ensemble is obtained by averaging the output data from two or more GCMs. In this way, biases inherent in individual models are minimised. Determination of appropriate models to be included in the ensemble are based the calibration results for the five selected models.

| Model | No Timesteps | Start Time | End Time | Rows | Columns | Resolution | Min_Lat |
|---|---|---|---|---|---|---|---|
| NNR | 720 | Jan-1948 | Dec-07 | 73 | 144 | 2.5° | 90° |
| CSIRO (20C3M) | 1560 | Jan-1871 | Dec-00 | 96 | 192 | 1.875° | -88.5722° |
| ECHO-G (20C3M) | 1692 | Jan-1860 | Dec-00 | 48 | 96 | 3.75° | -87.1591° |
| IPSL-CM4 (20C3M) | 1692 | Jan-1860 | Dec-00 | 72 | 96 | 2.53°x3.75° | -90° |
| MIROC (20C3M) | 1812 | Jan-1850 | Dec-00 | 64 | 128 | 2.8125° | -87.8638° |

Table 8 - Key parameters for NNR, CSIRO, ECHO-G, MIROC and MRI 20C3M model data

Two separate processes were used to calibrate the GCMs to the NNR data (Figure 2). The first process involved the use of the 12 *prototype vectors* derived from the SOM of the NNR data. Prototype vector is a term used to refer to the exemplar pattern of SLP values for each of the STs. Data from each model for the period from January 1968 to December 1996 was then compared to the 12 prototype vectors and the ST of the best matching unit assigned. Calibration of these models was conducted using the 20C3M model data only. The start time of each of the time series and the grid resolution varies for the selected GCMs (see Table 2). Regridding of the GCM data to the NNR 2.5° grid was performed to ensure the derivation of STs for the same spatial extent as that used for the NNR data (i.e. 112.5° to 177.5° longitude, -10° to -47.5° latitude).

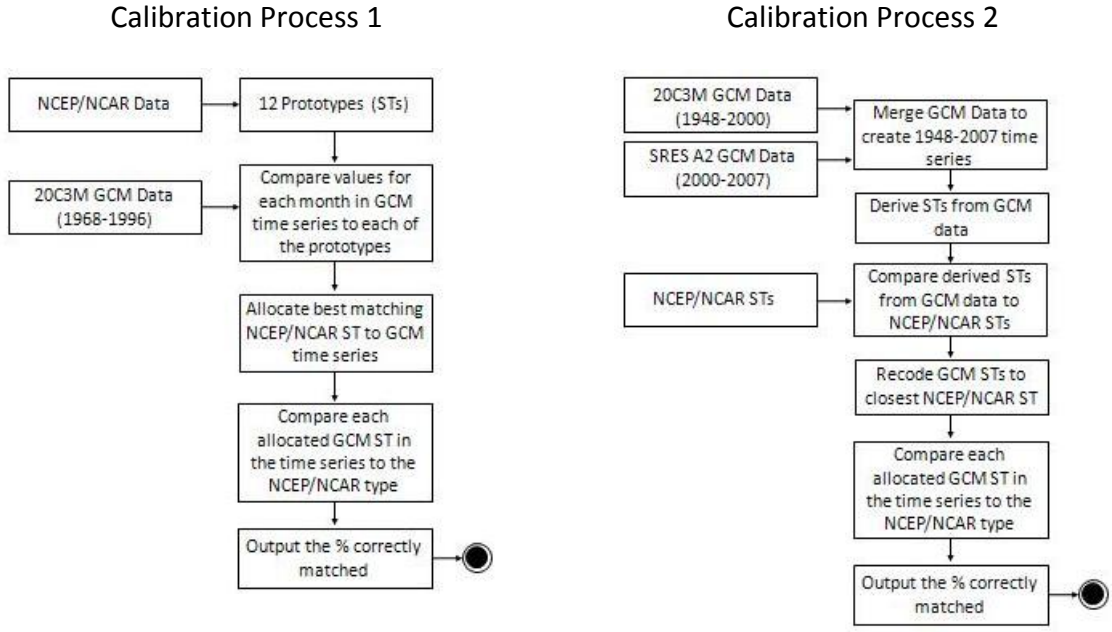


Figure 2 - Calibration processes for GCM data

These calibration processes were developed specifically for this project. Calibration process 1 assesses how well the raw GCM data aligns to the NNR derived prototype vectors. Calibration process 2 not only allows for the alignment between the NNR types and GCM derived types to be assessed, but also enables the evaluation of new GCM types. NNR types not produced by the GCM output can also be identified. In this way, the two processes provide a rigorous methodology for calibrating the data sets.

The second process involved using the GCM data for the 20C3M and the A2 scenario projected data to 2100AD to produce a time series from January 1948 to December 2007 (see Figure 2). This period is the same as that used for the NNR data SOM analysis. The GCM data was used as input data to derive a SOM for each of the selected models. These new STs

were then compared against those derived from the NNR data. Again, the model data was regridded to match that of the NNR data. The results of the calibration processes are presented in the following sections.

### 2.1.1 Calibration Using NNR Prototypes (Process 1)

The anomaly STs, derived using the SOM methodology from the NNR data for the period from January 1948 to December 2007, are shown in Figure 3. Although visualised as a two dimensional map, the actual output from the SOM process is a one dimensional prototype vector for each ST. These 12 one dimensional prototype vectors contain the SLP values for that ST.

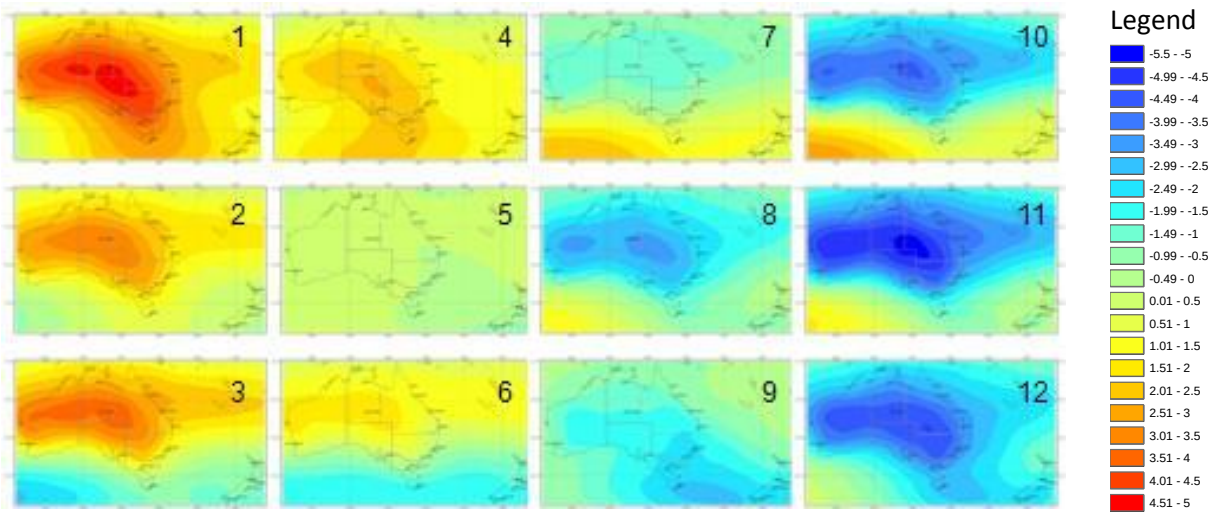


Figure 3 - 12 SLP anomaly STs derived using the SOM methodology from the NNR data for the time period from Jan 1948 to Dec 2007

The Matlab SOM toolbox used for this research includes an inbuilt function whereby new data can be compared to each of the existing prototype vectors and labelled according to the best matching unit (BMU). This function was used to assign the closest matching NNR ST to each month's SLP values for each of the selected GCMs. Analysis was then conducted to ascertain how well the ST allocations for each of the data sets matched. The results of this analysis are presented below.

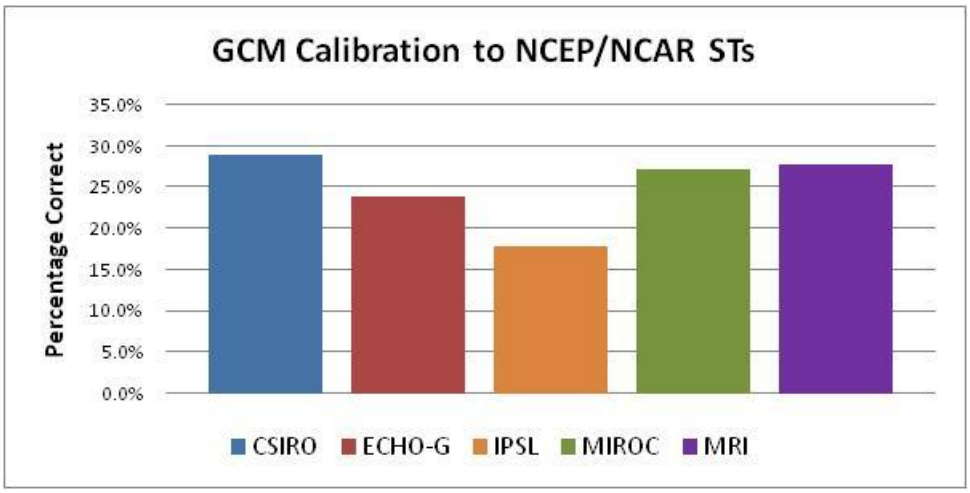


Figure 4 - GCM Calibration to NNR STs – Percentage Correct

Overall, total matches between the GCMs and the NNR are relatively low (Figure 4). The best performing GCM is the CSIRO model, with a 29% match between types. Performing poorest is the IPSL model, with only 18% of months in the time series correctly matched.

Figure 5 and Figure 6 show the number of hits per ST for each model and the percentage correct per ST respectively. STs 2, 5 and 8 have higher error rates than other STs, however these types also have significantly lower hits. No clear patterns in the error rates associated with the different STs are evident.

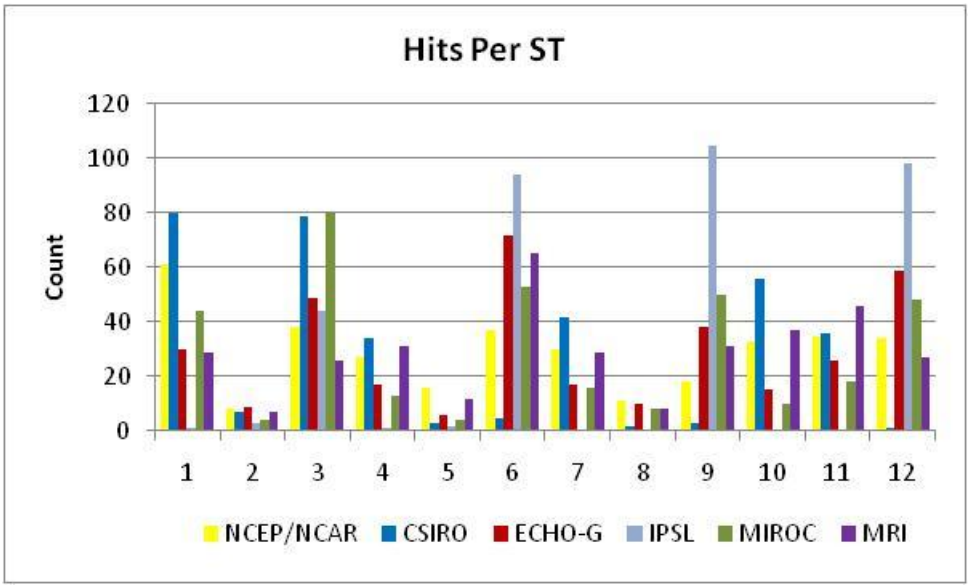


Figure 5 - GCM Calibration to NNR (NCEP/NCAR) STs - Hits per ST

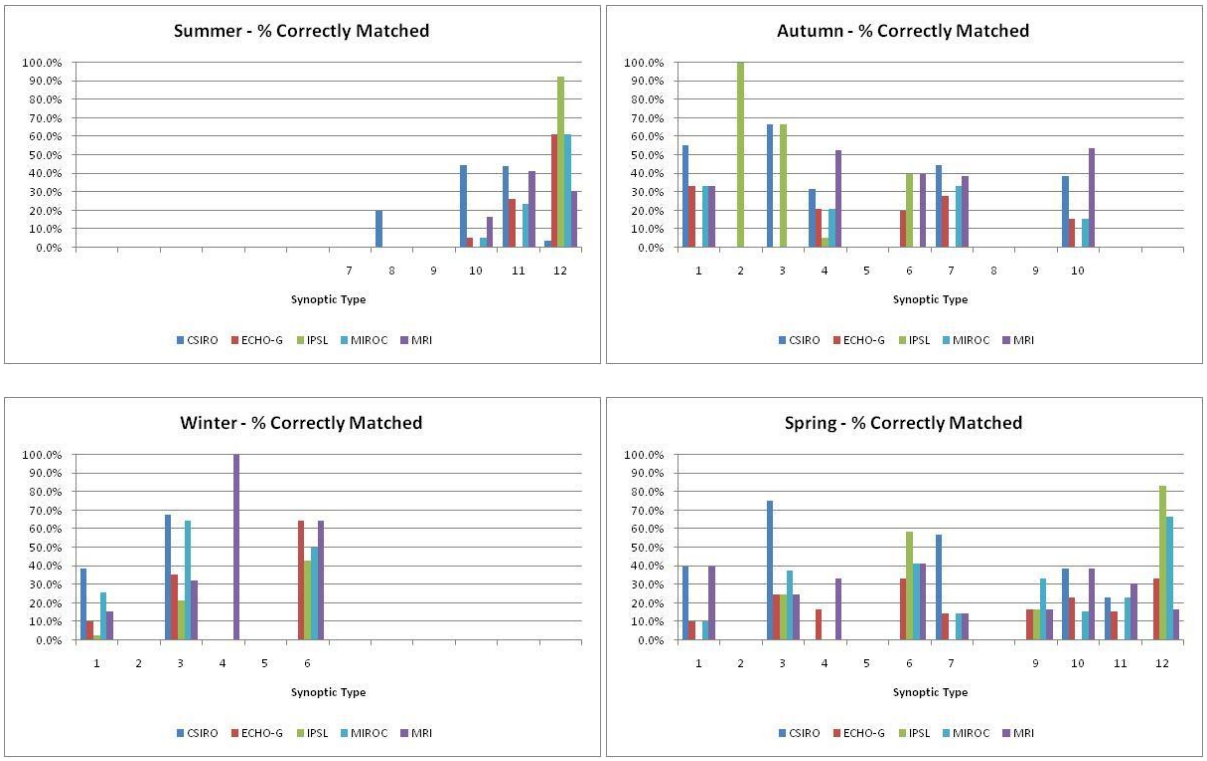


Figure 6 - Seasonal graphs of correctly matched STs

### 2.1.2 Calibration Using GCM Derived Synoptic Types (Process 2)

This calibration process involves generating new STs for each of the selected GCMs then matching the newly derived STs to the NNR derived STs. This process accounts for the possibility that the GCMs are producing synoptic patterns not evident in the STs produced by the NNR types.

As mentioned in Section 2 of this report, the 20C3M covers the time period from at least January 1901 (refer to Table 2 for specific details of the time horizons of each of the GCMs included in this analysis) to December 2000. The A2 scenario GCM output covers the period from January 2000 to December 2099. To derive synoptic types for the same time period as that used to derive the NNR STs (i.e. January 1948 to December 2007), the 20C3M and A2 scenario data for each GCM was merged to produce data sets covering the required time period.

For each of the models (i.e. CSIRO, ECHO, IPSL, MIROC, and MRI), 12 SLP STs are generated using the same SOM process used to derive the NNR types[1]. A closest match between the

[1] Although the same SOM process is used to derive the STs from the NNR data and all the GCMs, the ordering of the output STs from the SOM process may differ arbitrarily. That is, where NNR summer STs are located on the right hand edge of the 3x4 SOM (and therefore dominant summer types are 10, 11 and 12), SOMs derived from the GCM data may or may not mirror this ordering (i.e. ECHO dominant summer types are located along the bottom edge of the 3x4 SOM and are therefore labeled STs 3, 6, 9 and 12). Grids showing the position of seasonal types for the NNR and GCM SOMs are provided in Appendix B.

newly generated GCM type and existing NNR type was then determined[2] (Table 9), and the consistency between each of the GCMs and the NNR types was analysed. The best matching type was determined through a combination of visual comparison and analysis of seasonal types (i.e. the dominant seasonal types for each GCM were matched to the corresponding NNR type; intermediate types were then matched using seasonal hits). The anomaly STs produced from each of the GCMs are presented as figures and the results of the analysis are provided in the following sections.

| | Best Matching GCM Type | | | | |
|---|---|---|---|---|---|
| **NCEP** | **CSIRO** | **ECHO** | **IPSL** | **MIROC** | **MRI** |
| **1** | 1 | 10 | 3 | 9 | 10 |
| **2** | 2 | 4 | 12 | 12 | 12 |
| **3** | 3 | 7 | 9 | 3 | 9 |
| **4** | 4 | 2 | 2 | 2 | 6 |
| **5** | 5 | 5 | 5 | 5 | 5 |
| **6** | 6 | 11 | 6 | 6 | 11 |
| **7** | 7 | 1 | 1 | 8 | 3 |
| **8** | 8 | 8 | 8 | 10 | 2 |
| **9** | 9 | 3 | 11 | 11 | 7 |
| **10** | 10 | 6 | 4 | 4 | 8 |
| **11** | 11 | 9 | 10 | 1 | 1 |
| **12** | 12 | 12 | 7 | 7 | 4 |

Table 9 - Correspondence between NNR ST and derived GCM STs

[2] In some cases, NNR types were not present in the derived GCM types or vice versa. In these instances, a closest match is allocated from the available types. In this way, an estimation of the match between the models can be made.

### *CSIRO-Mk3.5*

The STs produced from the CSIRO-Mk3.5 data are generally in the same SOM positions as those produced from the NNR data (Figure 7). When compared to the closest matching NNR types, the CSIRO types appear to resolve the majority of types however they over-estimate the magnitude of the SLP anomalies, particularly over the Tasman. Additionally, the CSIRO types do not appear to be capturing the meridional variance associated with the planetary long-waves.

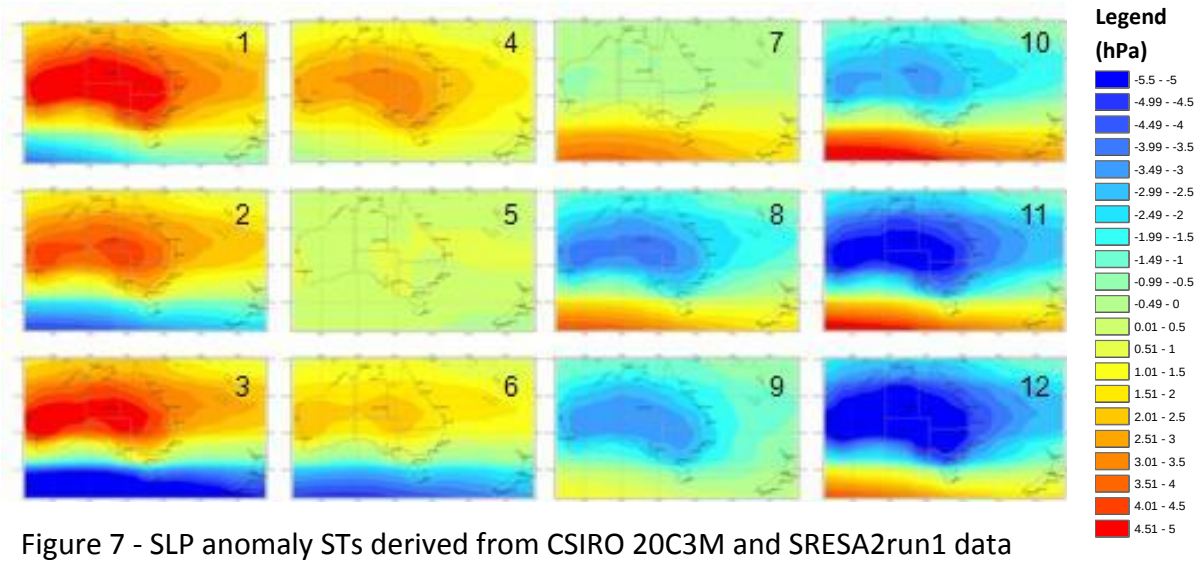


Figure 7 - SLP anomaly STs derived from CSIRO 20C3M and SRESA2run1 data

A total of 29.0% of the CSIRO types are correctly matched to the NNR types.

### *ECHO-G*

The STs produced from the ECHO-G data are in different SOM positions to those produced from the NNR data and significant differences in the synoptic patterns produced exist (Figure 8). In fact, the low correspondence between the types indicates that the output from this model is not appropriate for this research.

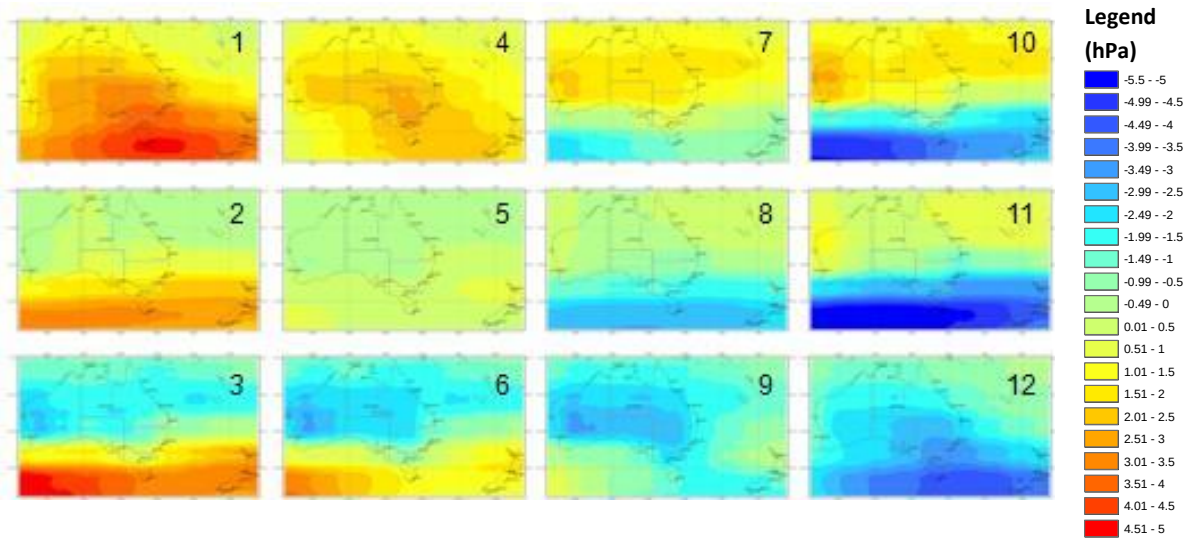


Figure 8 - SLP anomaly STs derived from ECHO 20C3M and SRESA2run3 data

For the time period from January 1948 to December 2007, only 15.3% of ECHO-G types were correctly matched to NNR types.

### *IPSL-CM4*

Despite little correlation between the NNR and IPSL types, the IPSL types do appear to capture some of the long-wave structures not captured by the types derived from the other GCM data (Figure 9).

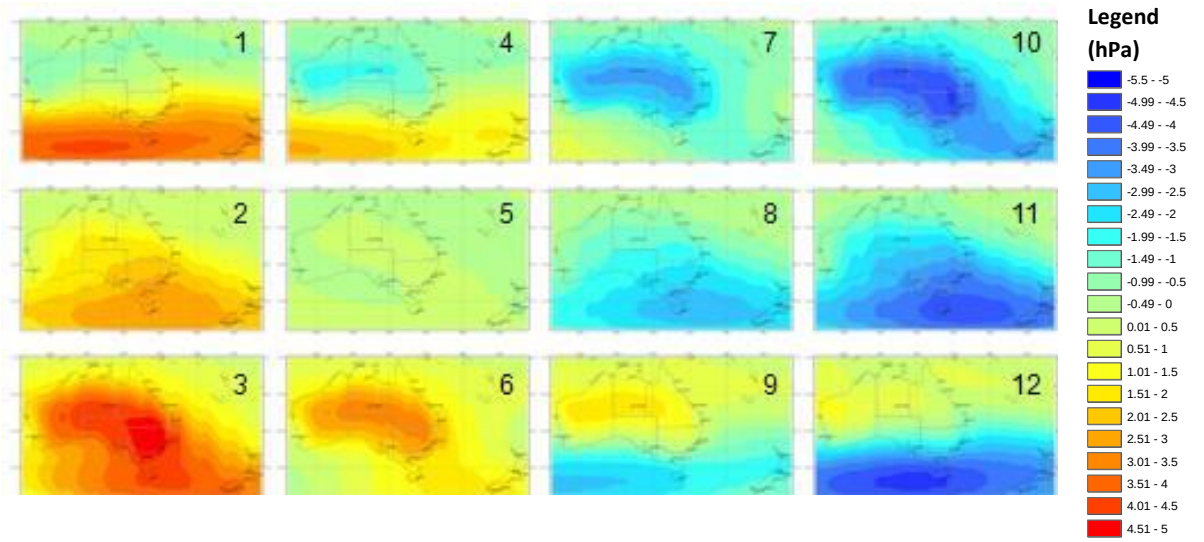


Figure 9 - SLP anomaly STs derived from MIROC 20C3M and SRESA2run1 data

For the time period from January 1948 to December 2007, only 6.1% of IPSL types were correctly matched to NNR types.

### *MIROC 3.2*

Little correlation exists between the STs SOM produced from the NNR data to those produced from the MIROC 3.2 data (Figure 10). As such, the output from this model is not appropriate for this research

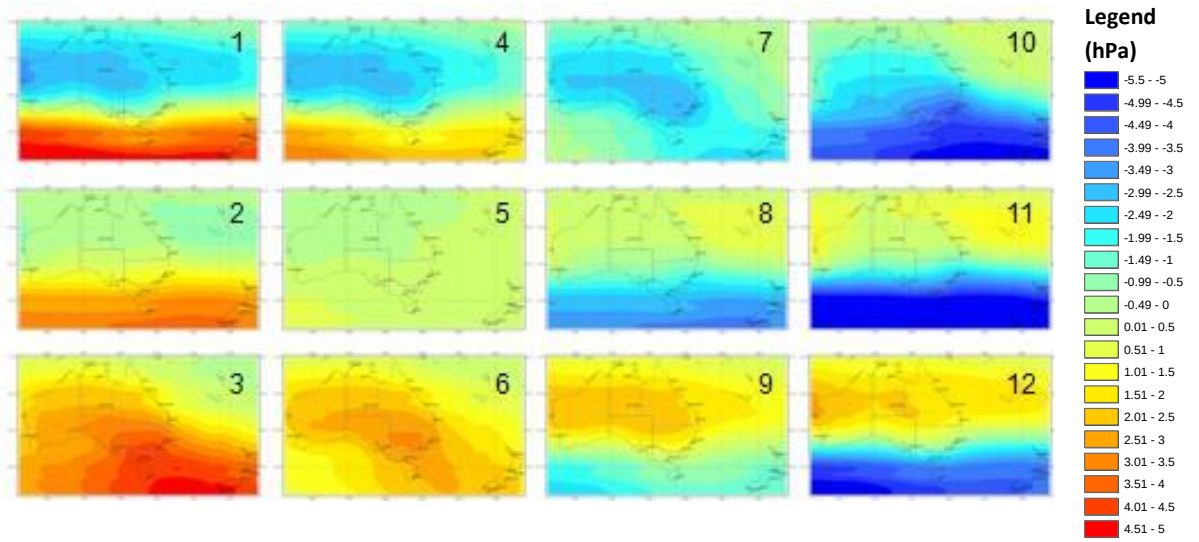


Figure 10 - SLP anomaly STs derived from MIROC 20C3M and SRESA2run1 data

For the time period from January 1948 to December 2007, 20.8% of MIROC 3.2 types were correctly matched to NNR types.

### *MRI-CGCM2.3.2*

The STs produced from the MRI-CGCM2.3.2 data are in the reverse SOM positions to those produced from the NNR data (Figure 11). That is, NNR ST1 corresponds to MRI ST12, NNR ST2 corresponds to MRI ST11, and so forth.

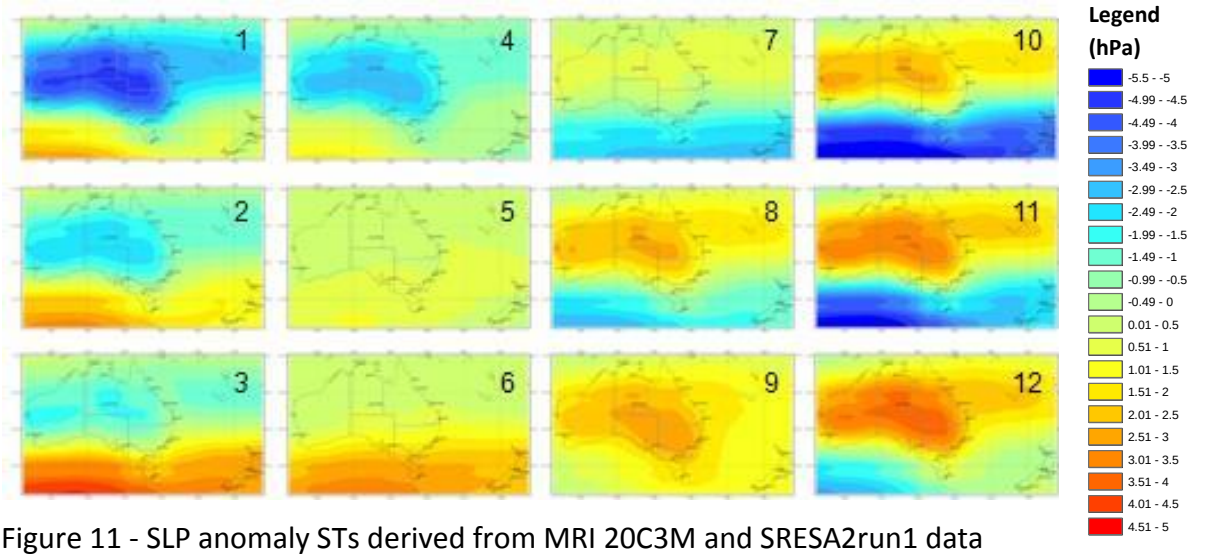


Figure 11 - SLP anomaly STs derived from MRI 20C3M and SRESA2run1 data

Correlation exists between the types produced from the NNR data and the MRI GCM derived types, although discrepancies are present. The MRI types appear to under estimate the magnitude of the anomalies (when compared to the NNR types) and do not fully capture the long-wave structure, and thus do not fully resolve the extremes in winter and summer anomalies. Additionally, types are included in spring and autumn that are not present in the NNR types.

For the time period from January 1948 to December 2007, 24.4% of MRI types were correctly matched to NNR types.

### 2.1.3 Summary of Calibration of GCMs (Processes 1 and 2)

The CSIRO model is the best performing of the individual GCMs, followed by MRI and MIROC. Although global models, these three GCMs are produced by Australasian countries (i.e. Australia and Japan) and thus may be optimised to the Australian region. The ECHO-G and IPSL GCMs perform poorly. Following previous logic, these European models (i.e. German and French) appear not to be optimised for Australasia.

| | CSIRO | ECHO-G | IPSL | MIROC | MRI |
|---|---|---|---|---|---|
| Callibration 1 | 29.0% | 23.6% | 18.1% | 27.0% | 27.9% |
| Callibration 2 | 24.4% | 15.3% | 6.1% | 20.8% | 24.4% |
| Average | 26.7% | 19.4% | 12.1% | 23.9% | 26.2% |

Table 10 - Summary of GCM correct matches using calibration processes 1 and 2

Although calibration process 1 results in higher matches to the NNR data than calibration process 2 (Table 10), the percentage correct is still poor. The major deficiency of the GCMs is their inability to capture long-wave structures. These errors primarily occur in the Southern Ocean, well beyond the extent of the area of interest for this study. As such, although statistical matching is poor, the best performing model (i.e. CSIRO) appears to capture the synoptic patterns relevant to the Lower North Coast, Hunter and Central Coast region.

### 2.1.4 Calibration of Ensemble Types

As briefly discussed in Section 3, the use of an ensemble may minimise the limitations of individual models. The 5 GCMs assessed in the previous sections are considered in this section as input for an ensemble. Three combinations of the GCMs, and therefore three different ensembles, are considered.

Firstly, an ensemble comprising all 5 GCMs is assessed. Secondly, an ensemble utilising only the two best performing GCMs (i.e. CSIRO and MRI) is assessed. Finally, an ensemble utilising the two best performing GCMs, and a third model which captures some of the long-wave structures not captured in the other two models (i.e. IPSL), is assessed. The results of matching to NNR STs using the two previously described calibration processes are provided in the following sections.

### *Ensemble – 5 GCMs*

The STs produced from the ENSEMBLE data are in the reverse SOM positions to those produced from the NNR data (Figure 12). That is, NNR ST1 corresponds to ENSEMBLE ST12, NNR ST2 corresponds to ENSEMBLE ST11, and so forth.

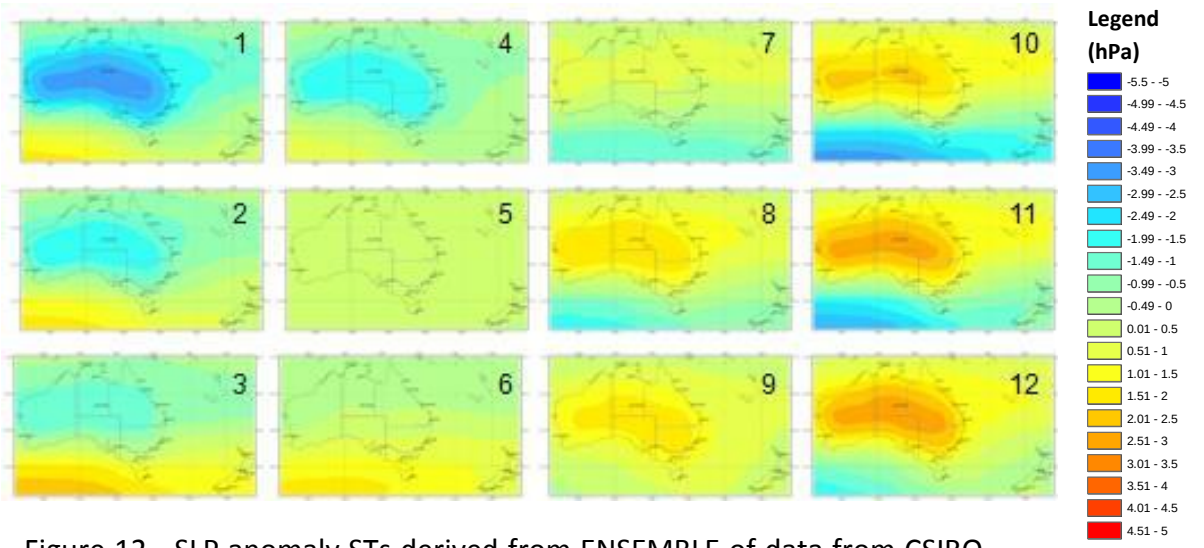


Figure 12 - SLP anomaly STs derived from ENSEMBLE of data from CSIRO, ECHO, IPSL, MIROC and MRI GCMs.

The 5 model ensemble appears to underestimate the anomalies across all STs. Despite this, the 5 model ensemble statistically matches the NNR STs better than the individual models, matching 31% using calibration process 1 and 24.7% using calibration process 2.

### *Ensemble – CSIRO and MRI GCMs*

The STs produced from the CSIRO and MRI GCM ensemble are in the same SOM positions as those produced from the NNR data (Figure 13). That is, NNR ST1 corresponds to ENSEMBLE ST1, NNR ST2 corresponds to ENSEMBLE ST2, and so forth.

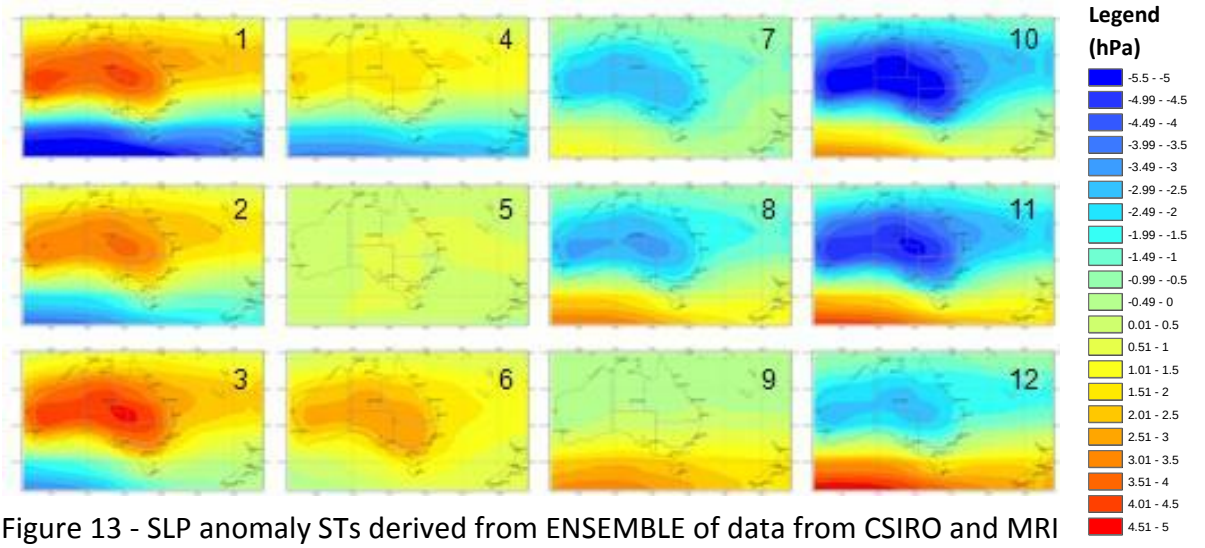


Figure 13 - SLP anomaly STs derived from ENSEMBLE of data from CSIRO and MRI GCMs

The CSIRO/MRI model ensemble appears to underestimate the low anomalies and overestimate highs. Additionally, the longwave structures present in the NNR types do not appear to be well captured. The CSIRO/MRI model ensemble matches the NNR STs better than the individual models, matching 30.5% using calibration process 1 and 23.5% using calibration process 2.

### *Ensemble – CSIRO, IPSL and MRI GCMs*

The STs produced from the CSIRO, IPSL and MRI GCM ensemble data are in the reverse SOM positions to those produced from the NNR data (Figure 14). That is, NNR ST1 corresponds to ENSEMBLE ST12, NNR ST2 corresponds to ENSEMBLE ST11, and so forth.

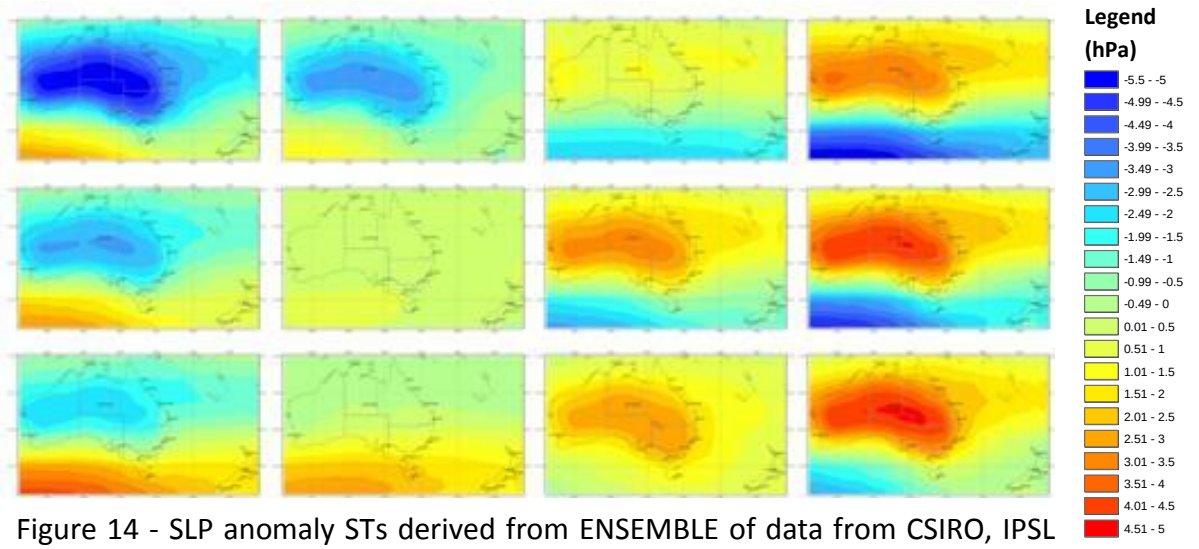


Figure 14 - SLP anomaly STs derived from ENSEMBLE of data from CSIRO, IPSL and MRI GCMs

The CSIRO, IPSL AND MRI ensemble appears to underestimate the low pressure anomalies. The ensemble matches the NNR STs better than the individual models, matching 31.3% using calibration process 1 and 24.9% using calibration process 2.

### 2.1.5 Discussion of Calibration Results

Overall, all models performed poorly with a best match of 24.4% achieved between the GCM and NNR STs (Figure 15 and Figure 16). Of the five GCMs assessed, the CSIRO and MRI models performed best using STs derived from the GCM data. The ensembles performed slightly better, with a best match of 31.3% achieved between CSIRO/MRI/IPSL ensemble and the NNR STs.

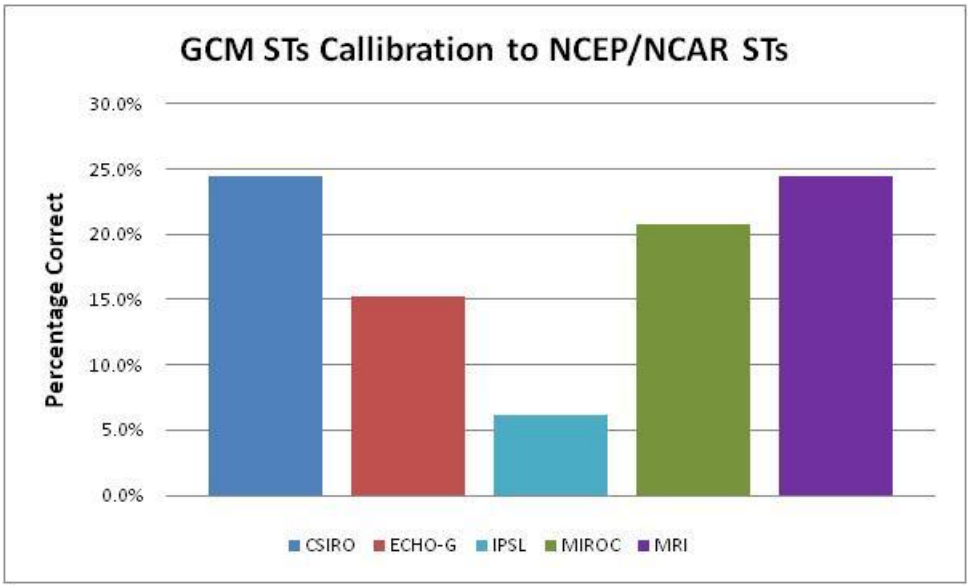


Figure 15 - Comparison of percentage correct matches for GCM derived STS to NNR STs

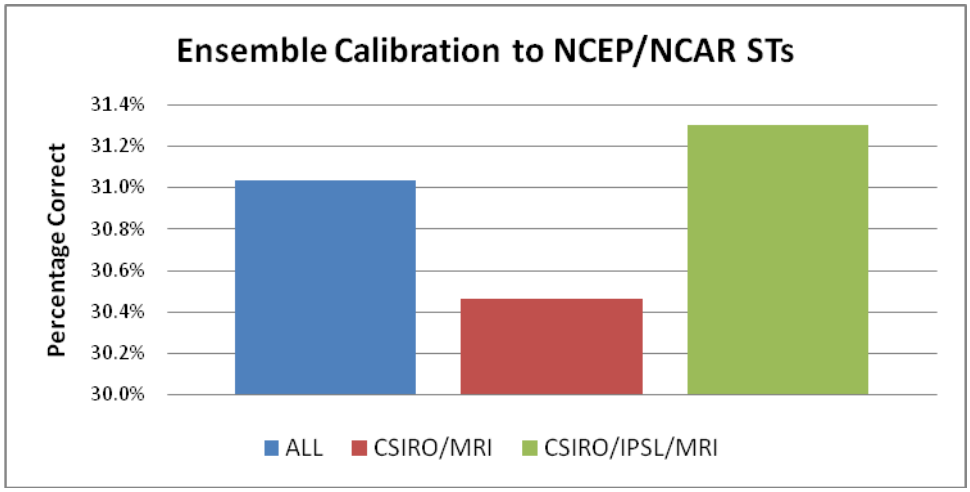


Figure 16 - Comparison of percentage correct matches for ensemble derived STS to NNR STs

A summary of the calibration results, expressed as the percentage of months correctly matched to the NNR ST, is provided in Table 11. Of the individual models, the CSIRO GCM performed best, followed by MRI. The three ensembles assessed performed better than the individual models, with the CSIRO/IPSL/MRI ensemble best matched. Higher percentage matches were achieved using calibration process 1. Generally however, there appears to be little correspondence between the synoptic patterns derived from the GCMs and those derived from the NNR reanalysis data.

| | CSIRO | ECHO-G | IPSL | MIROC | MRI | ALL | CSIRO/MRI | CSIRO/IPSL/MRI |
|---|---|---|---|---|---|---|---|---|
| Callibration 1 | 29.0% | 23.6% | 18.1% | 27.0% | 27.9% | 31.0% | 30.5% | 31.3% |
| Callibration 2 | 24.4% | 15.3% | 6.1% | 20.8% | 24.4% | 24.7% | 23.5% | 24.9% |
| Average | 26.7% | 19.4% | 12.1% | 23.9% | 26.2% | 27.9% | 27.0% | 28.1% |

Table 11 - Percentage correct matches for calibration 1, calibration 2 and an overall average for each GCM

Generally, percentage matches obtained using both calibration processes are low for all models and ensembles. A correlation or match greater than 75% is generally considered reasonable. Both calibration processes failed to produce matches greater than 31.3%. In the case of calibration process 2, some proportion of the poor matching may be attributed to closest match assignment between types when clearly some NNR types were not produced from the GCM output and vice versa. However, calibration process 1 overcomes this limitation but does not produce significantly superior results.

Although the ensemble models perform slightly better than the single GCMs, percentage matches still do not achieve close to the required 75% level. Given this, the best performing single GCM, the CSIRO Mk3.5 model, is selected as appropriate for the analysis of 2100AD climate change. Each GCM is constructed using a single forcing and is preferred over an ensemble where individual model forcings are combined. Dealing with a single forcing is preferred when the lack of statistical correlation may require a detailed understanding of the model dynamics.

Despite achieving poor statistical correlation to the NNR data, the CSIRO Mk3.5 model is considered appropriate for considering climate change in the region. The vast majority of the discrepancies between the STs produced from the NNR and CSIRO models occur in the southern ocean. Variations over the study region show little variation; in fact the differences between the CSIRO Mk3.5 STs and the NNR STs over this region are less than 1 hectopascal (hPa). These differences are further discussed in Section 3.

## 2.2 Statistical Downscaling

Following the calibration and evaluation of the GCMs, the best matching GCM is used to analyse projected changes in key climate variables using *statistical downscaling*. Statistical downscaling (SD) is a term given to techniques used to derive values for climate variables at a regional or sub-regional level from the coarse scale output of global climate models (GCMs). Some variability in the scale of output of GCMs exists; the models evaluated in this report range between a unit of analysis (grid cell size) of 1.875°x1.875° to 3.75°x3.75°. At these resolutions, the output of a single cell from the GCMs often covers an entire study region. For example, the CSIRO Mk3.5 model output resolution is 1.875°. This results in a grid cell size of approximately 208km × 208km at the equator and 180km × 208km at a latitude of 30°S. The study region for this climate change project encompasses an area of 39,021.58 sq/km, which is covered by parts of four 1.875 degree grid cells (Figure 17).

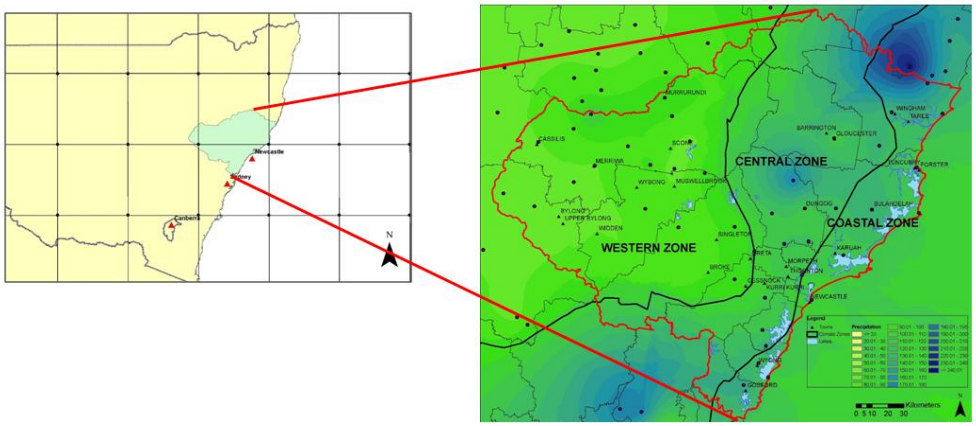


Figure 17 - The study region is covered by parts of four CSIRO Mk3.5 grid cells

Key climate parameters, such as precipitation, have been found to vary significantly within localised regions. In order to interpret the GCM output in a regional context, relationships between the output values for individual grid cells and the actual values of key climate variables for points within the study region are derived. These relationships can be derived using a number of different SD techniques. The main SD techniques can be broadly classified as:

- Regression models – derive statistical relationships between large scale climate variables and regional or local climate variables.
- Weather classification schemes – similar to regression models, however relationships are derived between large scale or synoptic patterns and regional or local climate variables.

- Weather generators – replicate the statistical attributes of a regional or local climate variable and artificially generate a long time series of climate information specific to the site (Wilby, et al., 2004).

Each of these techniques have associated strengths and weaknesses (Table 12).

| Method | Strengths | Weaknesses |
|---|---|---|
| **Weather typing** (e.g. analogue method, hybrid approaches, fuzzy classification, self organizing maps, Monte Carlo methods). | • Yields physically interpretable linkages to surface climate<br>• Versatile (e.g., can be applied to surface climate, air quality, flooding, erosion, etc.)<br>• Compositing for analysis of extreme events | • Requires additional task of weather classification<br>• Circulation-based schemes can be insensitive to future climate forcing<br>• May not capture intra-type variations in surface climate |
| **Weather generators** (e.g. Markov chains, stochastic models, spell length methods, storm arrival times, mixture modelling). | • Production of large ensembles for uncertainty analysis or long simulations for extremes<br>• Spatial interpolation of model parameters using landscape<br>• Can generate sub-daily information | • Arbitrary adjustment of parameters for future climate<br>• Unanticipated effects to secondary variables of changing precipitation parameters |
| **Regression methods** (e.g. linear regression, neural networks, canonical correlation analysis, kriging). | • Relatively straightforward to apply<br>• Employs full range of available predictor variables<br>• 'Off-the-shelf' solutions and software available | • Poor representation of observed variance<br>• May assume linearity and/or normality of data<br>• Poor representation of extreme events |

Table 12 – A summary of the strengths and weaknesses of the main SD methods (reproduced from Wilby et al., 2007).

A weather typing approach to SD is adopted for the research presented in this report. The GCM output sea level pressure (SLP) data is used to derive key synoptic types (STs) using the self-organising mapping (SOM) process. Relationships between these STs and BOM historic records for key climate variables are then derived. Changes in key climate variables for future time horizons are then estimated from changes in the frequency of occurrence of STs, using our understanding of how the region's weather is impacted by these STs. The key benefit of this approach is that we obtain a richer understanding of the drivers of weather patterns within the region and how these "drivers" are likely to change in the future.

## 2.3 Climate Zones

Projections for key climate variables are analysed and discussed in terms of the region's *climate zones*. Climate zonation is a process for dividing a region into distinct sub-regions or zones where climatic similarity is maximised within zones and minimised between zones. The development of climate zones for the region was conducted during Stage 2 of the project to allow the analysis of sub-regional climate variability at a level above the individual BOM station. The identified climate zones are shown in Figure 18.

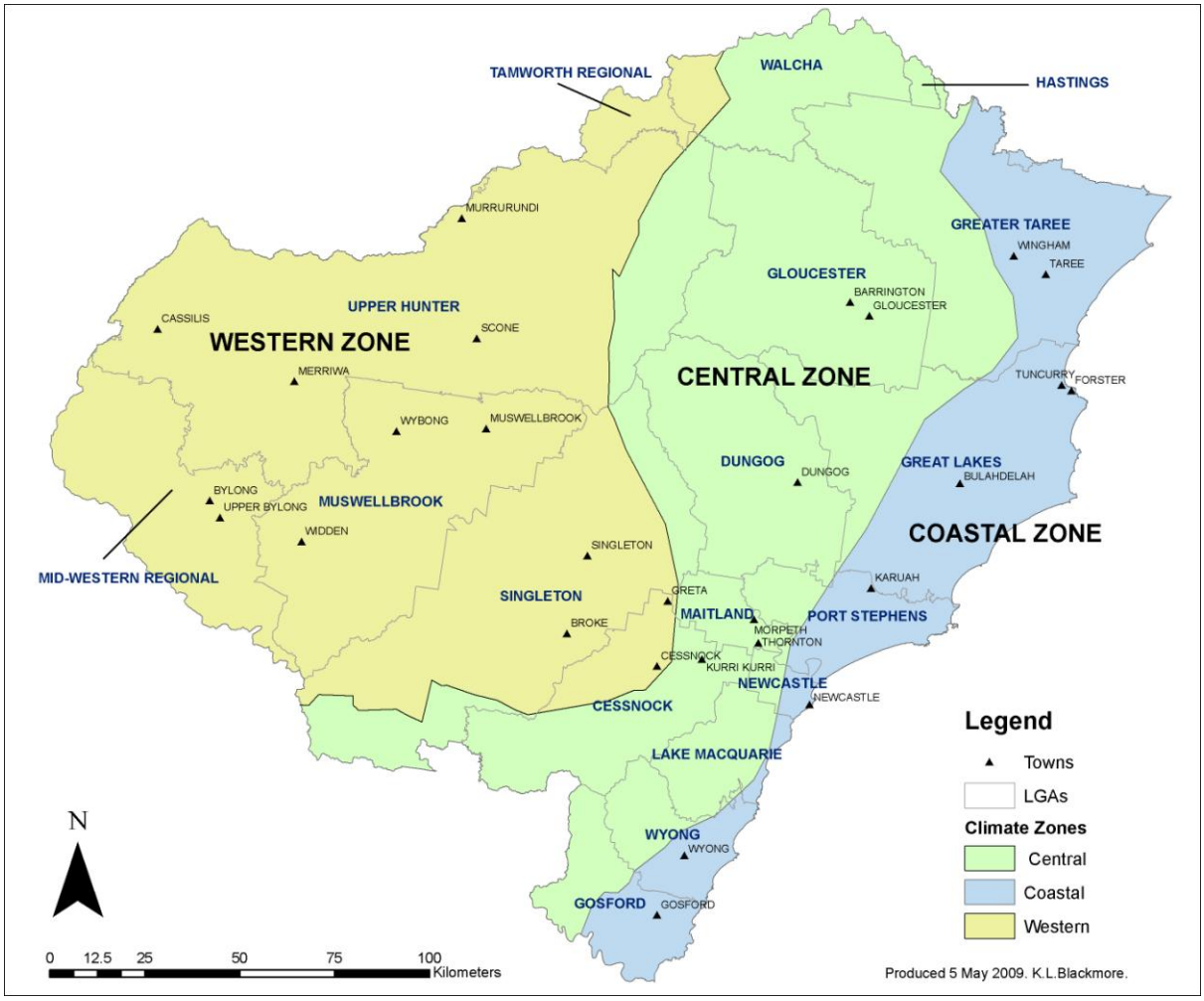


Figure 18 - The region's three climate zones identified in Stage 2 of the project

# 3 Analysis of the Matching of Sea-Level Pressure Synoptic Types using CSIRO Mk 3.5 and NNR for 1968-1996 calibration

The CSIRO Mk 3.5 global climate model (GCM) is selected to analyse projected climate change to 2100AD in the Lower North Coast, Hunter and Central Coast region (see previous section for a comparative analysis of different climate models). Despite being the best performing GCM of the five models assessed, the statistical match between the Sea-Level Pressure (SLP) STs generated from the CSIRO data and those derived from the NCEP/NCAR reanalysis data (NNR) for the calibration period (1968-1996) is low. Thus a more detailed analysis of the NNR and CSIRO STs is conducted to better understand the differences in characterizing the mean monthly atmospheric circulation. This analysis involves comparing the STs derived from the two different data sets to quantify the differences between the STs. The basic assumption here is that although the STs derived from the CSIRO GCM data may not statistically match the NNR STs, the CSIRO STs may still be capturing the essential synoptic patterns that drive climate variability in the region and are thus useful for analysing projected changes.

As a first step, each of the STs were compared and a difference map, obtained by subtracting the grid values of the NNR ST from the corresponding CSIRO ST, was derived (Figure 19). As part of this process, it was determined that NNR ST 9 did not have a corresponding CSIRO type and similarly, CSIRO ST 12 did not have a corresponding NNR type. Thus no difference maps are constructed for these types. The issue of these non matching types is further discussed in the following section.

The difference maps produced show seasonal trends. CSIRO STs 1 thru 6 (excluding 5) over-estimate low SLP anomalies in the circumpolar trough and some portions of the subtropical high over continental Australia. This is particularly evident for STs 1, 2 and 3; the dominant winter types. With the exclusion of NNR ST 9, CSIRO types 7 thru 11 over-estimate high SLP ridging anomalies over the Southern Ocean. CSIRO ST 7 also under-estimates the low pressure trough over inland Australia.

**COMPARISON OF NNR AND CSIRO STs**

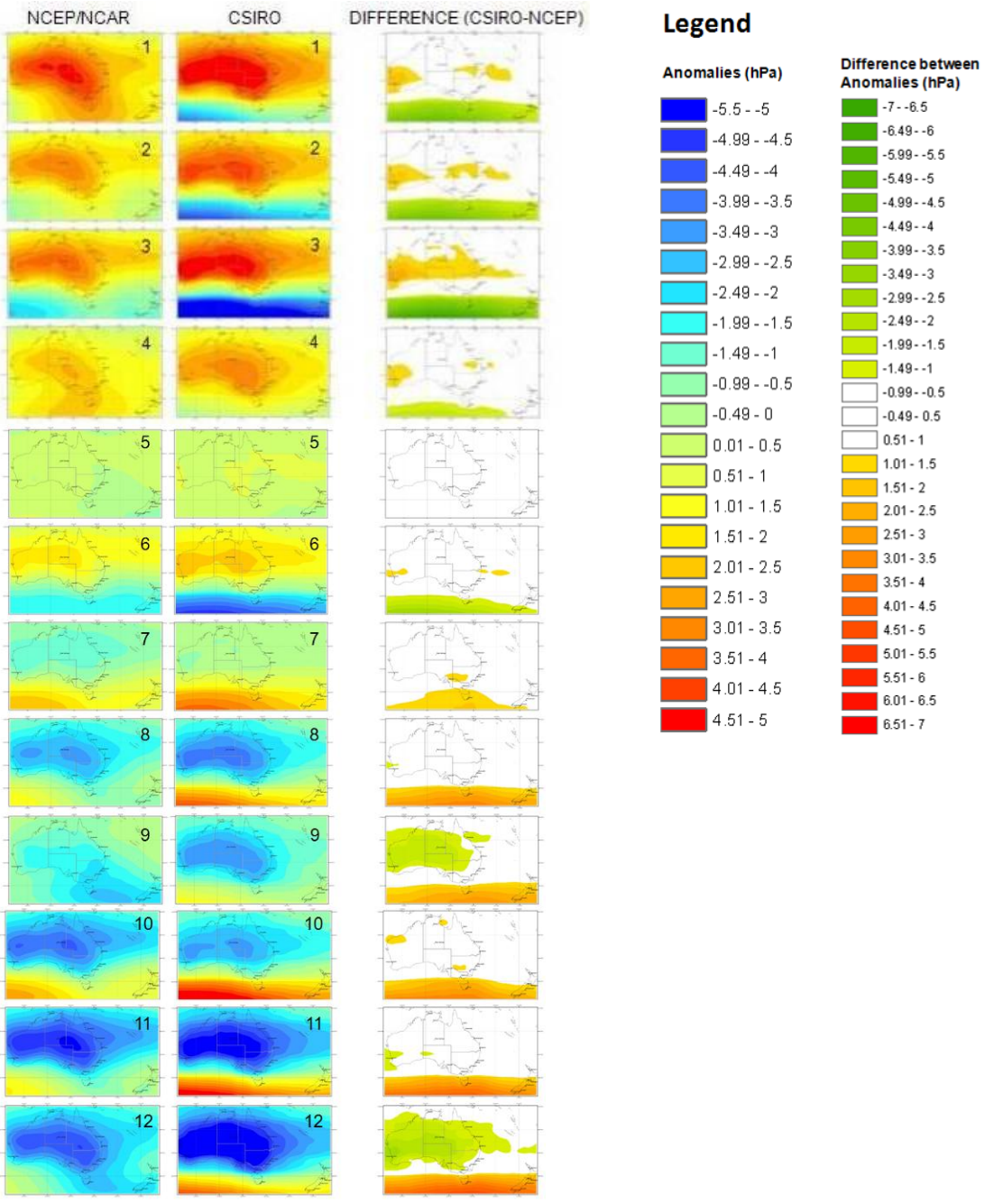


Figure 19 - Comparison of NNR and CSIRO anomaly STs including corresponding difference maps

Clearly the differences between STs varies, with some types exhibiting greater differences than others. STs 9 and 12 are poorly matched and the difference maps would suggest that these STs derived from the NNR data are not reproduced by the CSIRO GCM output. Further analysis of these differences is conducted using key climate variables for the region. The major limitation in the modeled SLP STs is the over estimation of the zonal pressure gradient, and the inability for the model to capture the characteristic meridional or longwave ridge and trough circulation, particularly over south-eastern Australia.

However, these shortcomings in the model simulated STs have minimal influence on the SLP field over the study region. In fact, the difference between the NNR and CSIRO SLP anomalies is less than plus or minus one hectopascal (hPa) for all twelve (12) STs. This contrasts to the differences between the NNR and MRI STs and the NNR and CSIRO/MRI ensemble STs (Appendix C). In both instances only four STs have differences of less than 1 hPa over the study region. Given the subtle differences in types over the study region, the use of seasonal frequency shifts in the ST's at the 2030, 2050 and 2070 time horizons for the determination of seasonal temperature and precipitation changes for the study region is valid for statistical downscaling.

## 3.1 Analysis of Key Climate Variables by Synoptic Type

In order to further assess the alignment between the STs derived from the NNR data and the CSIRO GCM data, precipitation, minimum and maximum temperature were analysed according to the ST allocated for each month in the time series (January 1948 to December 2007). The process used is shown in Figure 20. Average monthly values, derived from the frequency of occurrence of STs for each season, are compared against actual values for key climate variables. This process is repeated for each of the three climate zones in the region.

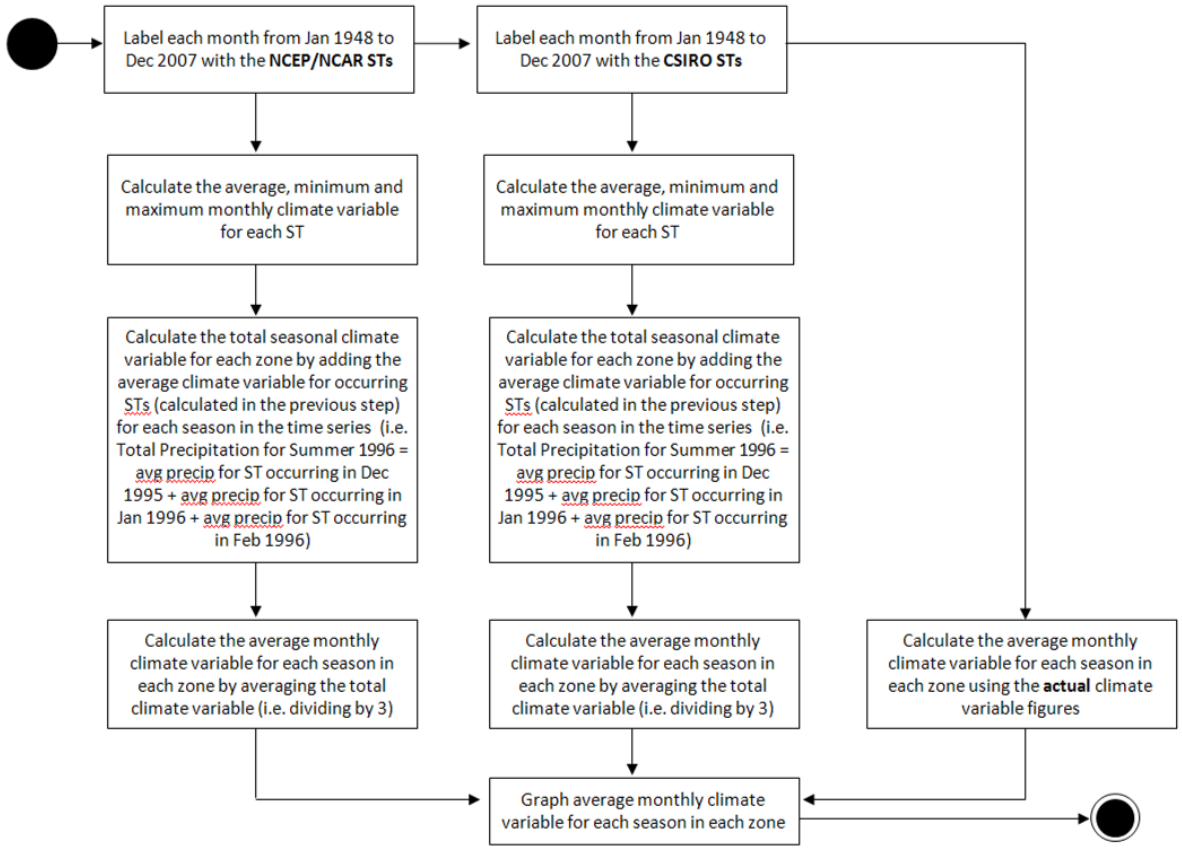


Figure 20 - Process for analysing key climate variables by synoptic type

The output from the process of comparing STs by key climate variables is a series of graphs (Figure 21 and Figure 22). Figure 22 represents the output from the 2nd step of the process and compares the average monthly precipitation, minimum and maximum temperature by NNR and CSIRO ST. Both models show similar average monthly precipitation for STs 1,2 and 8. STs 7 and 12 are generally least consistent for this climate variable. Minimum temperature is relatively well matched by ST for the two data sets. Despite slight discrepancies, the graph profiles are the same. This also applies to maximum temperature, with both the NNR and CSIRO STs recording very similar averages. Results do not appear to differ significantly according to zone.


Figure 21 - Average monthly precipitation, minimum temperature and maximum temperature for each ST by zone

Results for monthly averages by season as predicted by NNR and CSIRO STs perform well against actual seasonal monthly averages (Figure 22). Zonal differences do appear to impact on results for precipitation. In the coastal zone (1), both data sets achieve results similar to actual in summer and autumn. However during winter and spring, the NNR and CSIRO model over-estimate average monthly precipitation (based on comparison to actual precipitation records). This over-estimation is most pronounced for the CSIRO model. The over-estimation is seasonally reversed in Zone 3 where the NNR and CSIRO model over-estimation summer and autumn precipitation.

Average minimum temperatures are over-estimated by NNR and CSIRO during winter, regardless of zone. The STs for the datasets perform well at predicting average minimum temperatures for spring, and the CSIRO model results for summer align closely to actual values in summer. In autumn, the CSIRO model over-estimates actual values, whereas the STs for the NNR data only slightly under-estimate actual values. This pattern of over and under estimation is repeated for maximum temperatures.

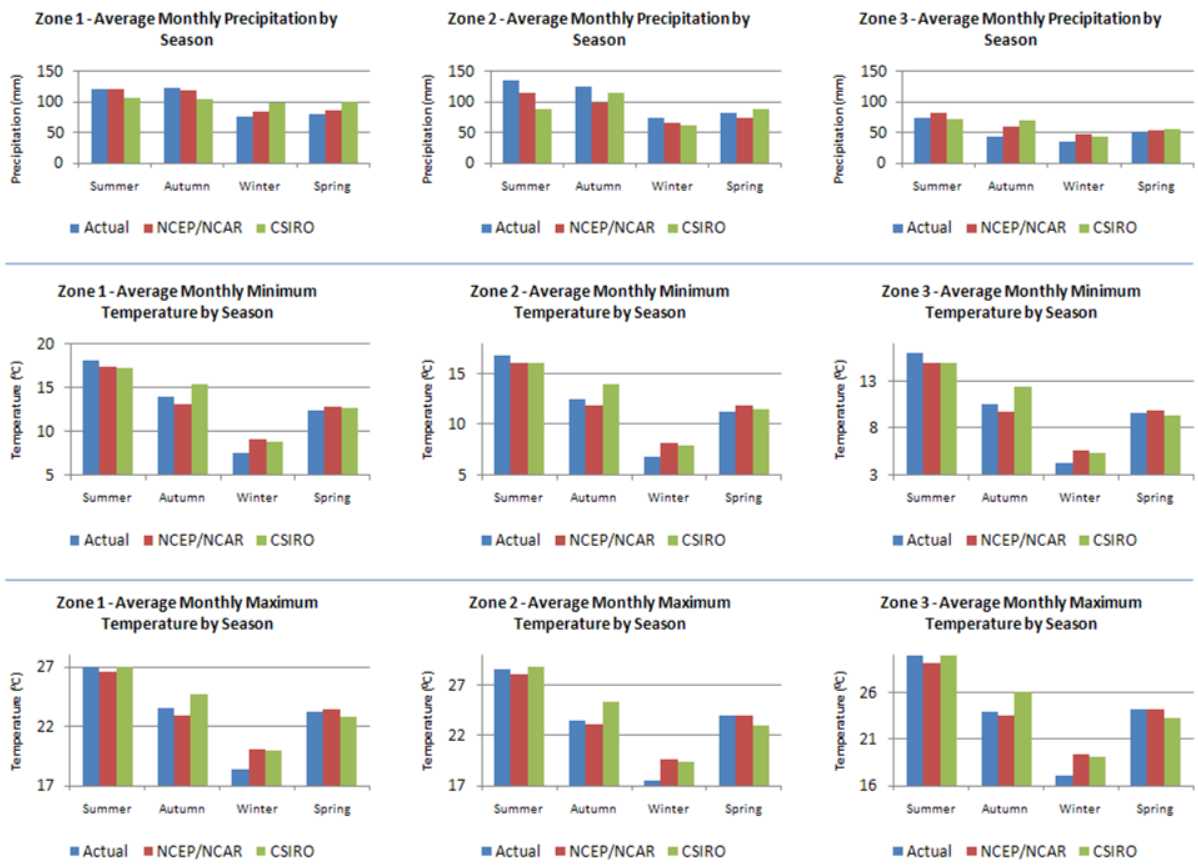


Figure 22 - Seasonal performance of NNR and CSIRO STs by actual records for key climate variables

# 4 Projected Climatic Change Impacts for the Hunter, Lower North Coast and Central Coast Region of NSW

Synoptic patterns are key drivers of regional climate. Understanding how mean synoptic patterns that influence key climate variables in the region are likely to change in the future provides insights into projected climatic change impacts. For example, if the frequency of occurrence of a synoptic pattern associated with high precipitation events in the region is projected to increase during future time horizons, the inference is that more high precipitation events will be observed. The following sections describe the CSIRO Mk3.5 GCM STs and associated weather patterns and discuss projected changes in key climate variables across the region.

## 4.1 Circulation Patterns and Weather Patterns

The 12 STs identified from the NNR data capture a range of significant large-scale synoptic features that are known to influence the weather of the region, including the clear seasonal trend in the location and intensity of the subtropical anticyclone, the monsoonal trough, the circumpolar trough, and the longwave trough and ridge features in the Pacific and Indian Ocean sectors (Appendix A). These monthly STs represent an average of the synoptic weather system occurrence at the daily time scale, including: cold frontal systems, simple and complex cold fronts, frontal waves, Southern Tasman Lows and cold-cored cut-off lows from the westerly airstream; the northern Australian monsoonal trough; warm-cored cyclones such as East Coast Lows and Easterly Dips; and, anticyclonic intensification over south-east Australia and blocking anticyclones over the Tasman Sea and New Zealand region (Sturman and Tapper, 2006).

The most frequent seasonal ST's that account for ~20 % of frequency are: ST 10, 11 and 12 in summer; ST 1, 4 and ST 6 in autumn; ST 1 and 3 in winter; and ST 6 and ST 9 in spring. The individual ST's represent the dominant large scale circulation for each month in the record, and many of the ST's can be associated with frequent occurrence or persistence of synoptic weather conditions. Synoptic weather systems and their associated ST's are listed in Table 13 below.

| SYNOPTIC WEATHER SYSTEM | SYNOPTIC CLIMATE TYPE |
|---|---|
| Southern Tasman Sea Lows | ST's 2 (eastern Tasman Sea), 3, 5, 6, 9 |
| Frontal waves in the Southern Tasman Sea | ST's 3, 6, 12 |
| Cut-off or Southern Secondary Low (central to southern Tasman Sea) | ST's 1, 2 |
| Blocking Highs over Tasman and New Zealand | ST's 7, 8, 10, 11 |
| Northern Australia or Monsoon Trough | ST's 7, 8, 10, 11, 12 |
| SE Australia Longwave Ridge | ST 1, 2, 4, 7 |
| SE Australia Longwave Trough | ST 8, 9, 11, 12 |
| Easterly Dips | ST's 7, 8, 10, 11 |
| East Coast Lows | ST 1 |
| Anticyclone intensification | ST's 1, 2, 3 |

Table 13 - Synoptic weather systems and their associated synoptic types

## 4.2 Projected Differences in the Frequency of Occurrence of Synoptic Types

The projected differences in the seasonal frequency of occurrence of STs derived from the CSIRO Mk3.5 GCM data are shown in Figure 23. Projected differences are shown for the 2020-2040, 2040-2060 and 2060-2080 time horizons. Significant differences are evident, particularly during autumn and winter. An approximate 10% decrease in the frequency of occurrence of ST10 with respect to the 1968-1996 calibration period is anticipated in Autumn. During winter, an approximate 15% increase in ST1 and 10% decrease in ST3 are projected.

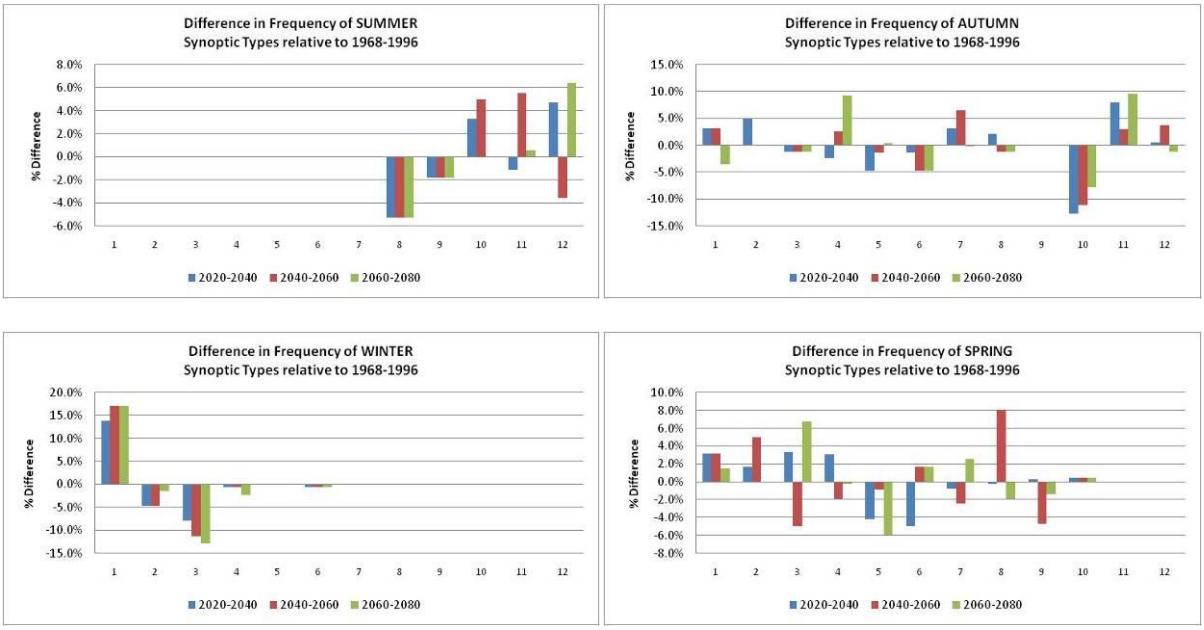


Figure 23 - Seasonal differences in the frequency of STs for projected time horizons relative to 1968-1996

Understanding the impact of these shifting synoptic patterns involves relating the STs to regional or station level measurements of key climate variables. This process is known as statistical downscaling (see Section 2). The following sections present the results of the statistical downscaling process for the key climate variables of precipitation, temperature (minimum and maximum), humidity, pan evaporation, and wind (gusts and average). Sea surface temperature (SST), sea-level rise (SLR) and extreme sea levels (ESL) are also considered. The downscaling process also accounts for interdecadal variability.

Interdecadal variability within the Australasian and South West Pacific regions is associated with the Interdecadal Pacific Oscillation (IPO). During the time period from 1948 to 2007 there have been two phases of this oscillation: IPO –ve phase (La Nina-like) from 1948 to 1976; and, IPO +ve phase (El Nino-like) from 1977 to 2007. To investigate the climate variability of the region, the ST time series was stratified according to these two time

periods. For purposes of comparison, the frequency of ST's for: (i) all years, 1948 to 2007; (ii) 1948 to 1976; and, (iii) 1977 to 2007 will be used for comparison of projected data to historic data.

## 4.3 Precipitation

An understanding of future changes can be obtained by contrasting projected values to those recorded historically. Figure 24 shows projected seasonal average precipitation for the 2020-2040, 2040-2060 and 2060-2080 time horizons together with average recorded values for the 1948-1976 and 1977-2007 time periods for each of the region's three climatic zones.

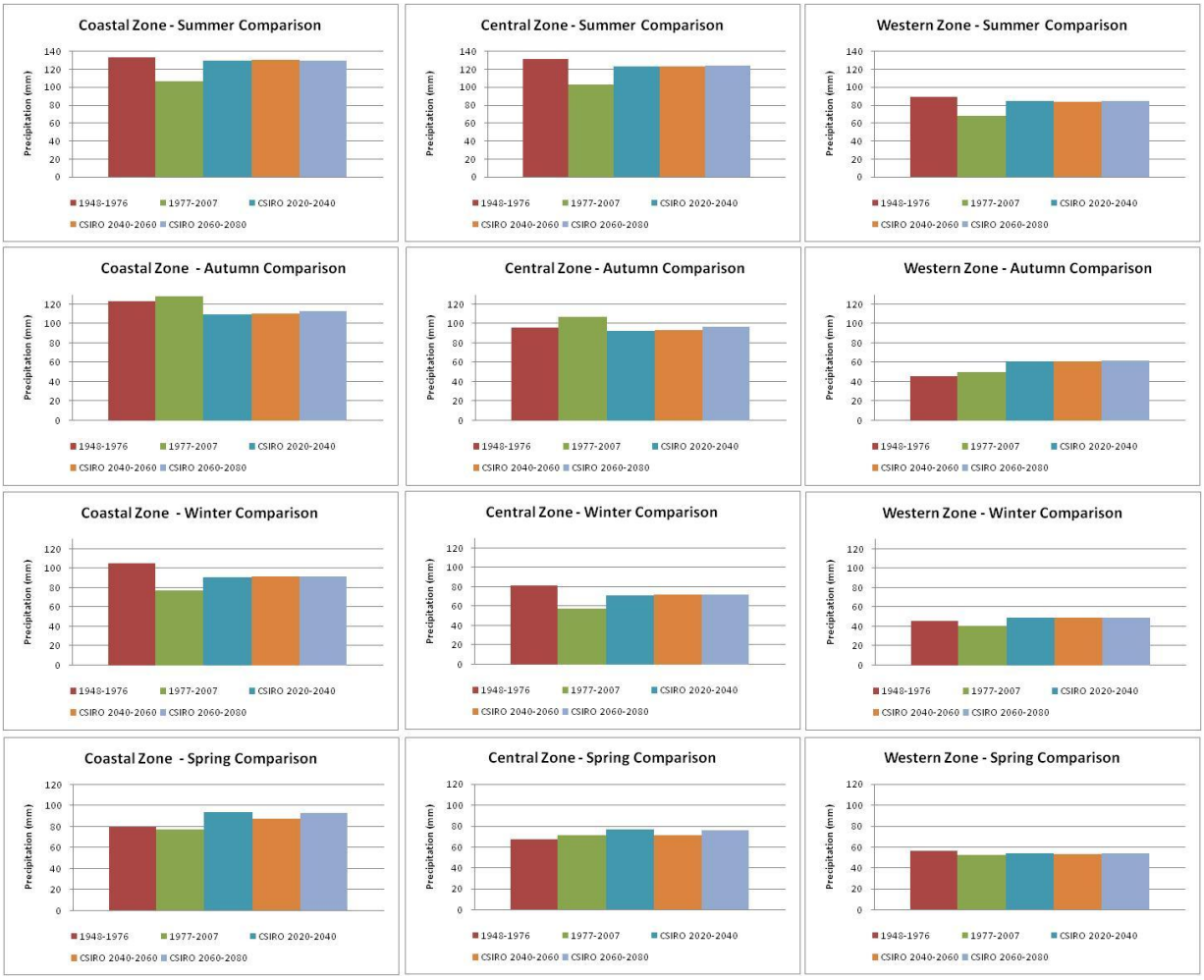


Figure 24 - Seasonal comparison of precipitation for historic interdecal time periods and future time horizons

Little variation in projected values is evident over the three projected time horizons (i.e. 2020-2040, 2040-2060 and 2060-2080 projections are all similar). Projections for summer show an increase in precipitation on the 1977-2007 seasonal average in all climatic zones in the region. The projected change in this season shows a future pattern similar to that recorded in the 1948-1976 interdecadal shift. Similar results are shown for winter, with an increase in precipitation more in line with the actual records for the 1948-1976 time period. Decreases in precipitation are projected for autumn in the coastal and central zones, with a slight increase shown for the western zone. An increase in spring precipitation is projected in the coastal zone only; a negligible increase is shown for the central zone with little or no change projected in the region's western zone.

Estimates of the magnitude of seasonal shifts, relative to the interdecadal periods, are presented in Figure 25 and Table 14. Seasonal averages for the interdecadal periods (1948-1976 and 1977-2007) are calculated from BOM data and compared with projected seasonal averages calculated from the CSIRO Mk3.5 STs for the period from 2020 to 2080 (CSIRO ALL). This time period is used for the projected data (rather than the three individual time horizons) as previous analysis shows little variation between the projected periods.

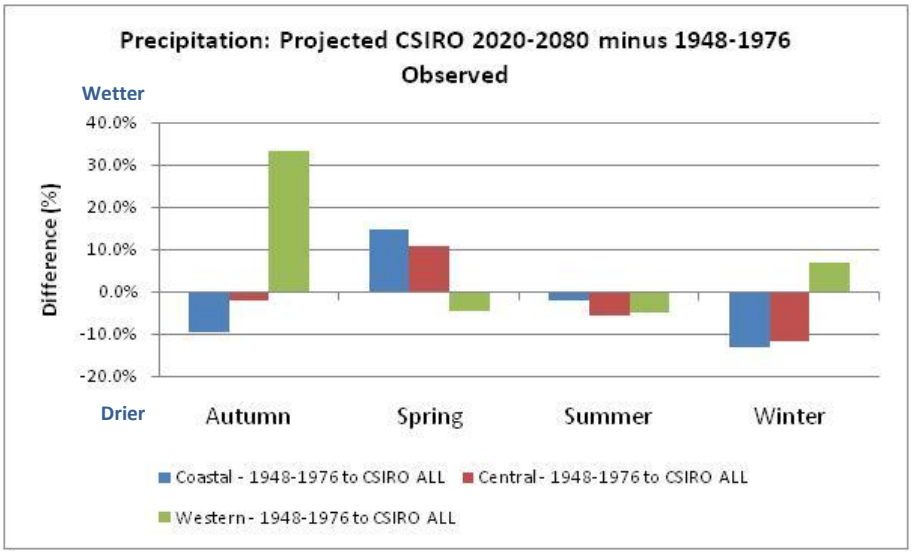


Figure 25 - Estimates of projected precipitation shifts relative to the interdecadal periods

| Season | Zone | Observed 1948-1976 | Projected Change (2020-2080) Relative to 1948-1976 (mm) | Projected Change (2020-2080) Relative to 1948-1976 (%) | Observed 1977-2007 | Projected Change (2020-2080) Relative to 1977-2007 (mm) | Projected Change (2020-2080) Relative to 1977-2007 (%) |
|---|---|---|---|---|---|---|---|
| Summer | Coastal (1) | 134 | -3 | -2% | 107 | 24 | 22% |
| | Central (2) | 132 | -7 | -6% | 103 | 21 | 20% |
| | Western (3) | 89 | -4 | -5% | 68 | 17 | 25% |
| Autumn | Coastal (1) | 123 | -12 | -9% | 129 | -17 | -14% |
| | Central (2) | 96 | -2 | -2% | 107 | -13 | -12% |
| | **Western (3)** | **46** | **15** | **33%** | 50 | 11 | 22% |
| Winter | **Coastal (1)** | **106** | **-14** | **-13%** | 77 | 15 | 19% |
| | **Central (2)** | **81** | **-10** | **-12%** | 58 | 14 | 24% |
| | Western (3) | 46 | 3 | 7% | 41 | 8 | 20% |
| Spring | **Coastal (1)** | **80** | **12** | **15%** | 78 | 14 | 18% |
| | **Central (2)** | **67** | **7** | **11%** | 71 | 4 | 5% |
| | Western (3) | 56 | -3 | -5% | 52 | 1 | 2% |

Table 14 - Projected changes in total precipitation relative to IPO periods

Projected precipitation in summer and winter is similar to that recorded during the 1948-1976 time period (i.e. the differences are smaller). This time period relates to a –ve phase (La Nina-like) of the Interdecadal Pacific Oscillation (IPO). Historic records indicate that summer and winter precipitation in the region was higher during this time period than that recorded during the following +ve phase (i.e. El Nino-like for 1977-2007). Summer estimates are for precipitation ~5% (3-7mm) less than that recorded for the 1948-1976 historic period. Winter projection estimates range between 13% less and 7% more (-14mm to +3mm) precipitation than that recorded in during 1948-1976. The western zone is projected to become wetter whereas the coastal region will receive less rainfall during winter.

Similar levels of autumn precipitation were recorded in the two IPO periods (see Table 14). Projections for 2020-2080 for the coastal and central zones are for between a 2% - 14% (2mm to 17mm) reduction in precipitation. An increase is projected in the western zone of between 22% and 33% (11-15mm). Spring also recorded similar levels of precipitation over the two IPO periods. Projected estimates for region are for 15%-18% increase (12mm to 14mm) in the coastal zone and a 5%-11% increase (4mm to 7mm) in the central zone. Little or no change is projected for the western zone.

The twenty year time periods analysed for each of the projected time horizons do not provide a sufficient length of record for the testing of the statistical significance of linear trends (due to the variability in the data). As such, changes in precipitation for the projected period from 2020 to 2080 are considered (Figure 26). In addition to showing linear trends (green line), total annual precipitation for the calibration period (1968-1996) is superimposed onto the projected data.

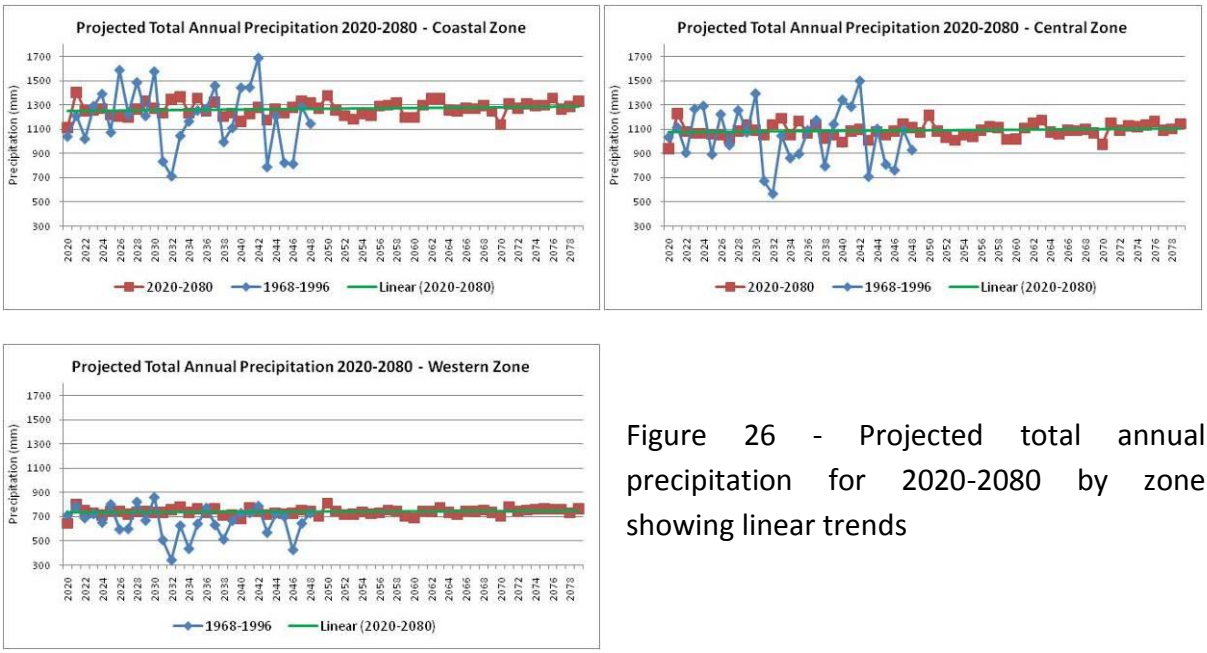


Figure 26 - Projected total annual precipitation for 2020-2080 by zone showing linear trends

Projected data for the coastal and central zones lies well within the bounds of natural variability recorded during the calibration period. Projections for the western zone, although still within the bounds of natural variability, show a tendency toward the upper bound. The statistical significance of the linear trends for precipitation for the 2020-2080 time period were tested using regression analysis. An increase of less than 50mm is projected for all three zones. Results from the regression analysis indicate that the increases are not statistically significant (i.e. $P>0.05$).

Projected changes in precipitation are ascertained using the STs derived from the CSIRO Mk3.5 GCM. Spatial precipitation patterns associated with the 12 CSIRO STs are shown in Figure 27. Coloured arrows indicate the dominant shift in the ST for the projected time period (2020-2080) relative to the calibration period (1968-1996). The highest levels of monthly precipitation in the region are produced by STs 8, 10, 11 and 12. These types are dominant during summer. ST10 produces primarily coastal precipitation. STs 3 and 9 are associated with low precipitation in the region. Seasonal differences in the frequency of these STs for the projected time horizons are evident (see Figure 23).

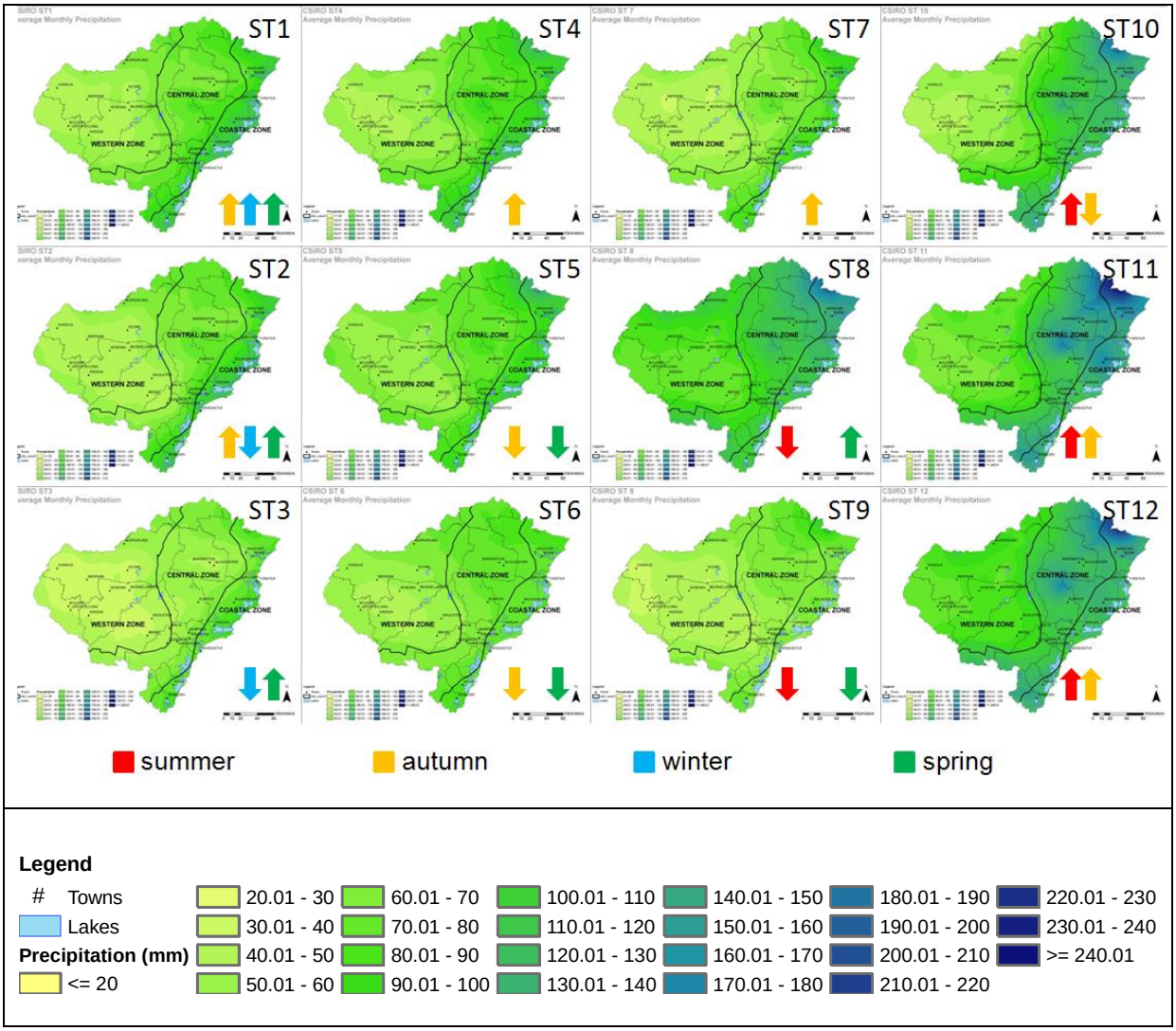


Figure 27 - Regional precipitation patterns for the period 1948 to 2007 derived from CSIRO STs

A decrease in ST10 in autumn of approximately 10% for each of the 2020-2040, 2040-2060 and 2060-2080 time horizons is likely to result in a decrease in autumn precipitation, particularly in the coastal region. A winter decrease in ST3 of approximately 10% and an increase in ST1 of approximately 15% should result in higher winter rainfall across the region. A decrease in ST8 during summer is offset by increases in STs 10 and 12. Generally, the projected changes in ST patterns balance out to produce little or no annual change in precipitation across the region. However, the seasonal changes will be important for a range of land use decision making and management.

## 4.4 Temperature

### 4.4.1 Minimum Temperature

Figure 28 shows projected seasonal average minimum temperature for the 2020-2040, 2040-2060 and 2060-2080 time horizons together with average recorded values for the 1970-2007 time periods for each of the region's three climatic zones.

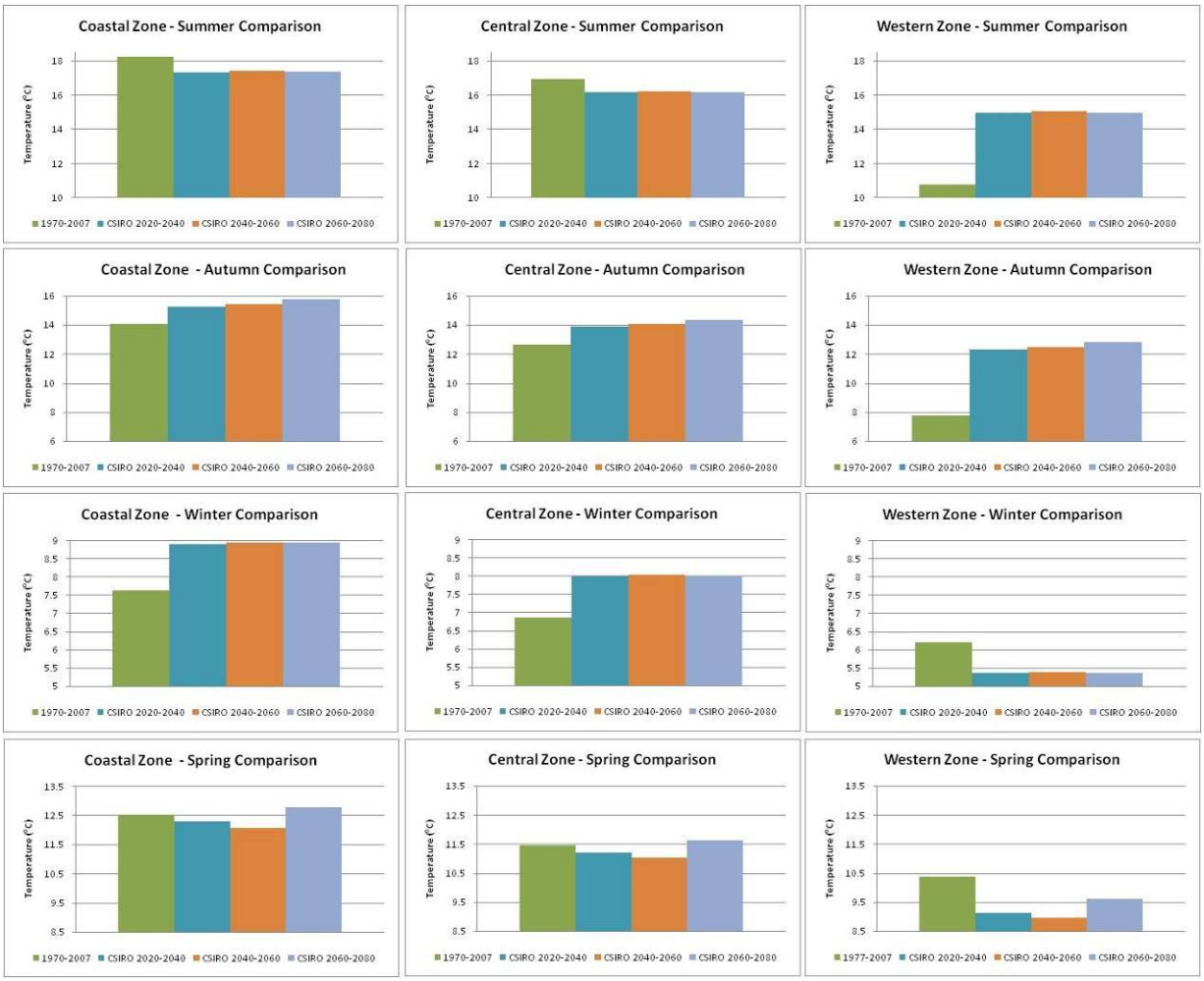


Figure 28 - Seasonal comparison of minimum temperature for the 1970-2009 time period and future time horizons

Little variation in projected values for summer and winter is evident over the three time horizons (i.e. 2020-2040, 2040-2060 and 2060-2080 projections are all similar). Projections for summer show a decrease in average minimum temperature for the coastal and central zones relative to the 1970-2007 time period. An increase is recorded for all time horizons in the western zone. Winter projections show increases in the coastal and central zones and a decrease in the western zone.

Projections for autumn show some variation across the three time horizons; a general increasing trend is evident. Increases are higher in the western zone. Projections for spring also show some variation for the three time horizons. A decrease is projected for the 2020-2040 time horizon (relative to the 1970-2007 time period) followed by a further decrease in 2040-2060. Projections for all zones show an increase in minimum temperatures, relative to the preceding time horizons, in the 2060-2080 period. Thus spring projections in the coastal and central zones show a decrease in minimum temperatures to 2060, at which point a shift to minimum temperatures similar to those experienced during the 1970-2007 time period are anticipated. A similar pattern is evident in the western zone, however decreases are greater and therefore anticipated increases during 2060-2080 fail to return minimum temperature to the levels experienced during the historic time period.

Estimates of the magnitude of seasonal shifts, relative to the 1970-2007 time period, are presented in Figure 25 and Table 14. Seasonal averages for the period from 1970-2007 are calculated from BOM data and compared with projected seasonal averages calculated from the CSIRO Mk3.5 STs for the period from 2020 to 2080 (CSIRO ALL). Note that these results should be considered in the context of the changes in the autumn and spring values for the projected time horizons discussed above. Additionally, consistent historic records are not available to cover the preceding two IPO phases (i.e. –ve La Nina–like for 1948-1976 and +ve phase El Nino-like for 1977-2007). Thus the time period from 1970-2007 covers a predominantly El Nino-like historic period.

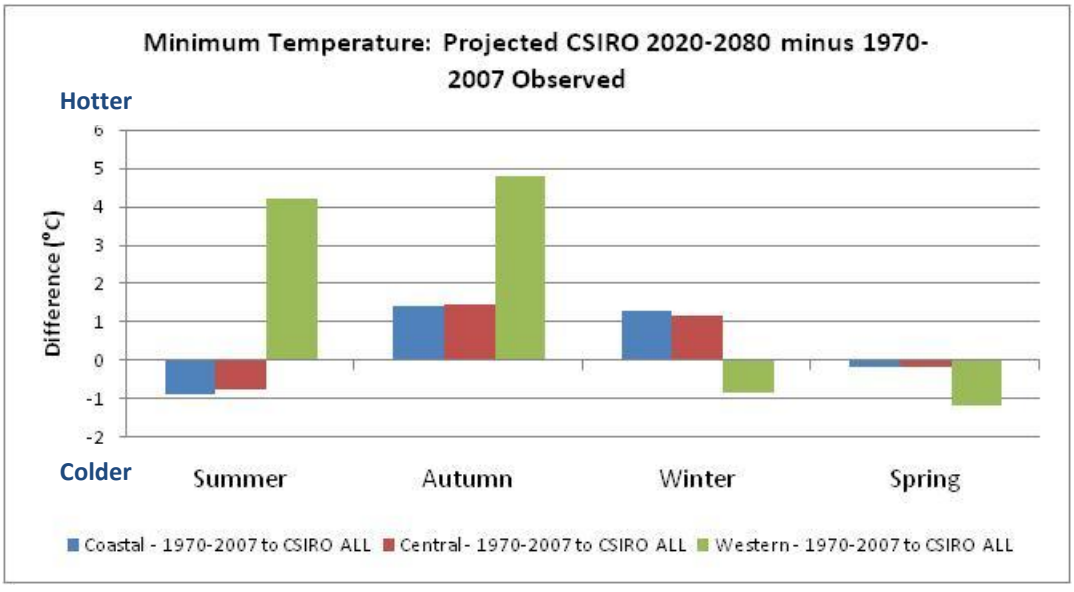


Figure 29 - Estimates of projected minimum temperature shifts (°C) relative to the 1970-2007 period

| Season | Zone | Observed 1970-2007 | Projected Change (2020-2080) Relative to 1970-2007 (°C) | Projected Change (2020-2080) Relative to 1970-2007 (%) |
|---|---|---|---|---|
| Summer | Coastal (1) | 18.2 | -0.9 | -4.7% |
| | Central (2) | 16.9 | -0.8 | -4.4% |
| | Western (3) | 10.8 | 4.2 | 39.1% |
| Autumn | Coastal (1) | 14.1 | 1.4 | 10.1% |
| | Central (2) | 12.7 | 1.5 | 11.5% |
| | Western (3) | 7.7 | 4.8 | 62.2% |
| Winter | Coastal (1) | 7.6 | 1.3 | 17.1% |
| | Central (2) | 6.9 | 1.2 | 16.7% |
| | Western (3) | 6.2 | -0.8 | -13.5% |
| Spring | Coastal (1) | 12.5 | -0.2 | -1.2% |
| | Central (2) | 11.5 | -0.2 | -1.6% |
| | Western (3) | 10.4 | -1.2 | -11.1% |

Table 15 - Projected changes in minimum temperature relative to the 1970-2007 period

Projections (2020-2080) in the coastal and central zones for summer are for decreases in average minimum temperature of ~0.8°C relative to the 1970-2007 period. A significant increase of ~4.2°C in average minimum temperature for summer is projected in the western zone. Increases in all three zones are projected for autumn; ~1.4°C in the coastal and central zones and again a significant ~4.8°C in the western zone. Winter projections are for warmer average minimum temperatures in the coastal and central zones (~1.3°C and ~1.2°C respectively) and lower temperatures in the western zone (~0.8°C). The study region is likely to experience lower average spring minimum temperatures with a decrease of ~0.2°C projected for the coastal and central zones, and ~1.2°C in the western zone.

Changes in average minimum temperature for the projected period from 2020 to 2080 are shown in Figure 30. In addition to showing linear trends (green line), average annual minimum temperature for the period from 1970-1996 is superimposed onto the projected data. Projected values for all zones show a propensity to extend beyond the bounds of natural variability experienced during the period from 1970-1996. Higher average annual minimum temperatures than those previously experienced are projected. Average minimum temperatures show an increasing trend over the period from 2020-2080. These trends are statistically significant at the 5% level ($P<0.05$).

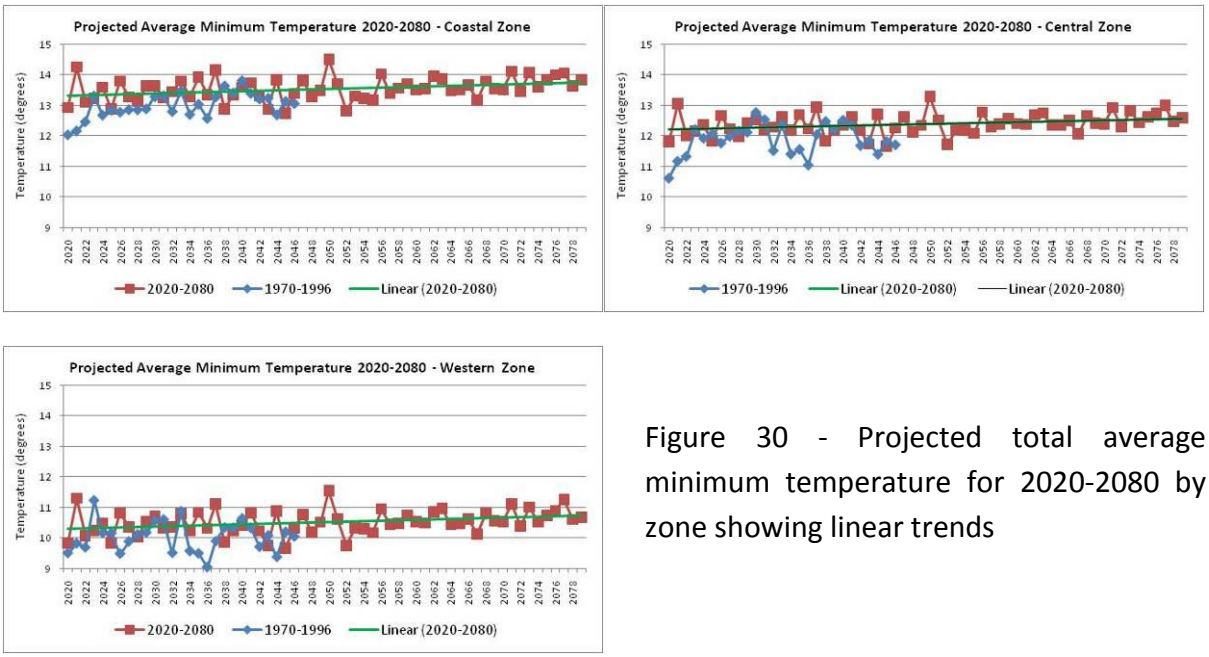


Figure 30 - Projected total average minimum temperature for 2020-2080 by zone showing linear trends

Spatial average annual minimum temperature patterns associated with each of the CSIRO STs are shown in Figure 31. Lowest average minimum temperatures in the region are produced by the dominant winter STs (1, 2 and 3). STs 4, 5, 6 and 7 produce warmer minimum temperature bands through the central parts of the region. STs 11 and 12 are dominant summer types and thus associated with the highest average minimum temperatures. Projected increases in the order of 5% for STs 10, 11 and 12 for the projected time horizons may result in higher minimum temperatures. An approximate 15% increase in the frequency of ST1 during winter is likely to produce colder winter average minimum temperatures with the possibility of increased frost incidence in the western parts of the region.

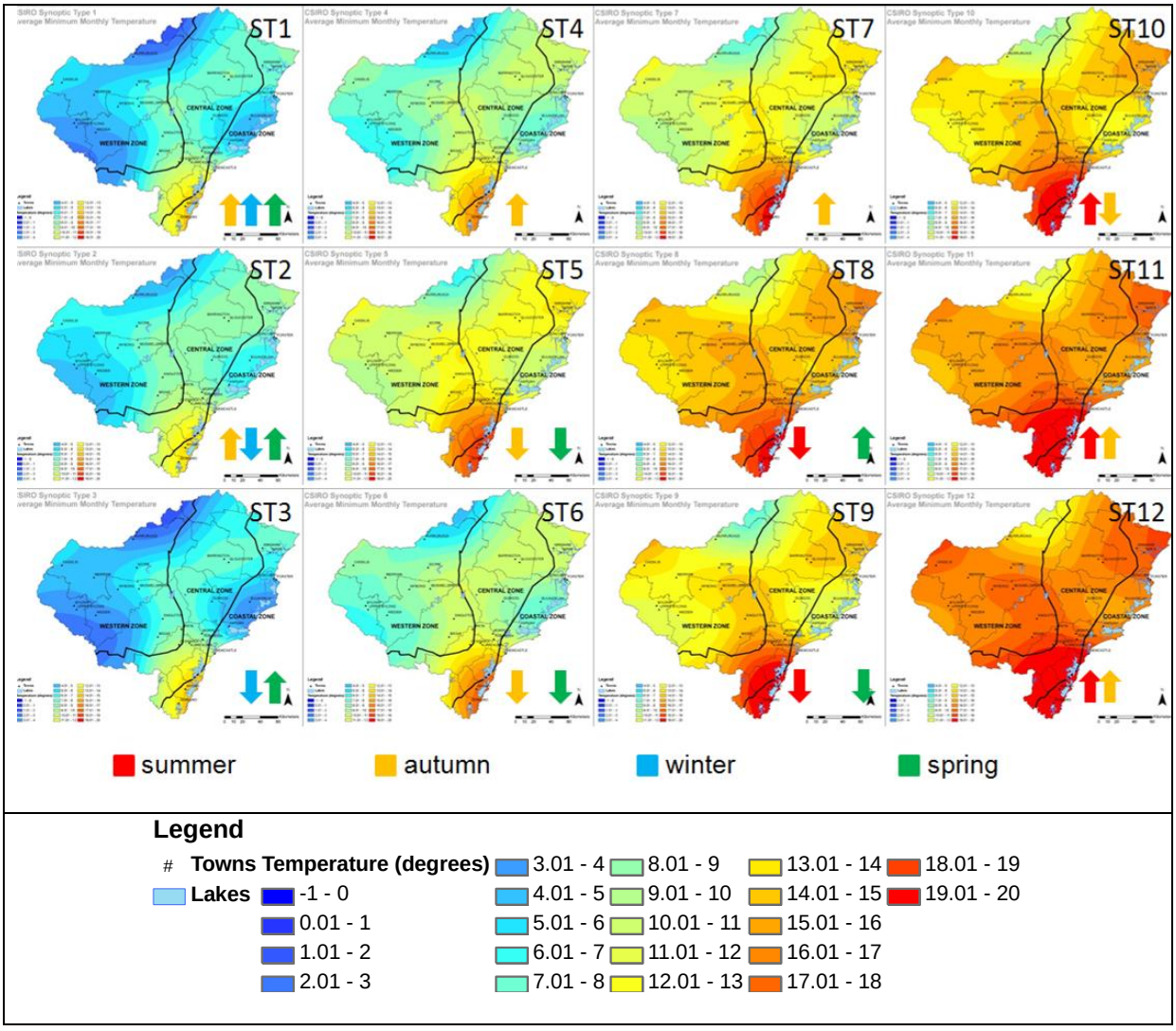


Figure 31 - Regional minimum temperature patterns for the period 1948 to 2007 derived from CSIRO STs with arrows indicating seasonal shifts.

### 4.4.2 Maximum Temperature

Figure 32 shows projected seasonal average maximum temperature for the 2020-2040, 2040-2060 and 2060-2080 time horizons together with average recorded values for the 1948-2007, 1948-1976 and 1977-2007 time periods for each of the region's three climatic zones.

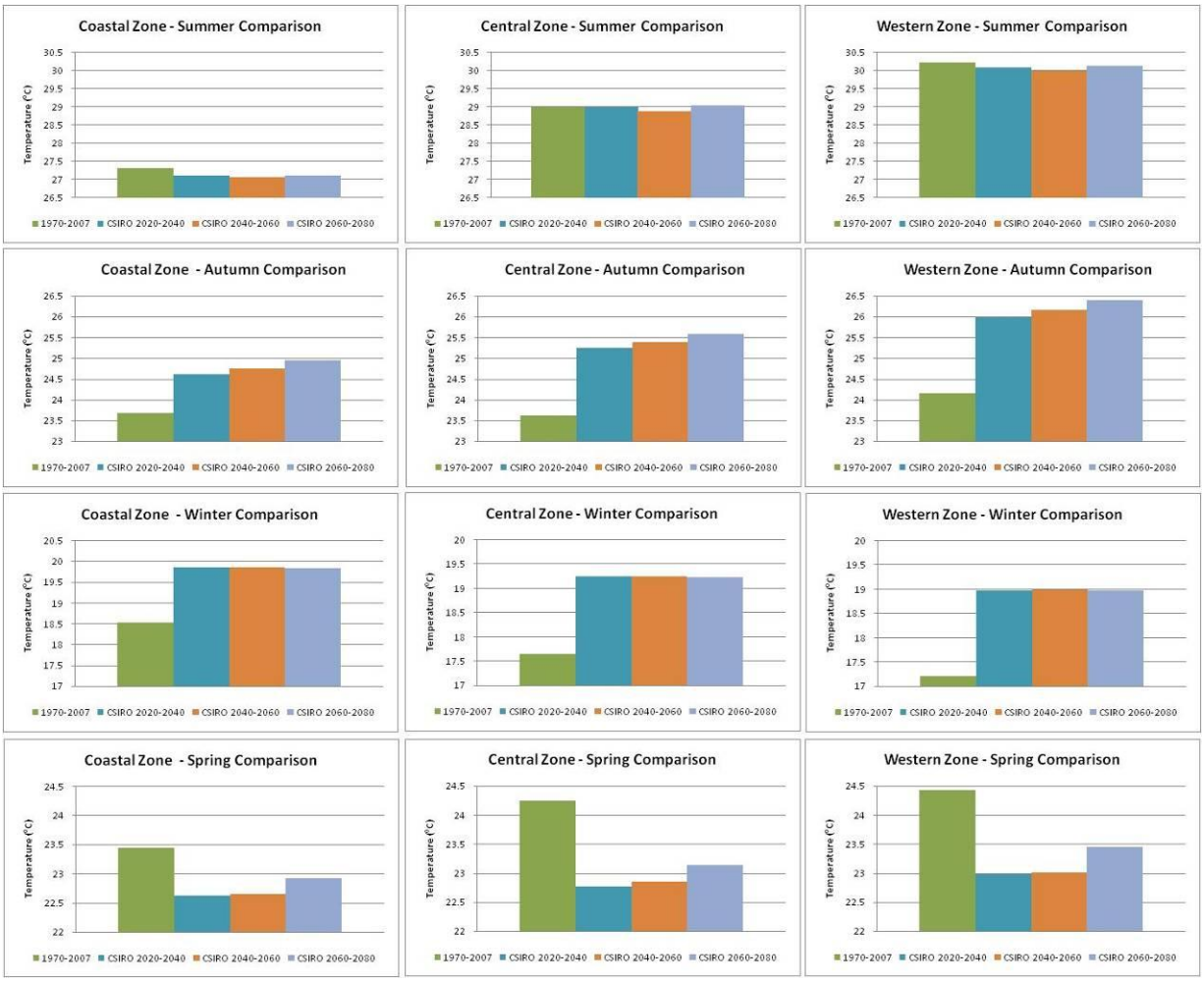


Figure 32 - Seasonal comparison of maximum temperature for the 1970-2007 time period and future time horizons

As with average minimum temperature, little variation in projected values for summer and winter is evident over the three time horizons (i.e. 2020-2040, 2040-2060 and 2060-2080 projections are all similar). Projections for summer show a decrease in average maximum temperature for the coastal zone relative to the 1970-2007 time period. Projections for the central and western zones show similar slight decreases. Winter projections show increases in the coastal, central and western zones.

Projections for autumn show increases in average maximum temperature with some variation across the three time horizons; a general increasing trend is evident. Projections for spring also show some variation for the three time horizons. A decrease is projected for the 2020-2040 time horizon (relative to the 1970-2007 time period) followed by increases (relative to the 2020-2040 time horizon) in the 2040-2060 and 2060-2080 time periods. Thus spring projections for all zones are for an initial decrease in average maximum temperature followed by moderate increases. These increases fail to return average maximum temperature to the levels experienced during the historic time period.

Estimates of the magnitude of seasonal shifts, relative to the 1970-2007 time period, are presented in Figure 33 and Table 16. Seasonal averages for the period from 1970-2007 are calculated from BOM data and compared with projected seasonal averages calculated from the CSIRO Mk3.5 STs for the period from 2020 to 2080 (CSIRO ALL). Note that these results should be considered in the context of the changes in the autumn and spring values for the projected time horizons discussed above.

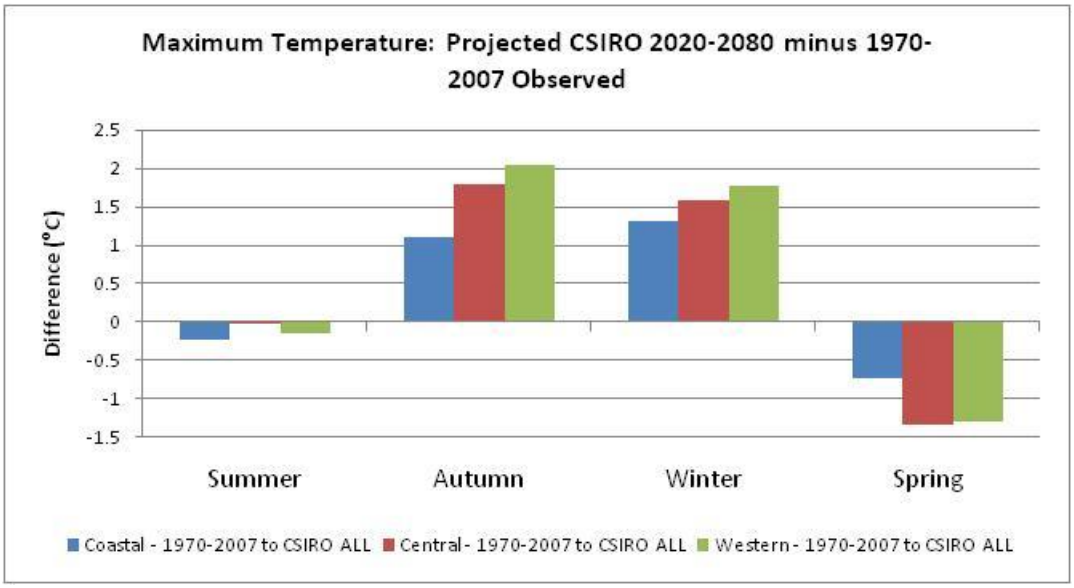


Figure 33 - Estimates of projected maximum temperature shifts (°C) relative to the 1970-2007 period

| Season | Zone | Observed 1970-2007 | Projected Change (2020-2080) Relative to 1970-2007 (°C) | Projected Change (2020-2080) Relative to 1970-2007 (%) |
|---|---|---|---|---|
| Summer | Coastal (1) | 27.3 | -0.2 | -0.8% |
| | Central (2) | 29.0 | 0.0 | 0.0% |
| | Western (3) | 30.2 | -0.2 | -0.5% |
| Autumn | Coastal (1) | 23.7 | 1.1 | 4.7% |
| | Central (2) | 23.6 | 1.8 | 7.6% |
| | Western (3) | 24.1 | 2.0 | 8.4% |
| Winter | Coastal (1) | 18.5 | 1.3 | 7.1% |
| | Central (2) | 17.7 | 1.6 | 9.0% |
| | Western (3) | 17.2 | 1.8 | 10.3% |
| Spring | Coastal (1) | 23.5 | -0.7 | -3.1% |
| | Central (2) | 24.2 | -1.3 | -5.5% |
| | Western (3) | 24.4 | -1.3 | -5.3% |

Table 16 - Projected changes in maximum temperature relative to the 1970-2007 period

Projections (2020-2080) in the coastal and western zones for summer are for decreases in average maximum temperature of ~0.2°C relative to the 1970-2007 period. No change for summer is projected in the central zone. Increases in all three zones are projected for autumn; ~1.2°C in the coastal zone, ~1.8°C in the central zone and ~2.0°C in the western zone. Winter projections are for warmer average maximum temperatures, ~1.3°C in the coastal zone, ~1.6°C in the central zone and ~1.8°C in the western zone. The study region is likely to experience lower spring average maximum temperatures with a decrease of ~0.7°C projected for the coastal zone, and ~1.3°C in the central and western zones.

Changes in average maximum temperature for the projected period from 2020 to 2080 are shown in Figure 34. In addition to showing linear trends (green line), average annual minimum temperature for the period from 1970-1996 is superimposed onto the projected data. Projected values for all zones show a propensity to extend beyond the bounds of natural variability experienced during the period from 1970-1996. Higher average annual maximum temperatures than those previously experienced are projected. Average maximum temperatures show an increasing trend over the period from 2020-2080. These trends are statistically significant at the 5% level ($P<0.05$).

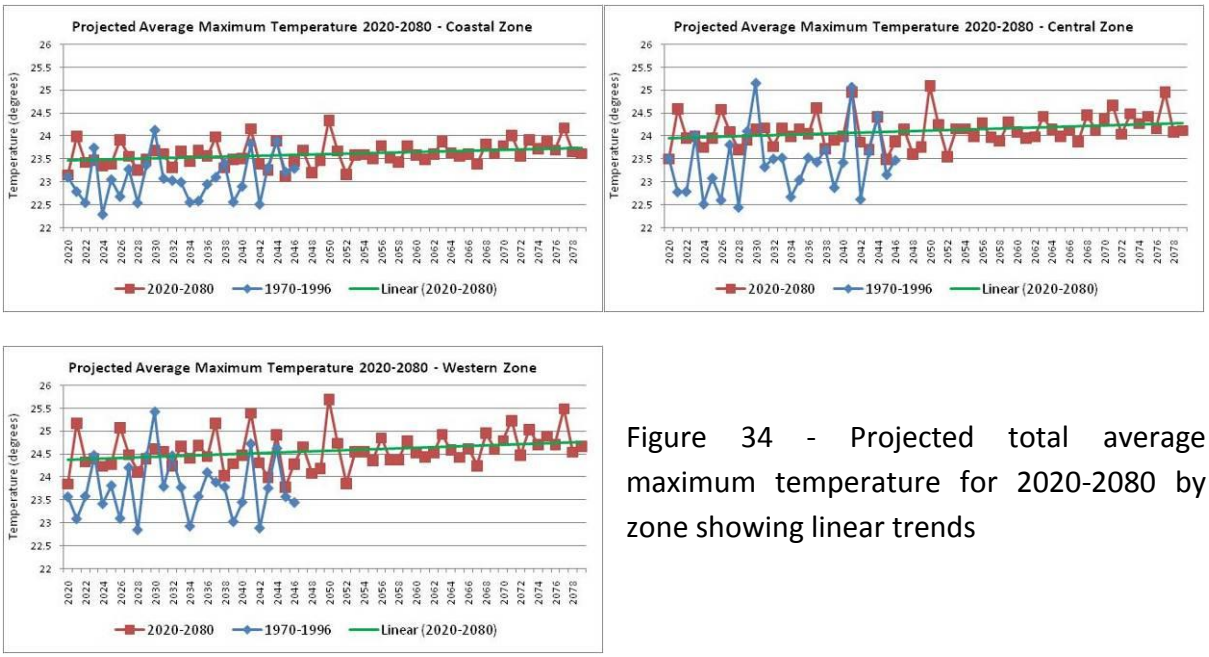


Figure 34 - Projected total average maximum temperature for 2020-2080 by zone showing linear trends

The spatial average annual maximum temperature patterns associated with each of the CSIRO STs closely follows the patterns produced for average minimum temperature (Figure 35). STs 11 and 12 are associated with the highest average maximum temperatures in the region. Projected increases in the frequency of occurrence of these STs for the projected time horizons, in both summer and autumn, are likely to produce warmer average annual temperatures in the region.

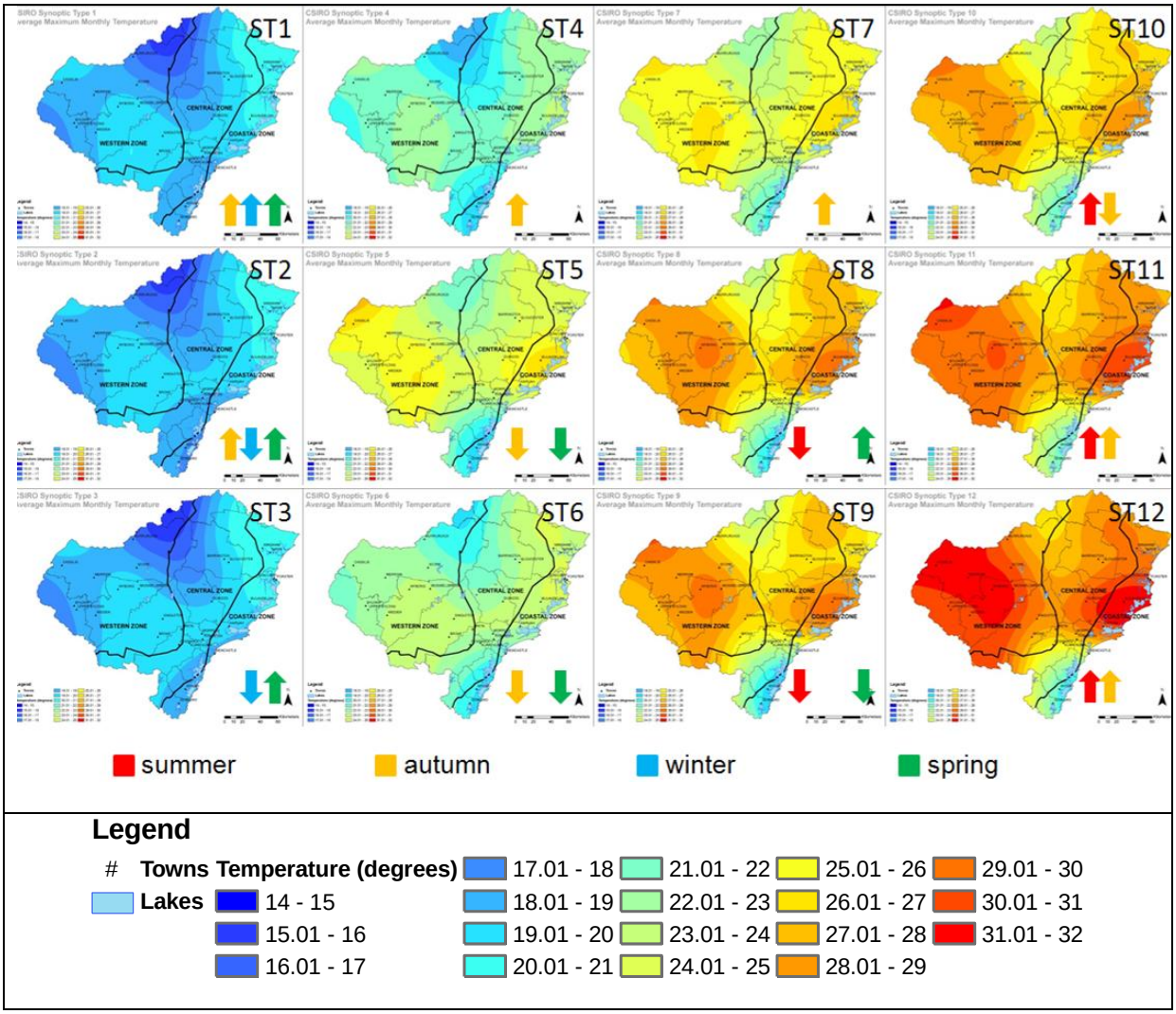


Figure 35 - Regional maximum temperature patterns for the period 1948 to 2007 derived from CSIRO STs with arrows indicating seasonal shifts.

### 4.4.3 Average Temperature and the Diurnal Cycle

Average temperature is calculated from the minimum and maximum temperature values (i.e. (minimum Temp + Maximum Temp) / 2). Figure 36 shows projected seasonal average maximum temperature for the 2020-2040, 2040-2060 and 2060-2080 time horizons together with average recorded values for the 1970-2007 time period for each of the regions three climatic zones.

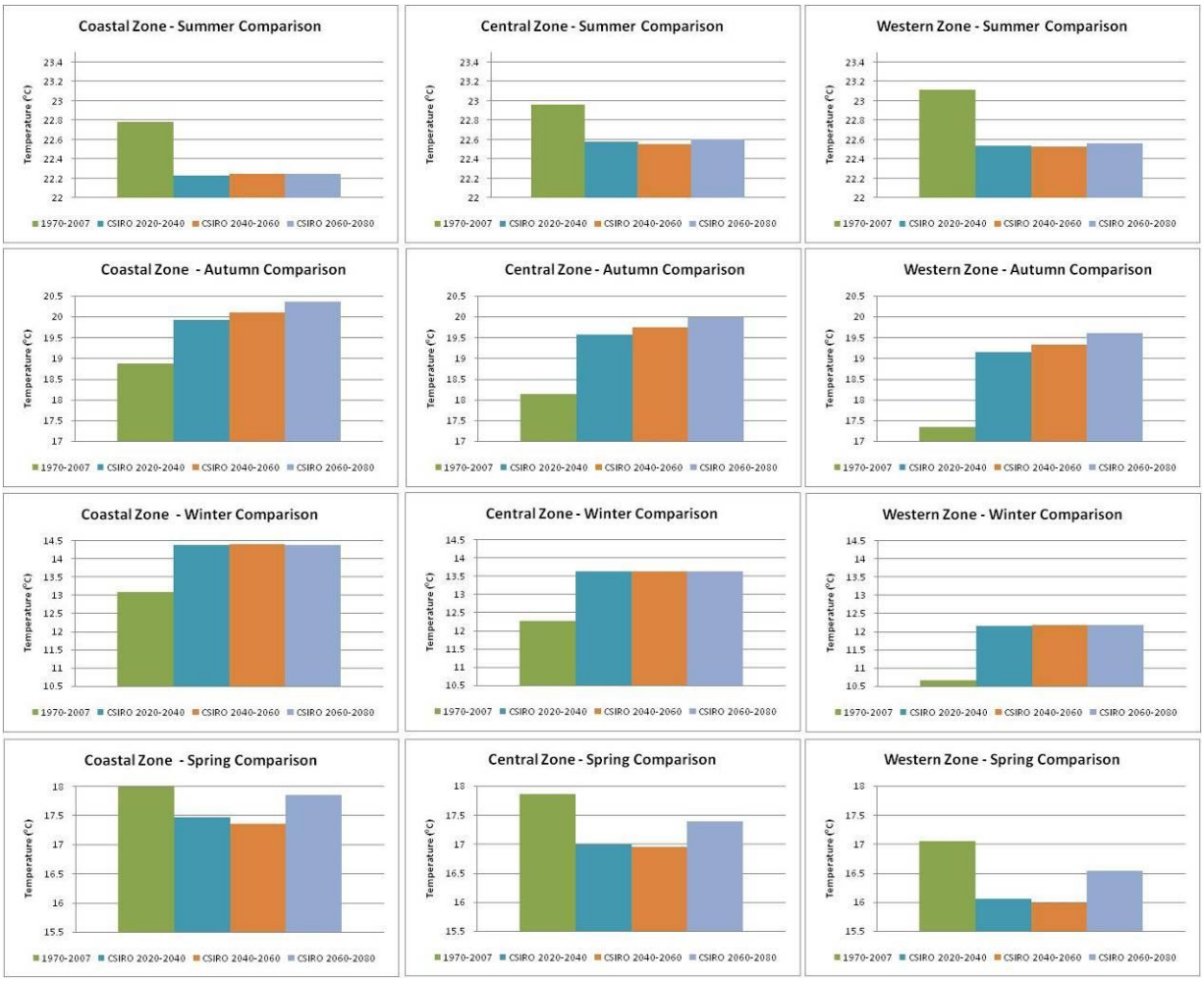


Figure 36 - Seasonal comparison of average temperature for the 1970-2007 time period and future time horizons

Generally, a decrease in average temperature is projected for the region. Following the average minimum and maximum temperature patterns, little variation in projected values for summer and winter is evident over the three time horizons (i.e. 2020-2040, 2040-2060 and 2060-2080 projections are all similar). Projections for summer show a decrease in average temperature for all three zones relative to the 1970-2007 time period. Winter projections show increases in the coastal, central and western zones.

Projections for autumn show increases in average temperature with some variation across the three time horizons; a general increasing trend is evident. Projections for spring also show some variation for the three time horizons. A decrease is projected for the 2020-2040 and 2040-2060 time horizons (relative to the 1970-2007 time period) followed by an increase (relative to the 2040-2060 time horizon) in the 2060-2080 time period. Thus spring projections for all zones are for initial decreases in average temperature followed by a moderate increase. This increase fails to return average temperature to the levels experienced during the historic time period thus an overall decrease in spring average temperature is projected.

Estimates of the magnitude of seasonal shifts, relative to the 1970-2007 time period, are presented in Figure 37 and Table 17. Seasonal averages for the period from 1970-2007 are calculated from BOM data and compared with projected seasonal averages calculated from the CSIRO Mk3.5 STs for the period from 2020 to 2080 (CSIRO ALL). Note that these results should be considered in the context of the changes in the autumn and spring values for the projected time horizons discussed above.

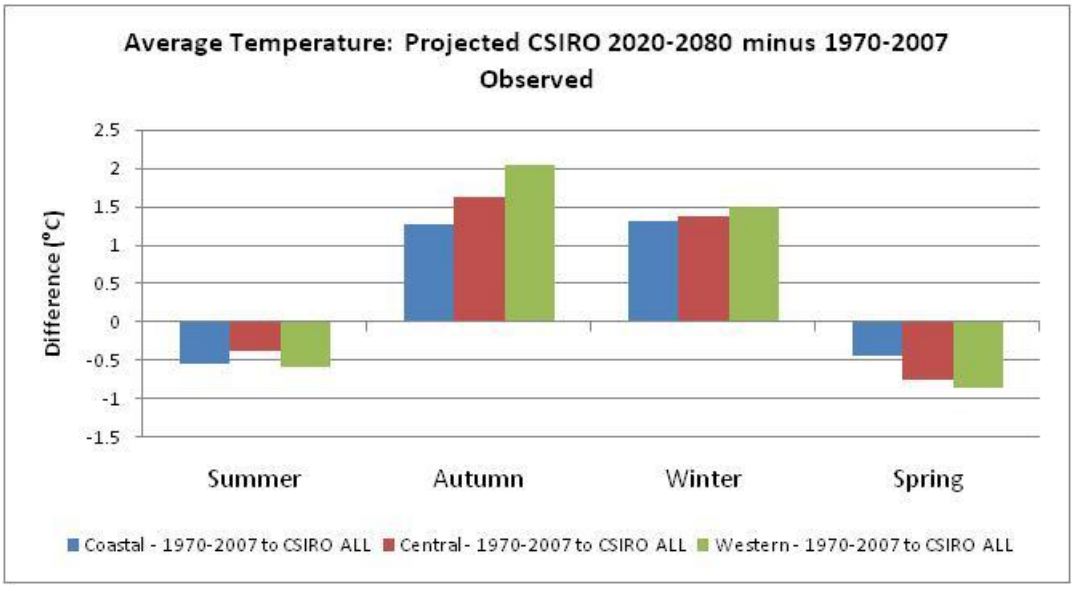


Figure 37 - Estimates of projected average temperature shifts (°C) relative to the 1970-2007 period

| Season | Zone | Observed 1970-2007 | Projected Change (2020-2080) Relative to 1970-2007 (°C) | Projected Change (2020-2080) Relative to 1970-2007 (%) |
|---|---|---|---|---|
| Summer | Coastal (1) | 22.8 | -0.5 | -2.4% |
| | Central (2) | 23.0 | -0.4 | -1.7% |
| | Western (3) | 23.1 | -0.6 | -2.5% |
| Autumn | Coastal (1) | 18.9 | 1.3 | 6.7% |
| | Central (2) | 18.1 | 1.6 | 8.9% |
| | Western (3) | 17.3 | 2.0 | 11.7% |
| Winter | Coastal (1) | 13.1 | 1.3 | 10.0% |
| | Central (2) | 12.3 | 1.4 | 11.1% |
| | Western (3) | 10.7 | 1.5 | 14.1% |
| Spring | Coastal (1) | 18.0 | -0.4 | -2.4% |
| | Central (2) | 17.9 | -0.8 | -4.2% |
| | Western (3) | 17.0 | -0.9 | -5.0% |

Table 17 - Projected changes in average temperature relative to the 1970-2007 period

Projections (2020-2080) in the coastal, central and western zones for summer are for decreases in average temperature of ~0.5°C relative to the 1970-2007 period. Increases in all three zones are projected for autumn; ~1.3°C in the coastal, ~1.6°C in the central zone and ~2.0°C in the western zone. Winter projections are for warmer average temperatures, ~1.3°C in the coastal zone, ~1.4°C in the central zone and ~1.5°C in the western zone. The study region is likely to experience lower spring average temperatures with a decrease of ~0.4°C projected for the coastal zone, and ~0.8-0.9°C in the central and western zones.

Changes in annual average temperature for the projected period from 2020 to 2080 are shown in Figure 38. In addition to showing linear trends (green line), average temperature for the period from 1970-1996 is superimposed onto the projected data. Projected values for all zones show a propensity to extend beyond the bounds of natural variability experienced during the calibration period from 1968-1996. Higher average temperatures than those previously experienced are projected. Average temperatures show an increasing trend over the period from 2020-2080. These trends are statistically significant at the 5% level ($P<0.05$).

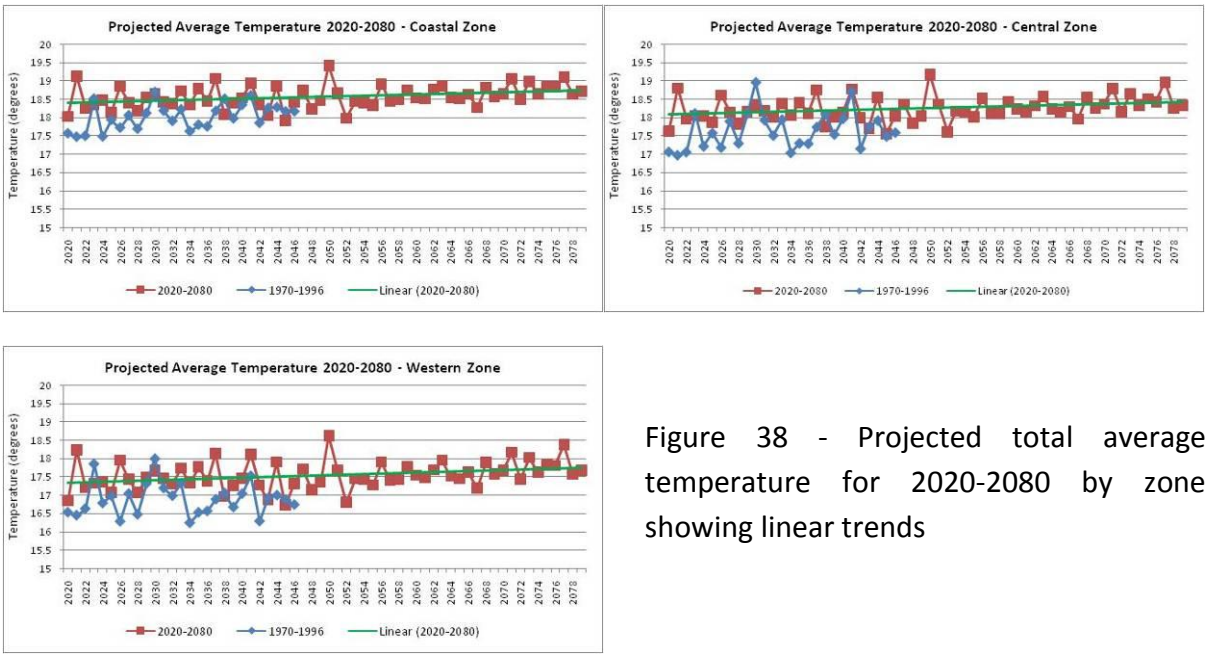


Figure 38 - Projected total average temperature for 2020-2080 by zone showing linear trends

The cycling between day and night is referred to as the diurnal cycle. The diurnal temperature range is typically obtained by subtracting the daily minimum temperature from the daily maximum temperature. These daily values are then averaged to obtain a mean diurnal range. Given the use of monthly GCM output in this analysis, the calculation of the daily diurnal temperature range is not possible. Thus the monthly diurnal temperature range is obtained by subtracting the average monthly minimum temperature from the average monthly maximum temperature. Figure 39 shows projected seasonal average maximum temperature for the 2020-2040, 2040-2060 and 2060-2080 time horizons together with average recorded values for the 1970-2007 time period for each of the regions three climatic zones.

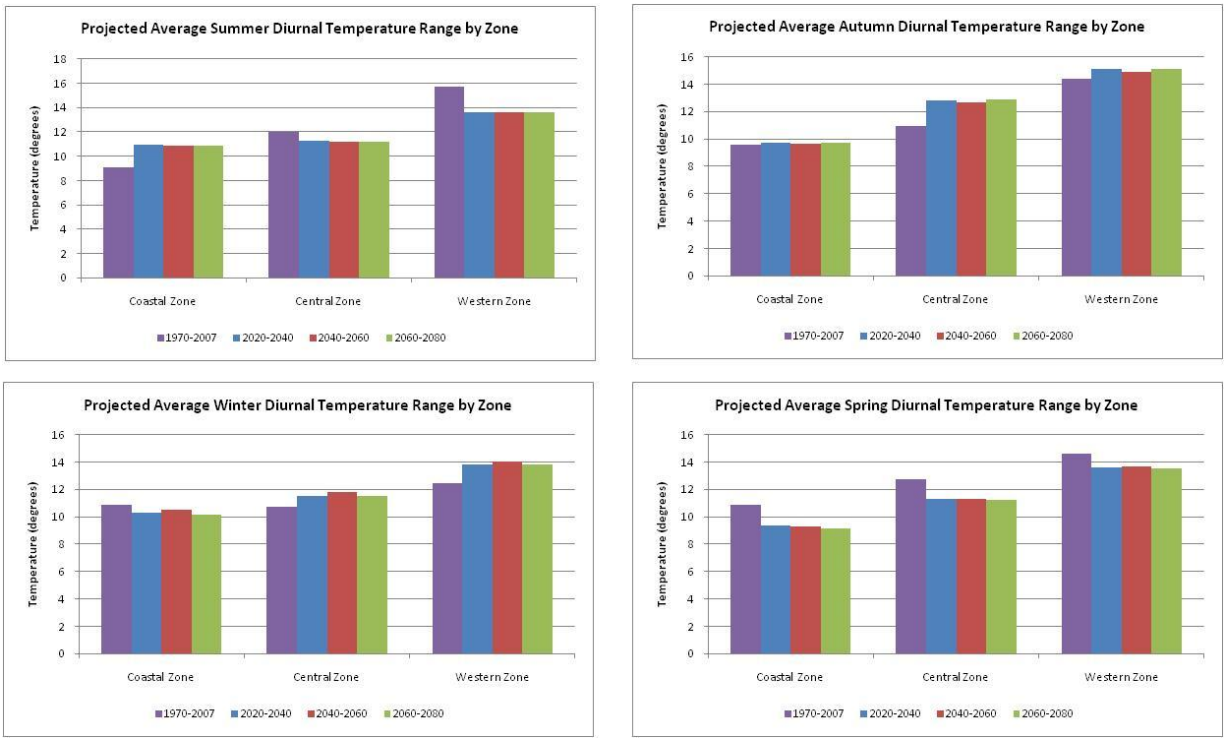


Figure 39 - Seasonal comparison of diurnal temperature ranges for the 1970-1996 time period and future time horizons

Projected changes in average minimum and maximum temperatures impact on the projected diurnal range. An increase in the diurnal range, relative to the 1970-2007 time period, is projected for summer in the coastal zone only; increases in the central and western zones are projected to occur during autumn. Slight increases in the central and western zones are also projected to occur during winter, however projections for spring are for decreases to occur within all climate zones in the region.

Estimates of the magnitude of seasonal shifts, relative to the 1970-2007 time period, are presented in Figure 40 and Table 18. Summer projections (2020-2080) for changes in the diurnal temperature range are for increases of approximately 0.6°C and 0.8°C in the coastal and central zones and a decrease of ~0.7°C in the western zone. Very little change is projected for autumn; decreases of ~0.3°C and 0.8°C are projected in the coastal and western zones whereas an increase of ~0.3°C is projected in the central zone. Increases in the diurnal temperature range are projected for winter in the central (~0.5°C) and western (~1.2°C) zones. Spring projections are for decreases in all zones; ~0.6°C in the coastal zone, ~1.2°C in the central zone and ~0.7°C in the western zone.

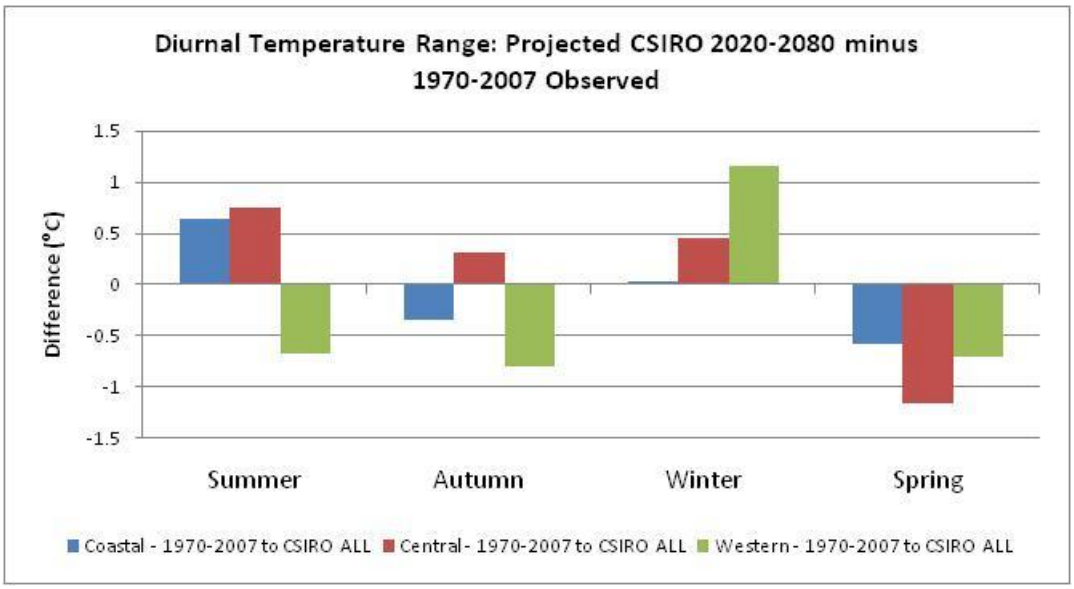


Figure 40 - Estimates of projected diurnal temperature range shifts (°C) relative to the 1970-2007 period

| Season | Zone | Observed 1970-2007 | Projected Change (2020-2080) Relative to 1970-2007 (°C) | Projected Change (2020-2080) Relative to 1970-2007 (%) |
|---|---|---|---|---|
| Summer | Coastal (1) | 9.1 | 0.6 | 7.0% |
| | Central (2) | 12.0 | 0.8 | 6.3% |
| | Western (3) | 15.7 | -0.7 | -4.3% |
| Autumn | Coastal (1) | 9.6 | -0.3 | -3.5% |
| | Central (2) | 11.0 | 0.3 | 2.9% |
| | Western (3) | 14.4 | -0.8 | -5.5% |
| Winter | Coastal (1) | 10.9 | 0.0 | 0.3% |
| | Central (2) | 10.8 | 0.5 | 4.3% |
| | **Western (3)** | **12.5** | **1.2** | **9.3%** |
| Spring | Coastal (1) | 10.9 | -0.6 | -5.3% |
| | **Central (2)** | **12.8** | **-1.2** | **-9.1%** |
| | Western (3) | 14.6 | -0.7 | -4.8% |

Table 18 - Projected changes in diurnal temperature range relative to the 1970-2007 period

Changes in average annual diurnal temperature range for the projected period from 2020 to 2080 are shown in Figure 41. In addition to showing linear trends (green line), average annual minimum temperature for the period from 1970-1996 is superimposed onto the projected data. Despite projected increases in minimum and maximum temperatures, projected diurnal temperature range values for all zones do not extend beyond the bounds of natural variability experienced during the period from 1970-1996.

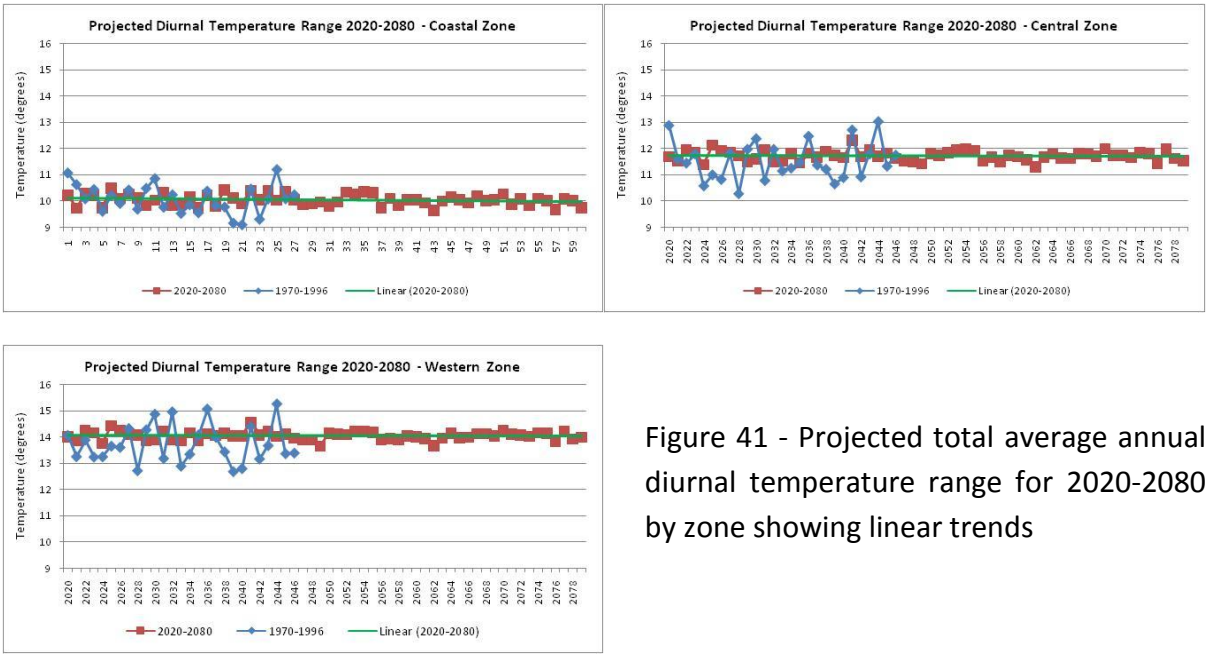


Figure 41 - Projected total average annual diurnal temperature range for 2020-2080 by zone showing linear trends

## 4.5 Relative Humidity

Previous analysis identified that an insufficient number of appropriate BOM relative humidity recording stations are present in the region to enable spatial distribution patterns to be produced (HCCREMS, UofN 2008). As such, relative humidity at 9am and 3pm is analysed by CSIRO ST averaged for the entire region rather than individual zones. Figure 42 shows the average, minimum and maximum humidity range for each of the CSIRO STs.

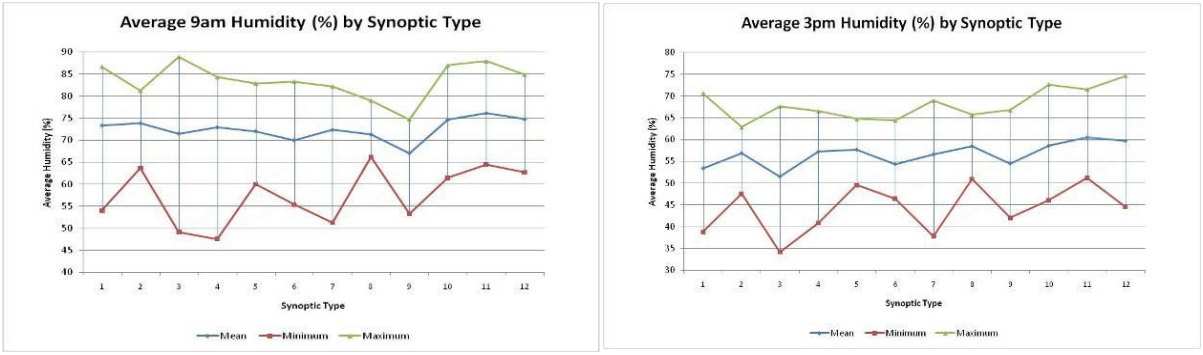


Figure 42 - 9am and 3pm humidity by CSIRO ST

Average 9am and 3pm humidity is higher during summer, although only marginally. The dominant summer STs (11 and 12) are associated with average humidity of approximately 75% at 9am and 60% at 3pm whereas the dominant winter types (1 and 3) are associated with average humidity of approximately 72% at 9am and 52% at 3pm. Substantial differences in the humidity range associated with each CSIRO ST are notable. In particular, STs 2 and 8 show low variability at both 9am and 3pm; ST5 also shows low variability at 3pm. These relationships suggest that changes in the frequency of occurrence of STs for the projected time horizons will have limited or no impact on average humidity due to the limited differentiation in this climate variable by CSIRO ST. However, differences in the frequency of occurrence of STs 2, 5 and 8 may impact on the variability of relative humidity in the region. Projected decreases in the frequency of occurrence of ST2 with a corresponding increase in ST1 for the 2020-2040 and 2040-2060 time horizons suggests a slight increase in winter humidity may be observed. Similarly, decreases in the frequency of occurrence of ST8 during summer in all of the projected time horizons should also result in increased variability during this season.

Figure 43 shows projected seasonal average humidity recorded at 9am and 3pm for the 2020-2040, 2040-2060 and 2060-2080 time horizons together with average recorded values for the 1970-1996 time period. No discernable change in humidity at either 9am or 3pm is projected to occur during summer. A slight decrease in both 9am and 3pm humidity is projected for autumn and winter, whereas a slight increase is projected for spring. Little

variation in projected values is evident over the three projected time horizons (i.e. 2020-2040, 2040-2060 and 2060-2080 projections are all similar).

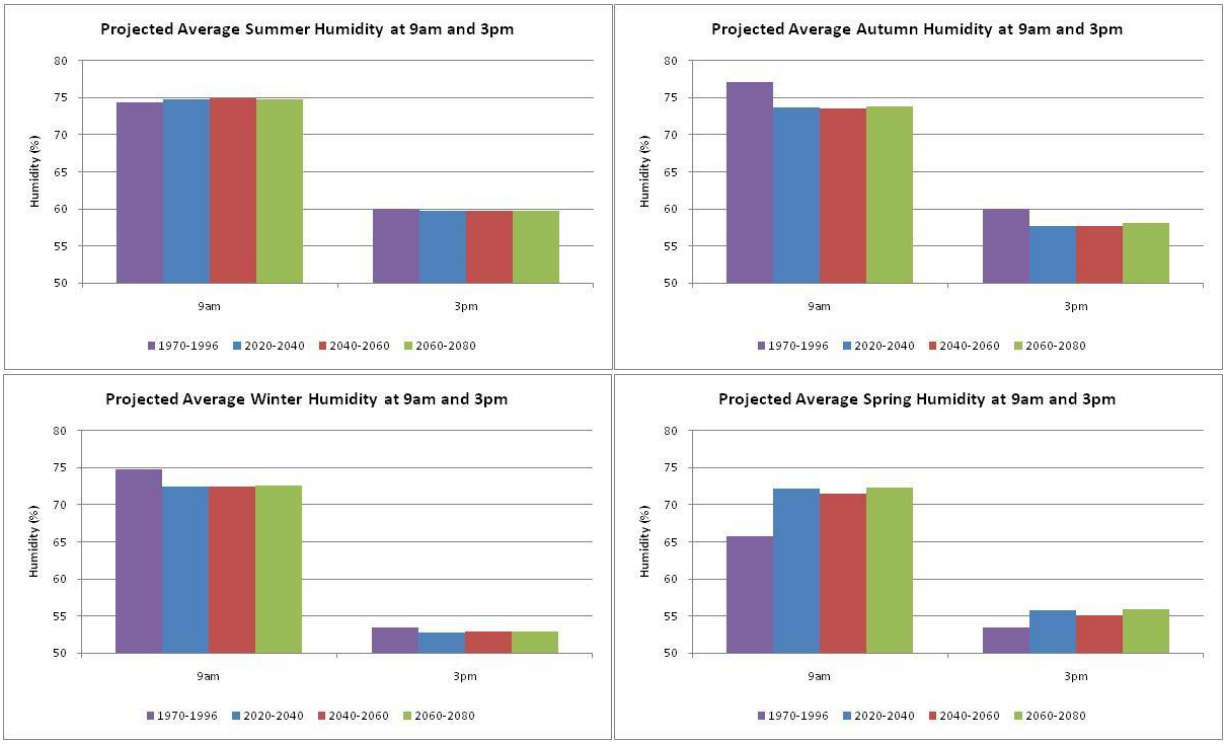


Figure 43 - Seasonal comparison of 9am and 3pm humidity for historic time period and future time horizons

Estimates of the magnitude of seasonal shifts, relative to the 1970-1996 period, is presented in Figure 25. Seasonal averages for the historic time period (1970-1996) are calculated from BOM data and compared with projected seasonal averages calculated from the CSIRO Mk3.5 STs for the period from 2020 to 2080 (CSIRO ALL). A negative change signifies a decrease in humidity over the projected time horizon (relative to the historic time period) whereas a positive change signifies an increase.

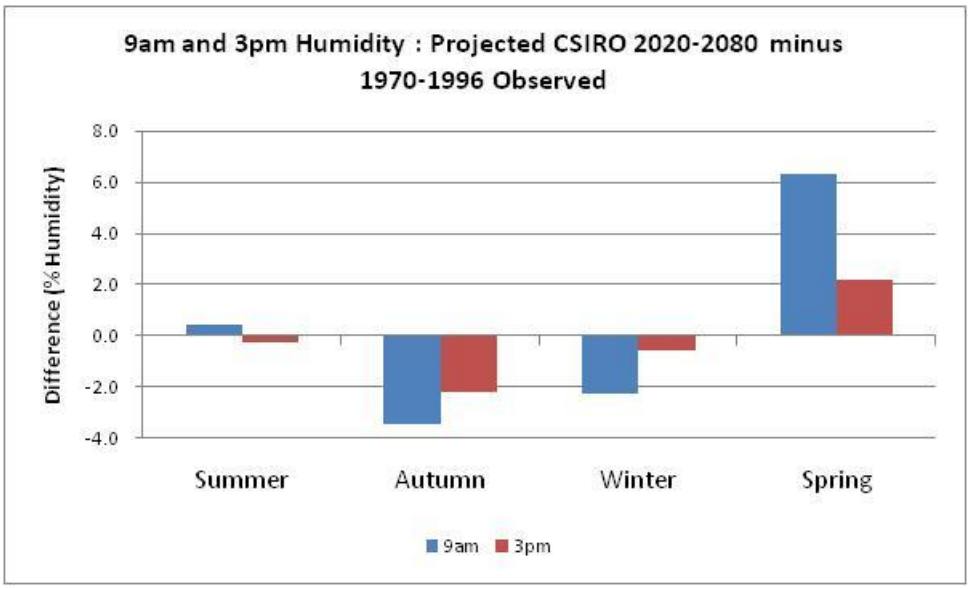


Figure 44 - Estimates of projected humidity shifts relative to the 1970-1996 period

Humidity is projected to remain relatively unchanged during summer with only a 0.4% increase projected in 9am humidity and a 0.2% decrease in 3pm. Lower humidity levels are projected for autumn and winter. Autumn 9am levels are projected to decrease by 3.4% and 3pm by 2.2%. Similarly, winter 9am humidity is projected to decrease by 2.2% and 3pm by 0.6%. The greatest shift is projected to occur in spring 9am humidity, with an increase of 6.3% anticipated. A 2.2% increase in 3pm humidity is also projected for spring.

Changes in relative humidity for the projected period from 2020 to 2080 are considered in Figure 45. In addition to showing linear trends (green line), average annual relative humidity for the period from 1970-1996 is superimposed onto the projected data. There is no evident increase in average annual relative humidity projected and projected values are within the bounds of natural variability experienced during the 1970-1996 time period.

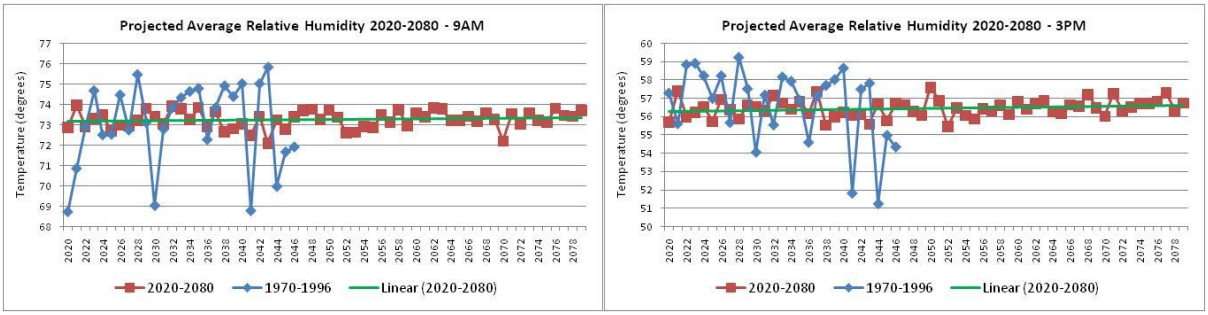


Figure 45 - Projected average annual 9am and 3pm relative humidity for 2020-2080 showing linear trends

## 4.6 Pan Evaporation

Figure 46 shows projected seasonal average pan evaporation for the 2020-2040, 2040-2060 and 2060-2080 time horizons together with average recorded values for the 1970-2007[3] time period for each of the regions three climatic zones.

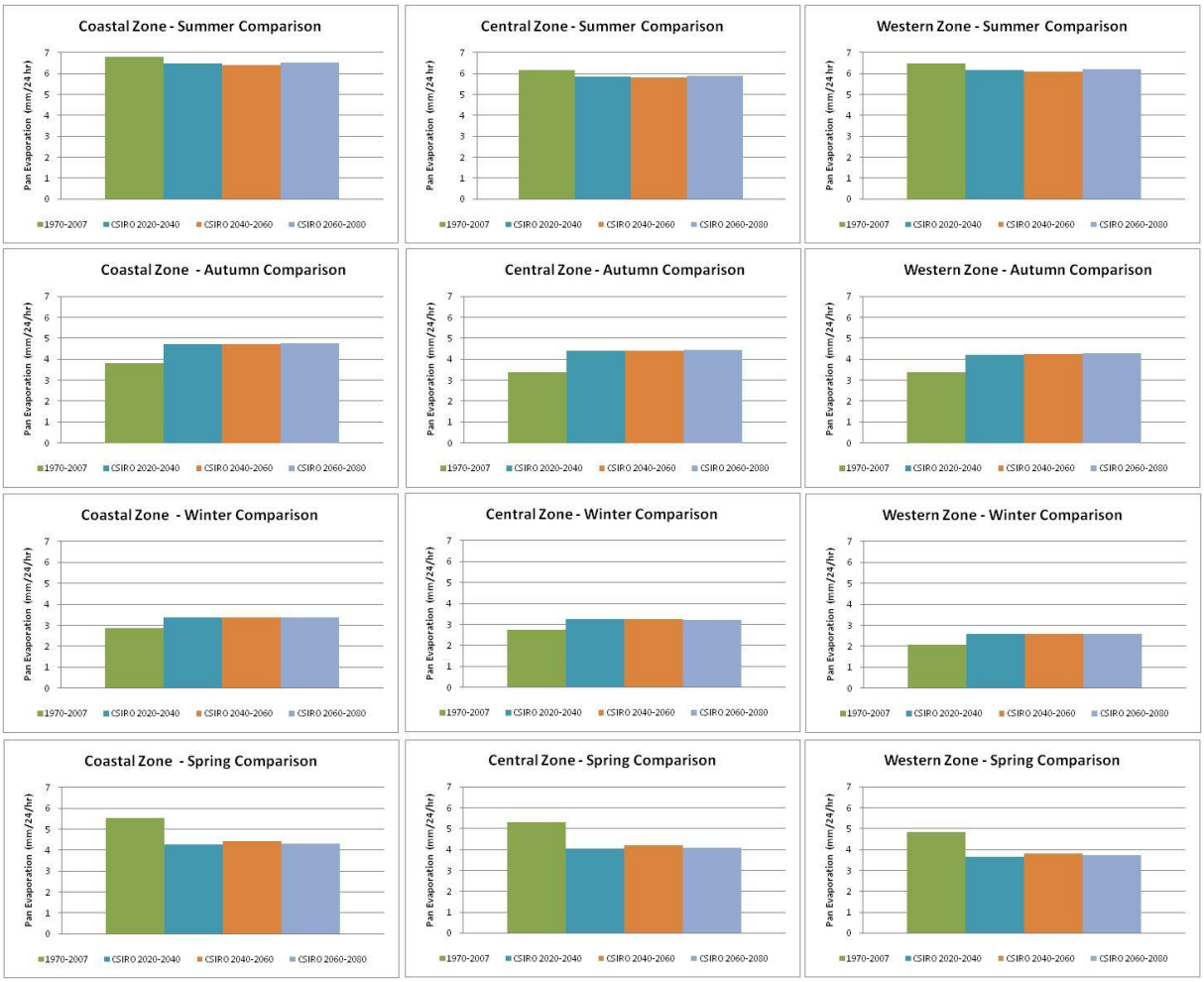


Figure 46 - Seasonal comparison of pan evaporation for historic time period and future time horizons

Little variation in projected values is evident over the three projected time horizons (i.e. 2020-2040, 2040-2060 and 2060-2080 projections are all similar). Projections for summer show a decrease in pan evaporation on the 1970-2007 seasonal average in all climatic zones in the region. Similar results are shown for spring, with a decrease in pan evaporation also projected, albeit larger. Increases in pan evaporation are projected for autumn and winter.

[3] Although the 1970-2007 time period is considered, only the central zone has BOM records extending back this far. Records for the coastal and western zones extend back to 1974 and 1972 respectively.

These seasonal increases and decreases in pan evaporation (for the entire 2020 to 2080 projected period), relative to the 1970-2007 observations, are shown in Figure 47. Seasonal shifts appear to balance out to produce no projected change in annual pan evaporation.

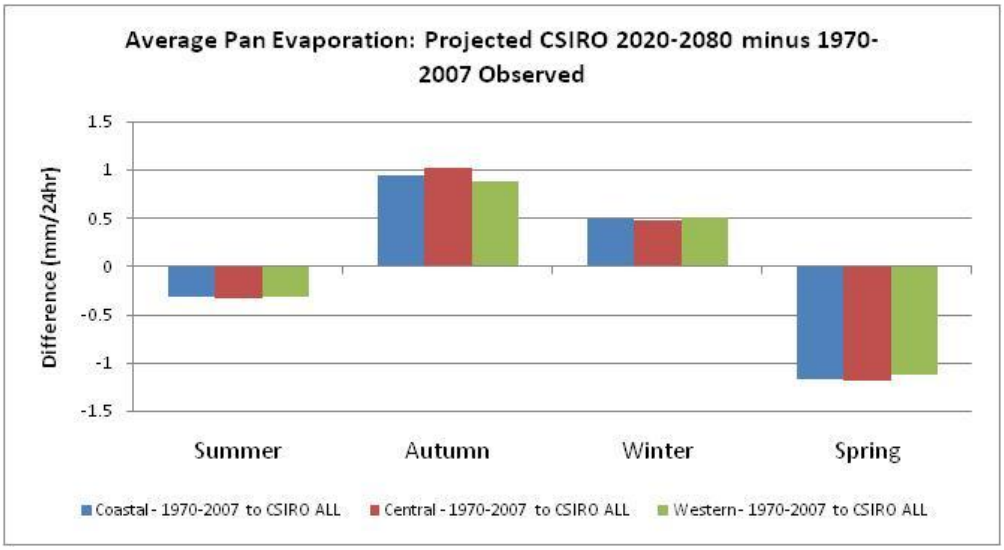


Figure 47 - Estimates of projected precipitation shifts relative to the 1970-2007 period

Changes in average annual pan evaporation for the projected period from 2020 to 2080 are considered using linear trends and regression analysis (Figure 48). In addition to showing linear trends (green line), average annual pan evaporation for as much of the calibration period (1968-1996) as is covered by the BOM data is superimposed onto the projected data. The years of coverage for each zone are: coastal zone = 1974-1996, central zone = 1970-1996 and western zone = 1972-1996.

Projected data for all zones lies well within the bounds of natural variability recorded during the calibration period. The statistical significance of the linear trends for average annual pan evaporation for the 2020-2080 time period were tested using regression analysis. No change is projected in any of the zones.

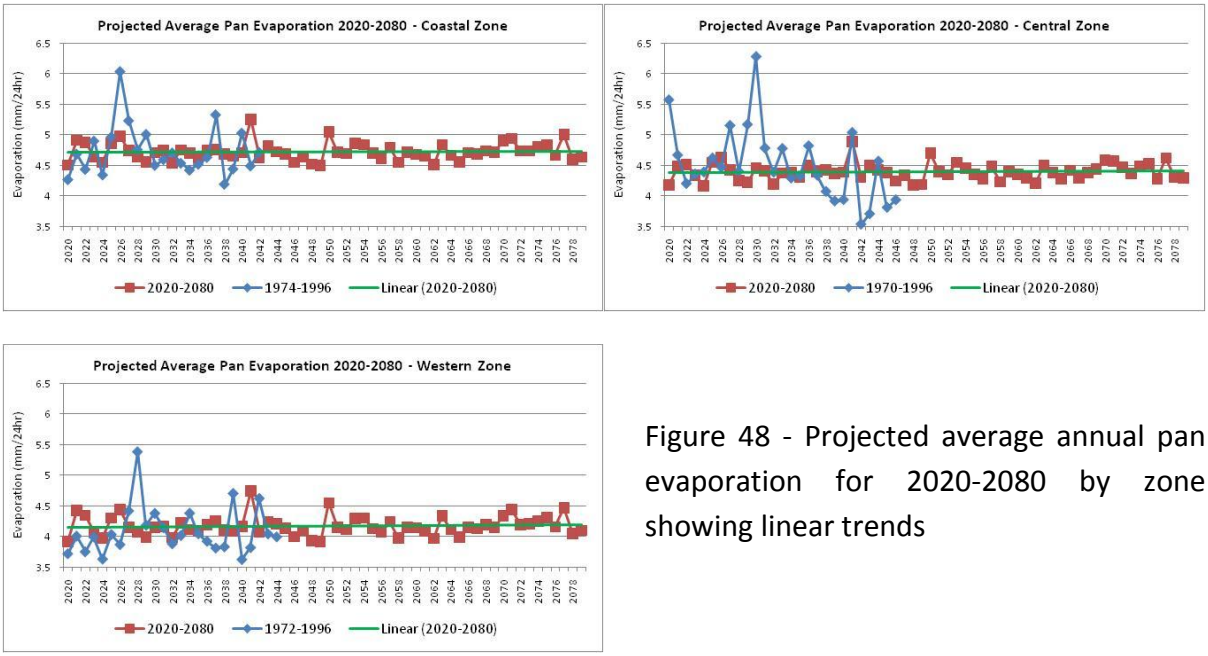


Figure 48 - Projected average annual pan evaporation for 2020-2080 by zone showing linear trends

An insufficient number of pan evaporation stations with sufficient length of record and complete data exist to allow the generation of spatial layers that cover the entire region. Thus spatial distributions for each of the 12 CSIRO STs do not offer complete regional coverage (Figure 49).

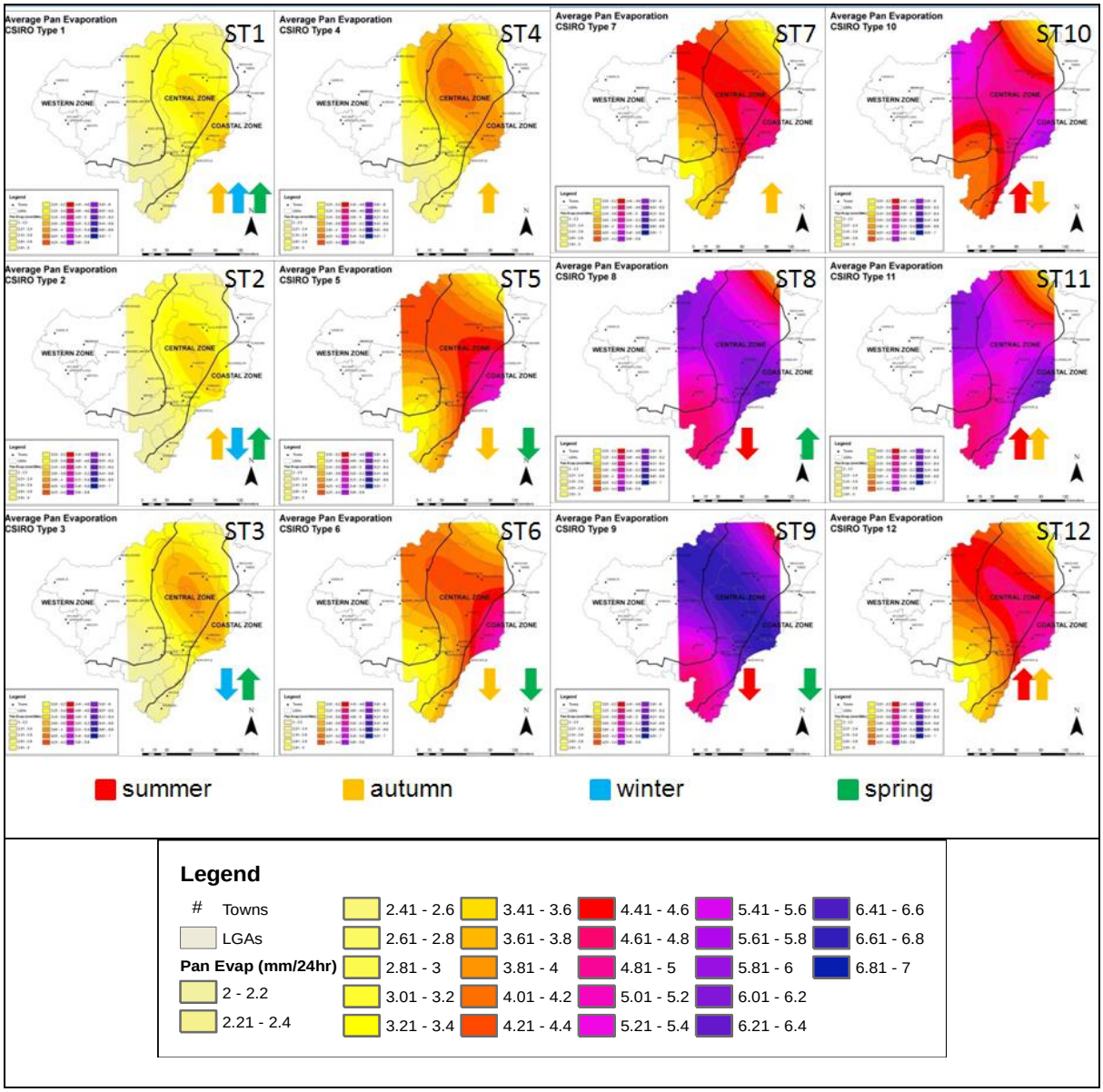


Figure 49 - Regional pan evaporation patterns for the period 1948 to 2007 derived from CSIRO STs with arrows indicating seasonal shifts

Highest average pan evaporation is recorded for ST9, followed by STs 8, 11 and 10 respectively. ST9 occurs during summer and spring; an approximate 2% decrease in frequency of occurrence of this synoptic type is projected during summer for all three time horizons to 2080. Similarly, an approximate 5% decrease is projected during spring for only the 2040-2060 time horizon. These decreases are counterbalanced by projected increases in the frequency of occurrence of STs 8, 10 and 11. As the previous analysis shows (see Figure 48), these changes in ST patterns are projected to have minimal impact on pan evaporation for the period from 2020-2080.

## 4.7 Water Balance

Water balance was calculated by subtracting the average daily pan evaporation (mm/24hr) from the average daily precipitation. These calculations were used to derive both seasonal and annual projections of water balance. Water balance values from this simple equation are presented as average daily millimeters (mm).

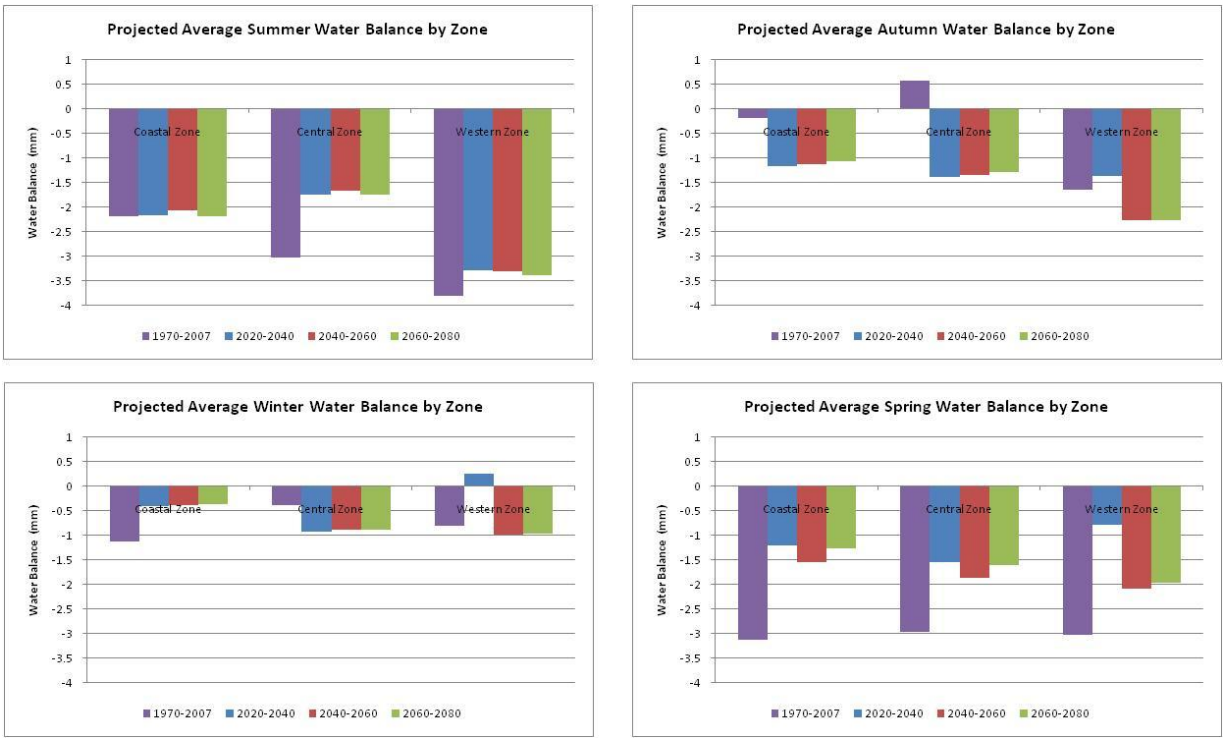


Figure 50 - Seasonal comparison of water balance for historic time period (1970-2007) and future time horizons

Little variation in projected values for summer is evident over the three time horizons (i.e. 2020-2040, 2040-2060 and 2060-2080 projections are all similar). Projections for summer show an increase in average water balance for the central and western zones relative to the 1970-2007 time period. Little change in summer average water balance is projected in the coastal zone. Autumn projections show a decrease in water balance in the coastal and central zones. A slight increase over each of the projected time horizons is also noted. Autumn projections for the western zone show an initial slight increase from 2020-2030, followed by a decrease in both 2040-206 and 2060-2080.

In winter, an increase in water balance is projected for all time horizons in the coastal zone. A slight decrease is projected for all time horizons in the central zone. The western zone shows a slight increase for 2020-2030 followed by decreases in 2040-2060 and 2060-2080. Average water balance projections for spring show increases in all zones and in all time

horizons relative to the 1970-2007 period. The strongest increase is projected to occur during the 2020-2030 time period, followed by a decrease (relative to the 2020-2030 time period) then a slight increase. This pattern is most evident in the western zone.

Estimates of the magnitude of seasonal shifts, relative to the 1970-2007 time period, are presented in Figure 51 and Table 19. Seasonal averages for the period from 1970-2007 are calculated from BOM data and compared with projected seasonal averages calculated from the CSIRO Mk3.5 STs for the period from 2020 to 2080 (CSIRO ALL). Note that these results should be considered in the context of the changes in the projected time horizons discussed above. Additionally, consistent historic records are not available to cover the preceding two IPO phases (i.e. –ve La Nina–like for 1948-1976 and +ve phase El Nino-like for 1977-2007). Thus the time period from 1970-2007 covers a predominantly El Nino-like historic period.

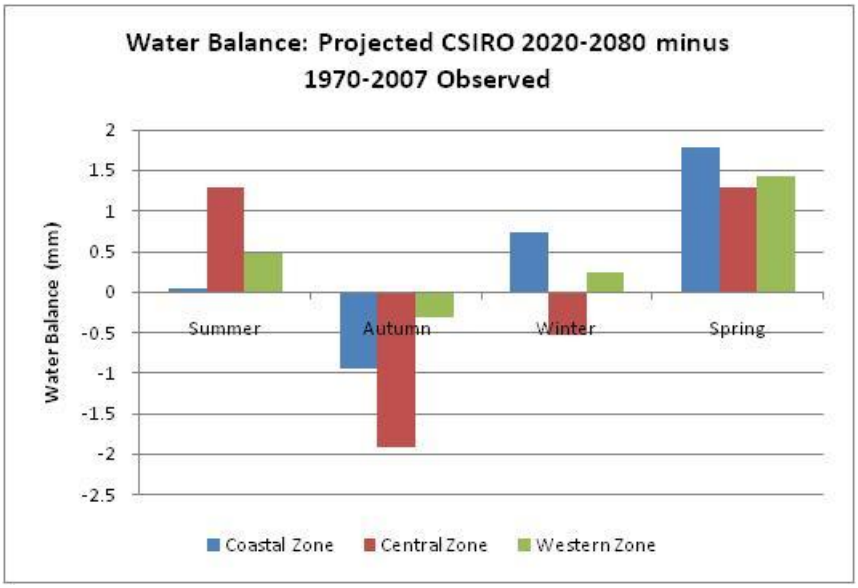


Figure 51 - Estimates of projected water balance shifts (mm) relative to the 1970-2007 period

Projections (2020-2080) for summer are for increases in average daily water balance of ~1.3mm in the central zone and ~0.5mm in the western zone relative to the 1970-2007 period. Water balance in the coastal zone remains relatively unchanged. A significant decrease of ~1.9mm in average daily water balance for autumn is projected in the central zone. Decreases of ~0.9mm and ~0.3mm are expected in the coastal and western zones respectively. Increases in the coastal and western zones are projected for winter; ~0.7mm in the coastal zone and ~0.2mm in the western zone. A decrease of ~0.5mm is projected in the central zone during winter. Spring projections are for increased average daily water balance in all zones; ~1.8mm in the coastal zone, ~1.3mm in the central zone and ~1.4mm in the western zone.

| Season | Zone | Observed 1970-2007 | Projected Change (2020-2080) Relative to 1970-2007 (°C) | Projected Change (2020-2080) Relative to 1970-2007 (%) |
|---|---|---|---|---|
| Summer | Coastal (1) | -2.2 | 0.1 | 2% |
| | **Central (2)** | **-3.0** | **1.3** | **43%** |
| | Western (3) | -3.8 | 0.5 | 13% |
| Autumn | **Coastal (1)** | **-0.2** | **-0.9** | **-533%** |
| | **Central (2)** | **0.6** | **-1.9** | **331.2%** |
| | Western (3) | -1.6 | -0.3 | -19.3% |
| Winter | **Coastal (1)** | **-1.1** | **0.7** | **66.2%** |
| | **Central (2)** | **-0.4** | **-0.5** | **-140.7%** |
| | **Western (3)** | **-0.8** | **0.2** | **29.7%** |
| Spring | **Coastal (1)** | **-3.1** | **1.8** | **57.0%** |
| | **Central (2)** | **-3.0** | **1.3** | **43.7%** |
| | **Western (3)** | **-3.0** | **1.4** | **47.0%** |

Table 19 - Projected changes in water balance relative to the 1970-2007 period

Changes in average annual water balance for the projected period from 2020 to 2080 are shown in Figure 52. In addition to showing linear trends (green line), average annual water balance for the period from 1970-1996 is superimposed onto the projected data. Projected values for all zones show no propensity to extend beyond the bounds of natural variability experienced during the period from 1970-1996. Average water balance shows a decreasing trend over the period from 2020-2080 in only the western zone. This trend is statistically significant at the 5% level ($P<0.05$).

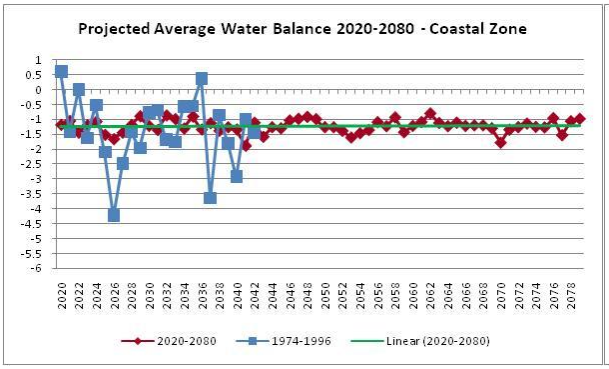


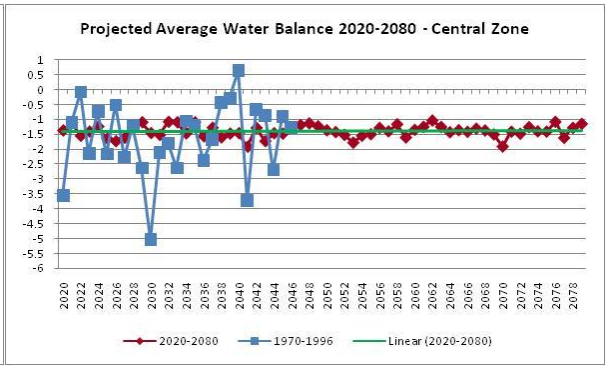


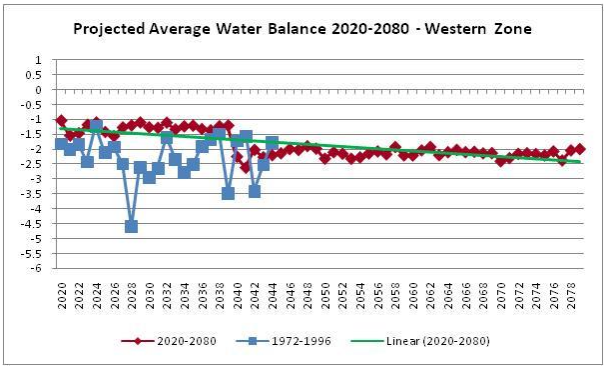


Figure 52 - Projected average water balance for 2020-2080 by zone showing linear trends

## 4.8 Wind

Figure 53 shows projected seasonal average wind speed for the 2020-2040, 2040-2060 and 2060-2080 time horizons together with average recorded values for the 1970-2007 time period for each of the region's three climatic zones. Note that average wind speed data from BOM recording stations does not include directional information.

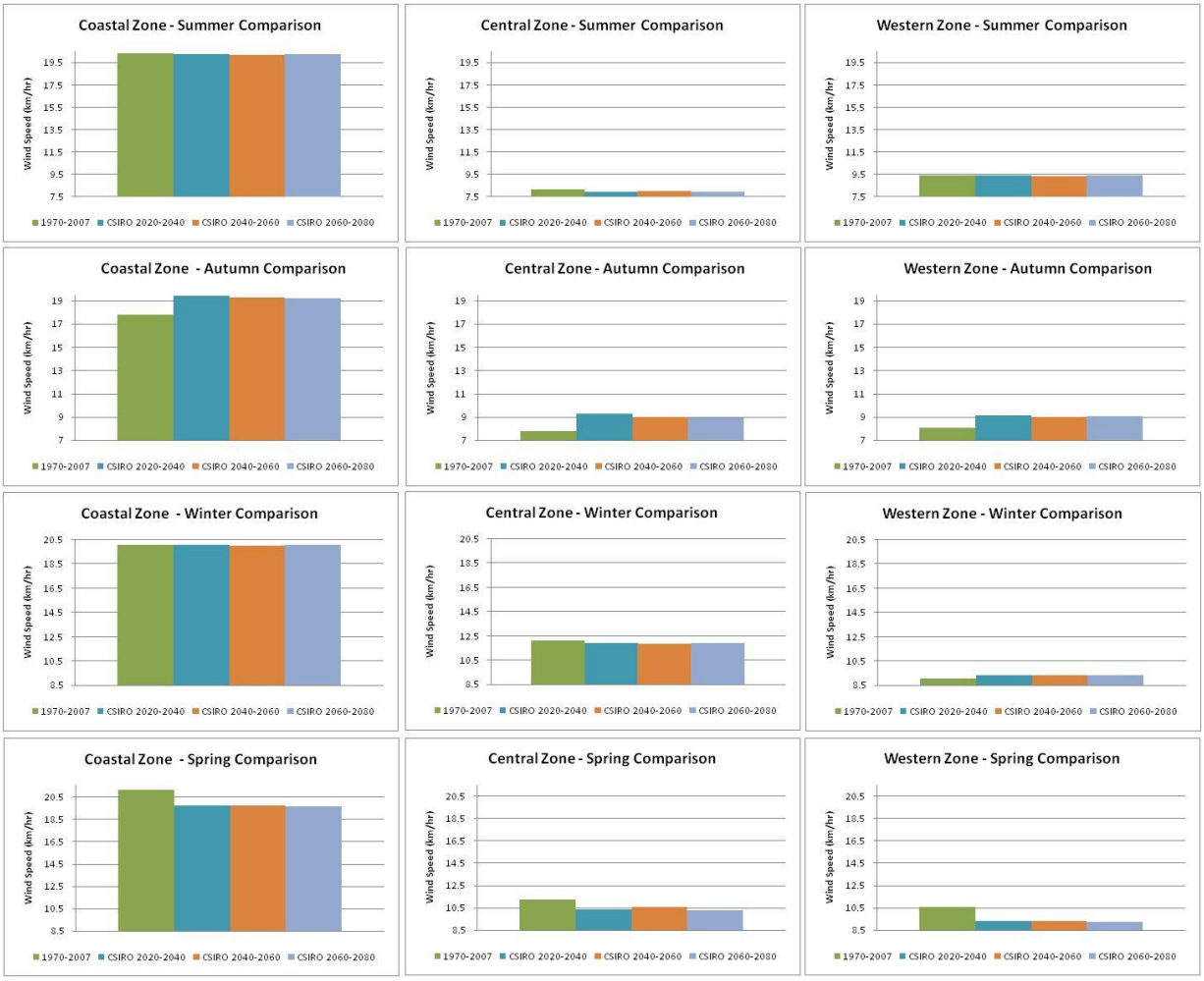


Figure 53 - Seasonal comparison of average wind speed for the 1970-2007 time period and future time horizons

Little variation in projected values is evident over the three time horizons (i.e. 2020-2040, 2040-2060 and 2060-2080 projections are all similar). Projections for summer and winter show little or no change in average wind speed relative to the 1970-2007 time period. Projections for autumn show an increase in average wind speed in all zones, whereas spring projections show a decrease.

Estimates of the magnitude of seasonal shifts, relative to the 1970-2007 time period, are presented in Figure 54 and Table 20. Seasonal averages for the period from 1970-2007 are calculated from BOM data and compared with projected seasonal averages calculated from the CSIRO Mk3.5 STs for the period from 2020 to 2080 (CSIRO ALL).

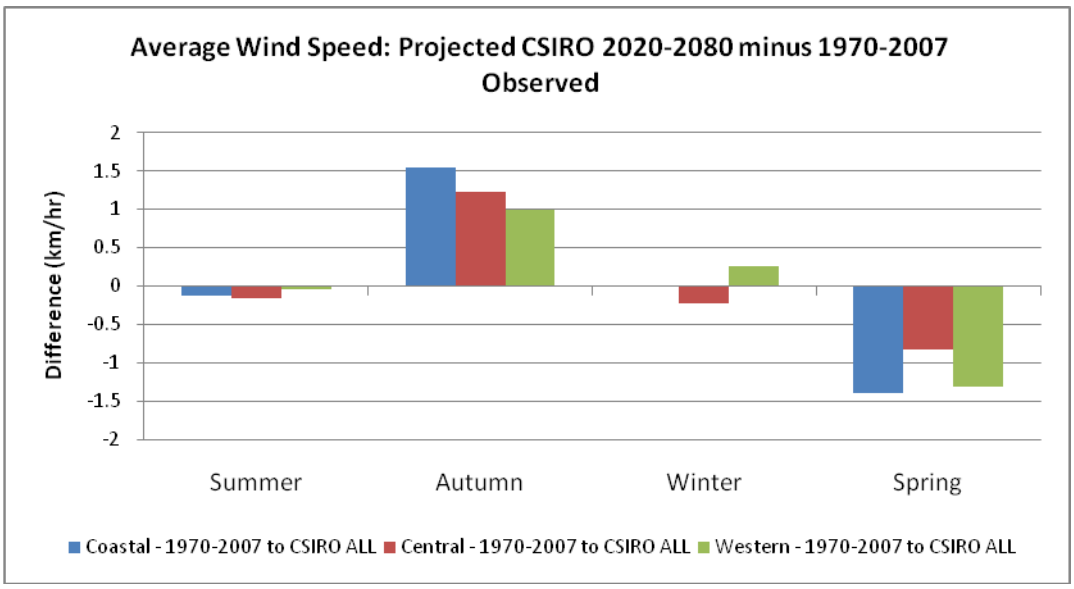


Figure 54 - Estimates of projected average wind speed (km/hr) shifts relative to the 1970-2007 period

| Season | Zone | Observed 1970-2007 | Projected Change (2020-2080) Relative to 1970-2007 (°C) | Projected Change (2020-2080) Relative to 1970-2007 (%) |
|---|---|---|---|---|
| Summer | Coastal (1) | 20.4 | -0.1 | -0.6% |
| | Central (2) | 8.1 | -0.2 | -1.9% |
| | Western (3) | 9.4 | 0.0 | -0.4% |
| **Autumn** | **Coastal (1)** | **17.8** | **1.5** | **8.7%** |
| | **Central (2)** | **7.8** | **1.2** | **15.9%** |
| | **Western (3)** | **8.1** | **1.0** | **12.4%** |
| Winter | Coastal (1) | 20.1 | 0.0 | -0.1% |
| | Central (2) | 12.1 | -0.2 | -1.9% |
| | Western (3) | 9.1 | 0.3 | 2.9% |
| **Spring** | **Coastal (1)** | **21.1** | **-1.4** | **-6.6%** |
| | **Central (2)** | **11.2** | **-0.8** | **-7.4%** |
| | **Western (3)** | **10.6** | **-1.3** | **-12.4%** |

Table 20 - Projected seasonal changes in average wind speed relative to the 1970-2007 period

Increases in average wind speed in all three zones are projected for autumn; ~1.5km/hr in the coastal zone, ~1.2km/hr in the central zone and ~1.0km/hr in the western zone. Spring projections are for decreased average wind speed, ~1.4km/hr in the coastal zone, ~0.8km/hr in the central zone and ~1.3km/hr in the western zone. Only minimal shifts occur during summer and winter. Increases occurring during autumn are balanced by decreases occurring in spring and thus should result in no overall change in annual average windspeed.

Changes in annual average wind speed for the projected period from 2020 to 2080 are shown in Figure 55. In addition to showing linear trends (green line), average annual wind speed for the period from 1970-1996 is superimposed onto the projected data. Projected values for all zones do not extend beyond the bounds of natural variability experienced during the period from 1970-1996. As suggested by the seasonal shifts in average wind speed, no change in annual average wind speed is projected.

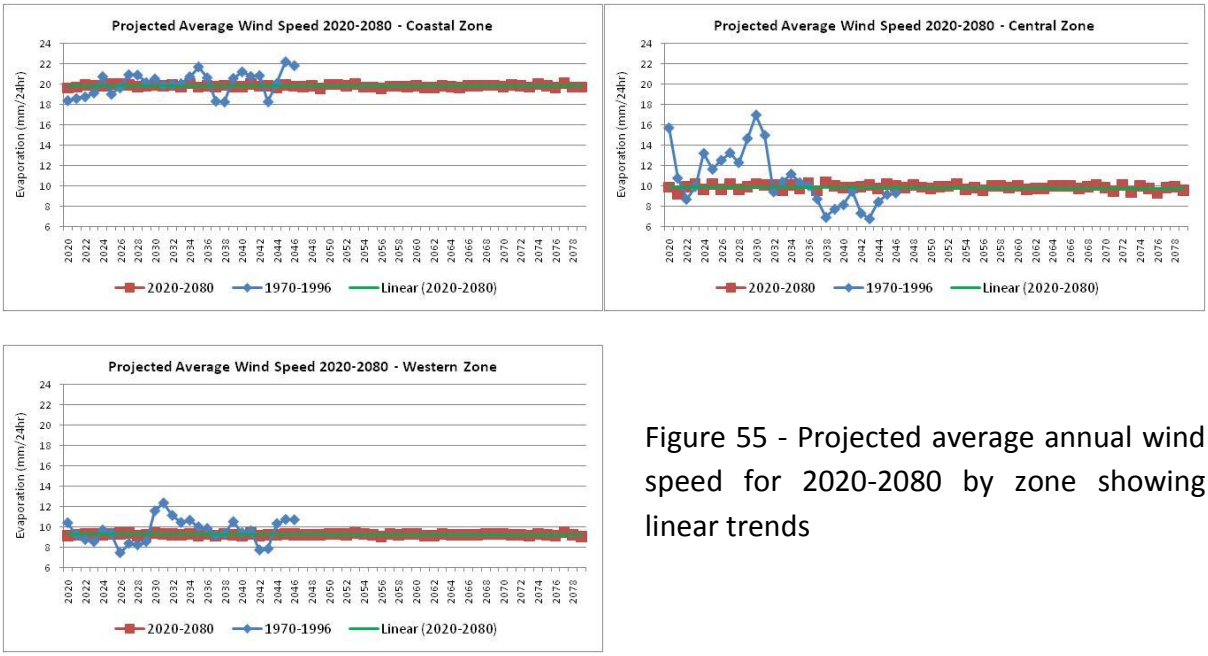


Figure 55 - Projected average annual wind speed for 2020-2080 by zone showing linear trends

Wind gust rose diagrams associated with each of the CSIRO STs are shown in Figure 56. ST 2 is associated with the highest wind gusts in the region. These gusts occur during winter and are from a predominately westerly direction. STs 1 through to 6 all produce primarily westerly winds. STs 7, 8 and 9 are associated with wind gusts from multiple directions, however strongest gusts occur from both the west and the south. ST10 is associated with gusts predominantly from the south and south east. STs 11 and 12 are associated with easterly on-shore gusts as well as those from the north east, south east and southerly directions. Projected decreases in the frequency of occurrence of STs 2 and 3 during winter should decrease the intensity of wind gusts in the region during this season. Conversely, increases in STs 11 and 12 should produce more onshore wind gusts during summer. There

is no indication from the ST patterns that the intensity of summer wind gusts will change. These changes are summarised in Table 21.

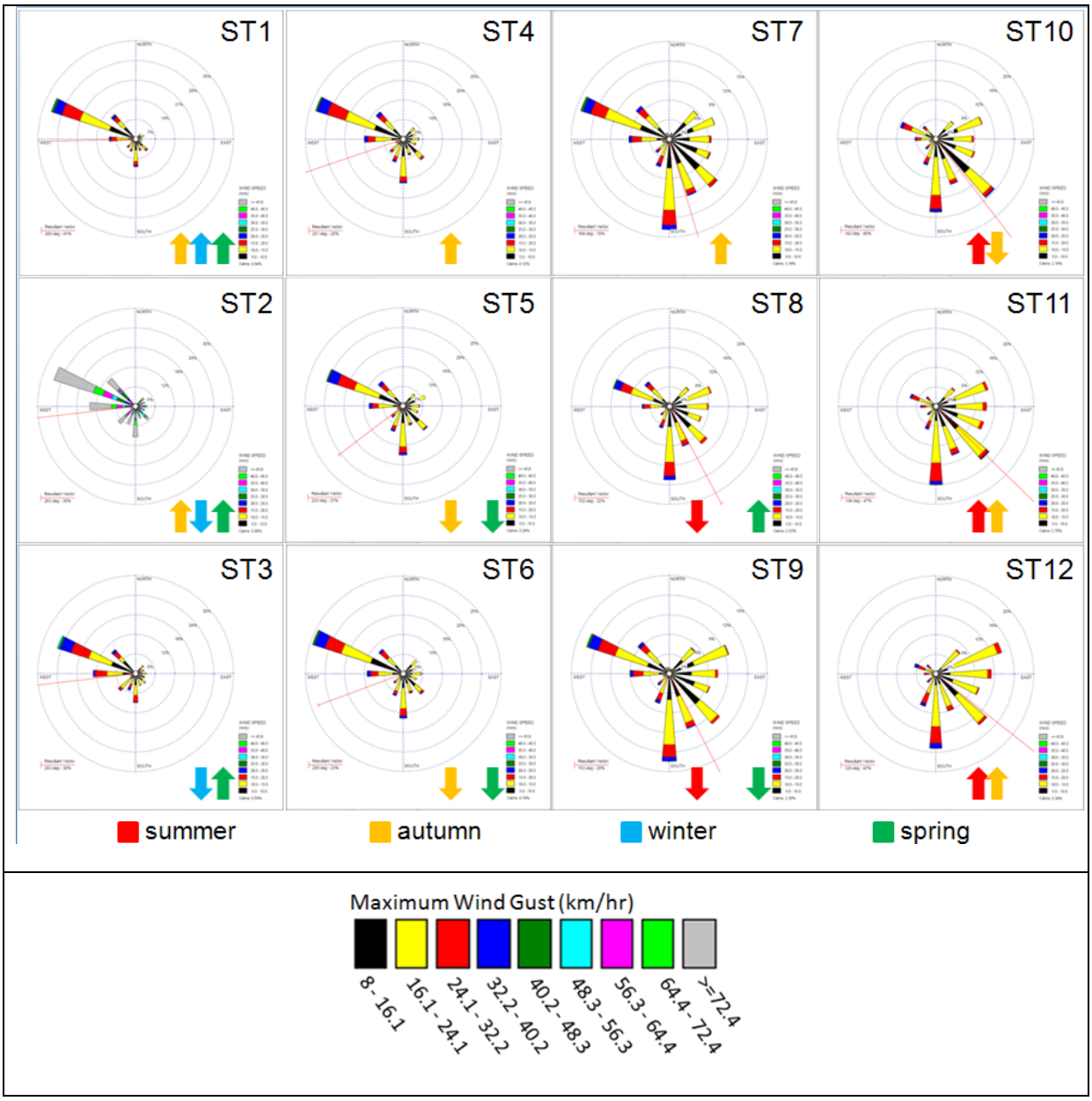


Figure 56 - Regional maximum wind gust patterns for CSIRO STs

| ST | Dominant Wind Direction | Change Projected |
|---|---|---|
| 1 | North-Westerly | Increase in autumn, winter and spring |
| 2 | North-Westerly | Increase in autumn and spring, decrease in winter |
| 3 | North-Westerly | Decrease in winter, increase in spring |
| 4 | North-Westerly, Southerly | Increase in autumn |
| 5 | North-Westerly, Southerly | Decrease in autumn and spring |
| 6 | North-Westerly, Southerly | Decrease in autumn and spring |
| 7 | Southerly, North-Westerly | Increase in autumn |
| 8 | Southerly, North-Westerly | Decrease in summer, increase in spring |
| 9 | Southerly, North-Westerly | Decrease in summer and spring |
| 10 | Southerly, South-Easterly | Increase in summer, decrease in autumn |
| 11 | Southerly, South-Easterly, Easterly | Increase in summer and autumn |
| 12 | Southerly, North-Easterly, South-Easterly | Increase in summer and autumn |

Table 21 - Summary of projected wind gust changes for each synoptic type

## 4.9 Sea-Level Rise and Extreme Sea Levels

Sea-level rise is a global process and the Hunter, Central and Lower North coast regions of NSW can expect to typically experience rates of sea-level rise as identified by the IPCC (2007). The adopted sea-level rise estimates by the NSW Government (Draft Sea-Level Rise Policy, 2008) are +0.4 m and +0.9 m above the 1990 sea-level by 2050 and 2100 AD. Hence, we adopt these values in this study and have ***not calculated sea-level rise estimates from the Global Climate Model output***. However, the regional impacts of sea-level rise depend upon the relative movement of the land to the ocean, caused by sedimentation, land subsidence, tectonism and millennial scale geodynamics (Goodwin, 2003). The latter has and will cause a small ongoing, relative sea-level lowering along the NSW coast of ~0.5 mm/yr which reduces the relative sea-level rise along the regional coastline, by this amount. In addition, spatial variability in mean-sea-level rise (MSLR) exists across the latitudinal extent of the south-east Australian coast. Church et al. (2004) indicate that maximum rates of sea-level rise in Australia in excess of 2 mm per year are observed between Sydney and Brisbane, and rates of between 1 and 1.5 mm per year along the southern NSW coast. McInnes et al. (2007) examined projections of the relative mean sea level rise along the NSW coast due to thermal expansion in two CSIRO global climate models. In both models the MSLR along the NSW coast due to thermal expansion (and uncorrected for land motion) was greater than the global average values, and indicated considerable spatial variability

due to the warming of sea surface temperatures in this region, and the strengthening of the East Australian Current. The projected sea level rise estimate of IPCC (2007a) differed by up to 4 cm from present to 2030 (approx 1 mm per year) between Batemans Bay and Wooli Wooli on the NSW coast. With respect to coastal behaviour, this differential in MSL rates of rise is probably insignificant on multi-decadal time scales.

However, the return period of extreme sea levels due to storm surges and high waves during storm events is an important consideration for coastal management. The storm systems that produce these elevated sea levels are East Coast lows, cut-off lows and southward moving tropical cyclones. The latitudinal difference in extreme water levels has an important effect on the spatial variability of coastal responses on decadal timescales, and is coupled to wave direction changes (e.g. Storm waves with east mean wave direction are coupled to frequent extreme high water levels). Our analysis of the projected changes in the frequency of Synoptic Types (ST's) from the CSIRO Mk3.5 GCM indicate an 4% increase in the mean circulation pattern (ST1) during autumn and winter. Extreme East Coast Lows preferentially develop within ST1. Accordingly there is a higher probability of ECL's formation over the future decades. Unfortunately the current generation of GCM's are not sophisticated enough to provide information on the probability of changes in the magnitude nor frequency of these extreme maritime storms (CSIRO, 2007). Hence, we can only conclude that the increase in the monthly frequency of ST1 will be accompanied by an increase in the frequency of extreme maritime storm events along the NSW coast. The recent historical observations below, provide some information of the magnitude-frequency relationship.

Church et al. (2004) found that extreme sea levels were 2-3 times more frequent in the period since 1950 when compared to the pre 1950 period, and that enhanced interannnual variability due to ENSO and the IPO was contributing to this. Lord and Kulmar (2000) calculated that the return period for severe storms such as those in 1974 was 1 in 70 years for peak wave height and 1 in 200 for extreme water level. Analysis of a new 1000 year IPO record suggests that multi decades where frequent extreme storms equivalent to the 1974 storms occur, have a return period of about 250 years (Goodwin and Browning, in prep 2009). However, both the historical analysis and the future modelling predictions do not discount the possibility of an extreme 1 in 250 to 1 in 1000 recurrence year storm event from occurring. The probability of such an event impacting the central and mid-north coast NSW is higher during La Niña years in the ENSO cycle (You and Lord, 2007), and further increased during the La Nina-like phase of the IPO.

## 4.10 Wave Climate

Recently, McInnes et al. (2007) have used the CSIRO MK3.5 GCM output to assess the likely changes to swell and storm-wave climate along the NSW coast as an outcome of latitudinal climate change. Their results were inconclusive due to the GCM's inability to replicate the meridional variability in the atmospheric circulation, particularly in the mid-latitudes. In addition the GCMs do not fully capture the inherent decadal variability which has been observed to cause major changes in coastal stability, sand supply rates and shoreline alignment in the past 60 years of instrumental data. The GCM analysis by McInnes et al. (2007) indicated that changes to mean deepwater swell wave direction were insignificant at -0.5° to +1.2° (compared to observed interannual and interdecadal variability) with a corresponding average change in significant wave height of ± 8% by 2070. This highlights that the prediction of wave climate changes using GCMs is immature with respect to their higher skill in predicting sea-level change.

**Methodology and Skill Testing**

Taking into account the results of the McInnes et al. (2007) methodology, we applied the same approach used throughout this study to investigate whether the alternative approach could yield improved wave climate projections. We have used the monthly ST's determined from the NNR, CSIRO MK3.5 GCM, MIROC GCM, and an Ensemble of the CSIRO/MIROC GCM output. The ST's identified by the SOMS analysis of the GCM output was calibrated to the monthly mean Waverider Buoy data from Sydney for the calibration period July, 1987 to June, 2007 (Goodwin and Blackmore, in prep). The monthly significant wave height (Hsig), monthly maximum wave direction (HMax), monthly mean wave direction (MWD), and monthly peak period (Tp), together with the respective standard deviations were calculated for ST1 to ST12. The monthly mean wave statistics for each NNR ST were listed in the Stage 2 report (HCCREMS & UofN, 2008). The monthly mean wave statistics for each Ensemble CSIRO/MIROC ST are listed in Table 22.

| ST | Average of SYD MWD Waverider buoy data (°T) | Average of SYDNEY TP1 (s) | Average of Sydney HSIG (m) | Average of Sydney HMAX (m) | StdDev of SYD MWD Waverider buoy data (°T) | StdDev of SYDNEY TP1 (s) | StdDev of Sydney HSIG (m) | StdDev of Sydney HMAX (m) |
|---|---|---|---|---|---|---|---|---|
| 1.00 | 140.11 | 10.14 | 1.69 | 2.65 | 11.13 | 0.69 | 0.40 | 0.46 |
| 2.00 | 130.87 | 10.12 | 1.75 | 2.97 | 20.98 | 0.97 | 0.23 | 0.38 |
| 3.00 | 141.52 | 10.07 | 1.63 | 2.77 | 10.79 | 0.55 | 0.23 | 0.39 |
| 4.00 | 137.28 | 9.09 | 1.66 | 2.84 | 11.13 | 0.39 | 0.21 | 0.34 |
| 5.00 | 131.71 | 9.39 | 1.69 | 2.85 | 16.19 | 0.49 | 0.22 | 0.36 |
| 6.00 | 138.80 | 9.87 | 1.64 | 2.67 | 12.07 | 0.58 | 0.29 | 0.45 |
| 7.00 | 125.47 | 8.93 | 1.56 | 2.66 | 12.37 | 0.53 | 0.16 | 0.27 |
| 8.00 | 133.30 | 8.78 | 1.58 | 2.69 | 7.82 | 0.44 | 0.24 | 0.40 |
| 9.00 | 135.90 | 9.64 | 1.65 | 2.80 | 11.43 | 0.70 | 0.31 | 0.51 |
| 10.00 | 126.57 | 8.90 | 1.64 | 2.72 | 12.61 | 0.50 | 0.26 | 0.37 |
| 11.00 | 125.05 | 9.12 | 1.60 | 2.73 | 12.59 | 0.67 | 0.18 | 0.30 |
| 12.00 | 128.99 | 9.71 | 1.78 | 2.89 | 12.98 | 0.71 | 0.26 | 0.44 |

Table 22 - Mean Sydney region mid-shelf wave parameters for each Ensemble CSIRO/MIROC ST

The mean interdecadal wave statistics were calculated for the two Interdecadal Pacific Oscillation (IPO) phases: 1948-1976; 1977-2007, for the instrumental-derived NNR ST's, and the ST's determined from the CSIRO MK3.5 GCM, MIROC GCM, and an Ensemble of the CSIRO/MIROC GCM output. A comparison of the interdecadal mean values for Sydney mean wave direction (MWD), peak wave period (TP1), significant wave height (HSig) and maximum wave height (HMAX) was made to assess the suitability of the GCM output to replicate the data for the calibration period. The standard deviation of the mean interdecadal values was: mean wave direction (± 11.7°); peak wave period (±0.6 sec); significant wave height (±0.3 m); and, maximum wave height (±0.4 m). The Ensemble CSIRO/MIROC derived wave parameters had the highest correlation to the NNR wave parameters for the calibration period. Hence, the Ensemble CSIRO/MIROC output was used to project the Sydney wave climate out to 2100 AD. However, it is important to note that the Ensemble CSIRO/MIROC output is best fitted to the El Nino-like phase of the IPO (Figure 57), and therefore lacks sensitivity to the IPO related shifts in atmospheric circulation. Accordingly, the projected wave parameters to 2100 AD should be interpreted as indicative of the potential wave climate trend only, with limited application to projecting the magnitude of the changes. It is suggested that the projected seasonal wave parameters be interpreted in the context of the statistical fit between the NNR and Ensemble CSIRO/MIROC derived values for the IPO phases.

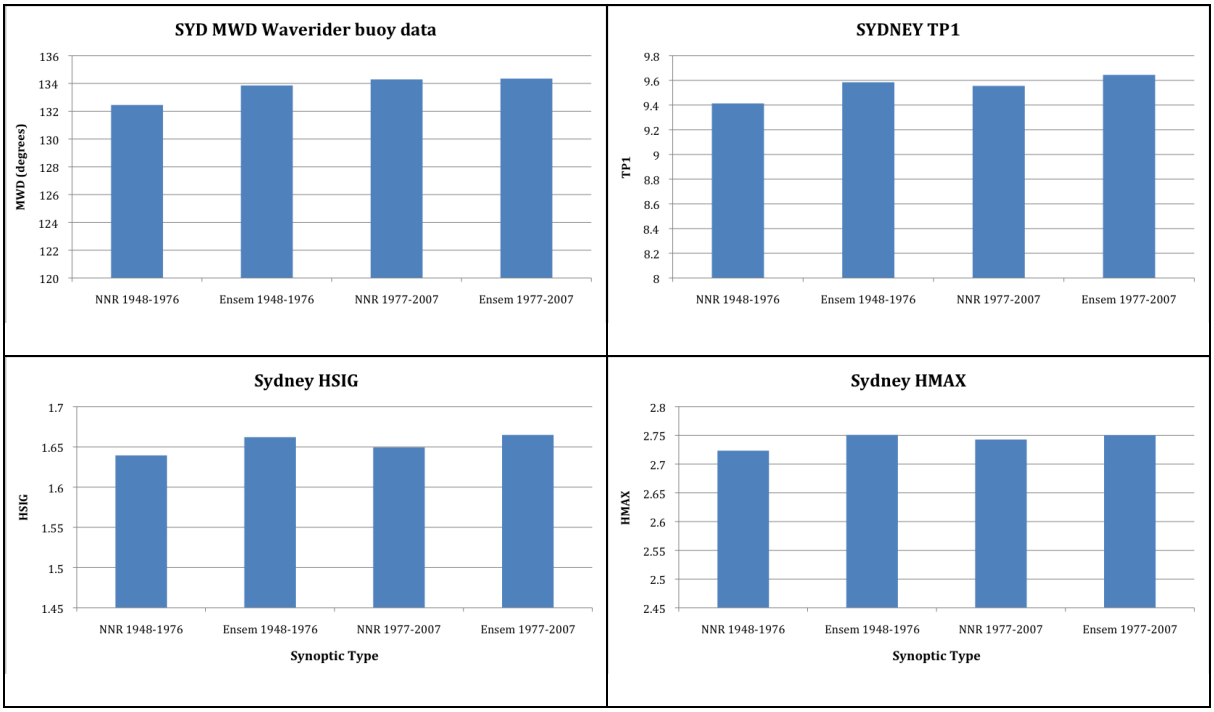


Figure 57 - The ensemble output for the 1948-2007 time period best matches the El Nini-like phase of the IPO

The seasonal wave characteristics were then calculated for the decadal periods: 2020-2040, 2040-2060 and 2060 to 2080, based on the frequency occurrence of each ST. The seasonal wave statistics for each multi-decadal period are shown in Figure 58. Whilst the CSIRO MK 3.5 model output on pressure and windfields is limited in sensitivity and simulation of longwave circulation, the trends in wave statistics can be used as a guide to the likely changes in seasonal wave climate. The magnitude of the changes is indicative only. For planning purposes the projected decadal wave climate can be interpreted with respect to the observed variability in the decadal wave climate associated with the Interdecadal Pacific Oscillation (IPO) phases: 1948-1976; 1977-2007.

An overall summary relative to the 1948-2007 period is that: ***Summer*** wave climate is projected to experience a slight increase in significant wave height to 2030-2040, followed by a decrease, coupled with no trend in mean wave direction; ***Autumn*** wave climate is projected to experience a slight decrease in wave height, coupled with no trend in mean wave direction; ***Winter*** wave climate is projected to experience a decrease in significant wave height, coupled with no trend in mean wave direction; ***Spring*** wave climate is projected to experience no clear trend. Note that the last two histogram columns in each seasonal block in Figure 58 are the historical interdecadal values for the past two IPO periods. The variability in the projected values to 2080 is significantly less than for the historical IPO periods.

The methods used in this study to project wave climate variables to 2080 have produced no statistically significant trends. We conclude that this is most likely a product of the resolution in the GCM sea-level pressure fields, particularly in the lack of simulation of the atmospheric long wave circulation in the Southern Hemisphere. The results confirm those of McInnes et al (2007) and imply that the historical variability over the past 60 years, most likely reflects the range of possible wave climates over the next century.

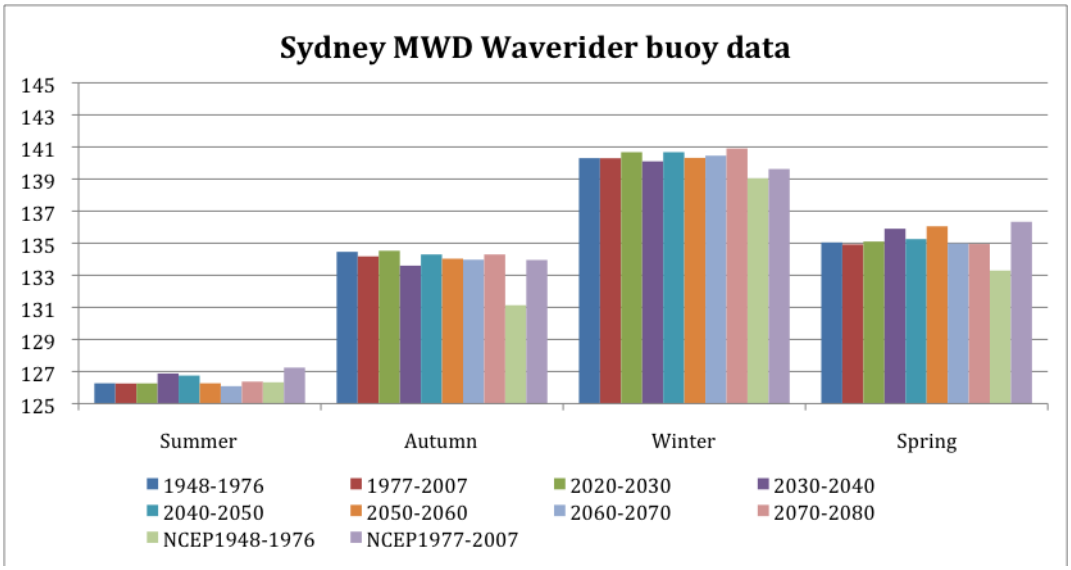


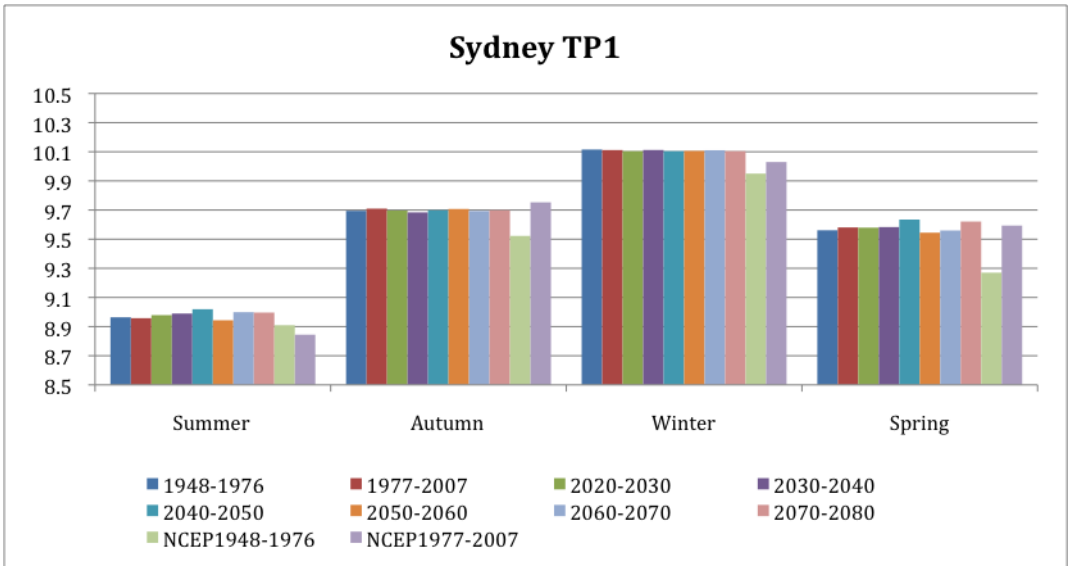

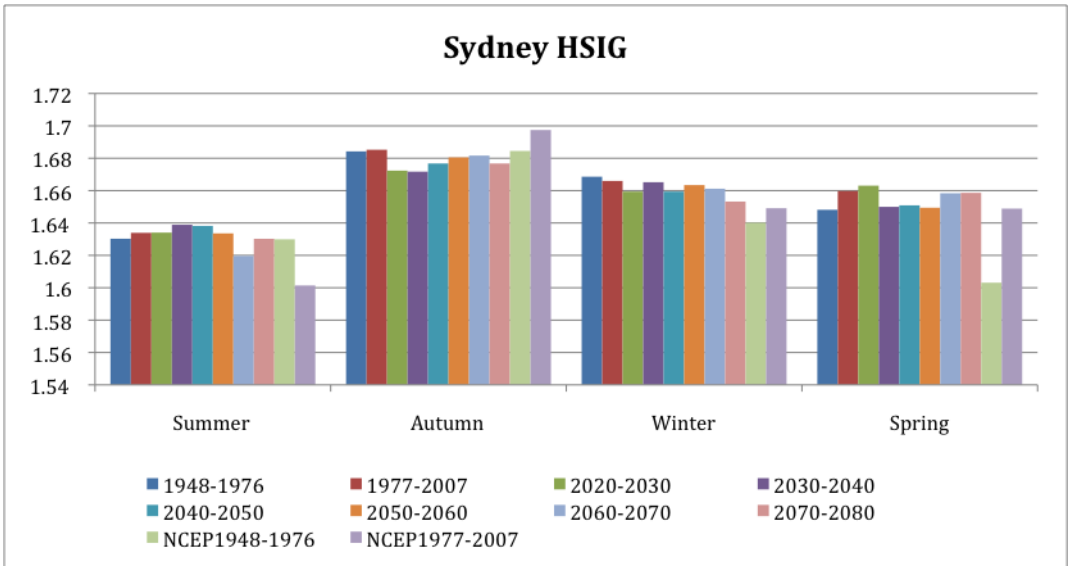


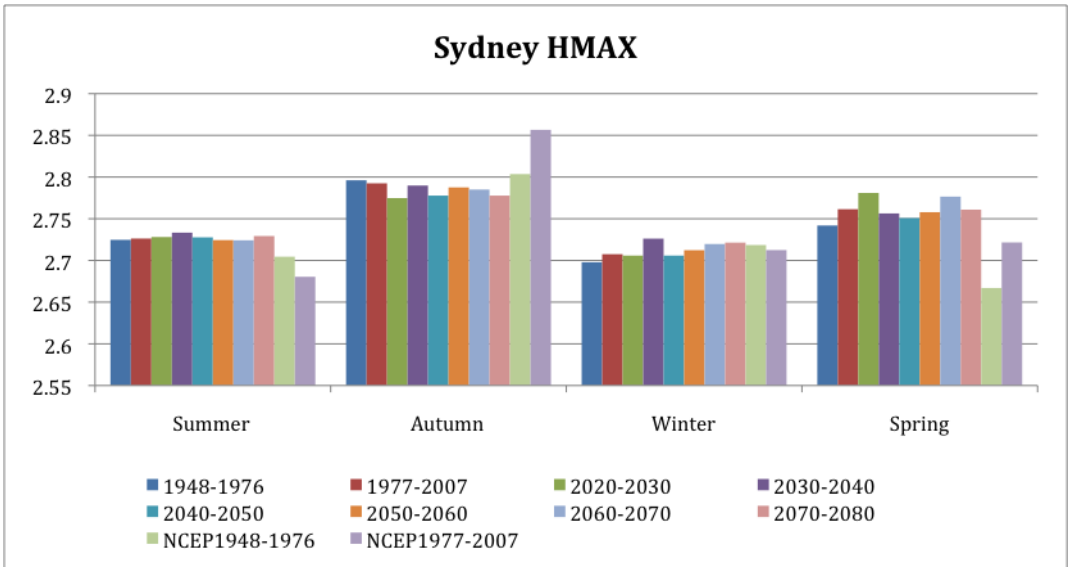


Figure 58 - Sydney monthly mean wave direction (MWD) and monthly peak period (Tp) comparisons for the 1948-1976, 1977-2007, 2020-2040, 2040-2060 and 2060-2080 time periods

## 4.11 Extreme Event Projections

In this section extreme events are considered in terms of:

- daily precipitation readings occurring in the 95$^{th}$ percentile;
- daily maximum temperatures above 37 (number of extreme heat days); and
- daily minimum temperature below 0 (number of frost days).

In the case of precipitation, the percentiles are calculated from daily records with precipitation recorded (i.e. above 0mm). The data used for this analysis is provided by the BOM. Data from January 1948 to December 2007 are analysed for precipitation whereas data from January 1970 to December 2007 are analysed for temperature. This difference occurs as a result of the length of available records.

Variables with high spatial variability such as precipitation may result in only localised extreme events. Thus analysis on a regional level distorts results in that extreme localised events may be missed. For this reason, five (5) representative stations within the study boundary are selected for the analysis of extreme precipitation and temperature events (Figure 59). Three of the five selected stations record both precipitation and minimum/maximum temperature (i.e. Murrurundi, Jerry's Plains and Newcastle). These stations provide an indication of extreme event behaviour in two of the region's three climate zones. Unfortunately stations within the central zone do not have a sufficient length of record to allow analysis of extremes events for a sufficient length of time to discern trends.

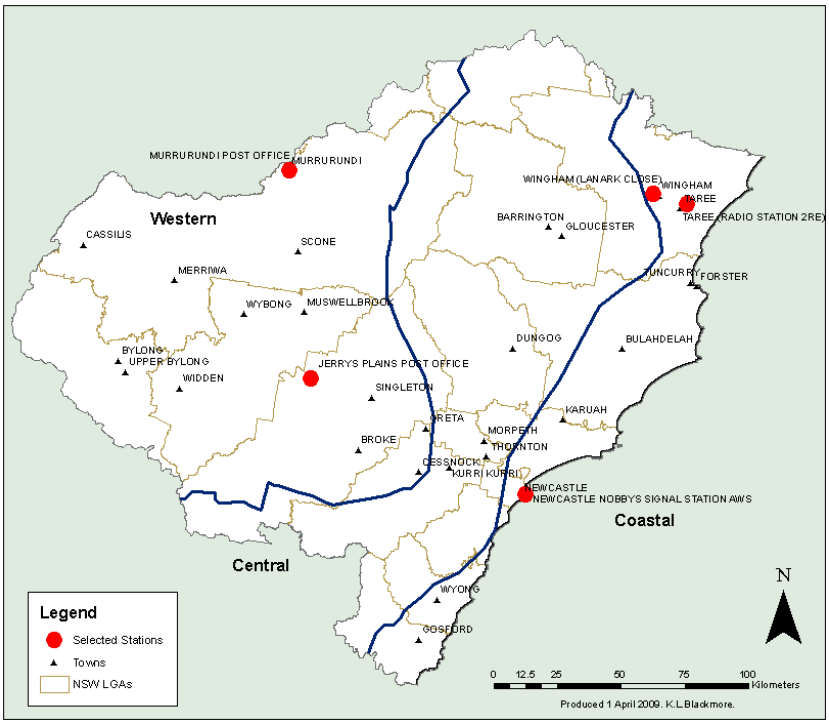


Figure 59 - Selected stations for analysis of extreme events

A single station recording both variables was not available in the north of the region, thus Wingham and Taree stations are selected for precipitation and minimum/maximum temperature respectively. This station(s) ensures longitudinal effects are captured. All of the selected stations provide reasonable spatial coverage of the region and have been recording data for the maximum available time period.

### 4.11.1 Precipitation (High Rainfall Events)

High rainfall events can occur under any of the 12 STs however a greater likelihood of precipitation events in the 95$^{th}$ percentile (95$^{th}$%ile) occurs under some STs. The frequency of precipitation events in the 95$^{th}$%ile by ST for four selected stations is shown in Figure 60. The frequency is shown as the percentage of 95$^{th}$%ile rain events associated with each ST. For example, when ST 12 occurs in the region, this ST produces a rainfall event in the 95%ile in Murrurundi 2.65% of the time. Additionally, red, orange, blue and green upward and downward arrows are used to indicate the dominant shift in the ST for the projected season for summer, autumn, winter and spring respectively. For example, displayed with the ST7 frequency of precipitation is an orange upward arrow indicating that an increase in frequency of this ST during autumn is the dominant shift for the projected period.

During summer and autumn, ST 12 is most likely to produce a high rainfall event in the western zone (Jerrys Plains and Murrurundi). On the coast (Newcastle) and to the north (Wingham) of the region, ST11 is associated with the highest frequency of high rainfall events. The frequency of occurrence of both of these STs are projected to increase during the period from 2020-2080. This would suggest an increase in the frequency of occurrence of high rainfall events in summer and autumn during the projected period.

ST 8 is associated with a relatively high frequency of extreme rainfall events in all zones during winter and spring. Projected decreases in the frequency of occurrence of this type during winter, and increases during spring, suggest a corresponding shift to occur in high rainfall events. An association between high rainfall events and ST2 is also noted in Newcastle. Projected changes in the frequency of occurrence of this ST are likely to impact on this location, however, extrapolation of these impacts to the entire coastal zone is not possible without analysis of additional locations.

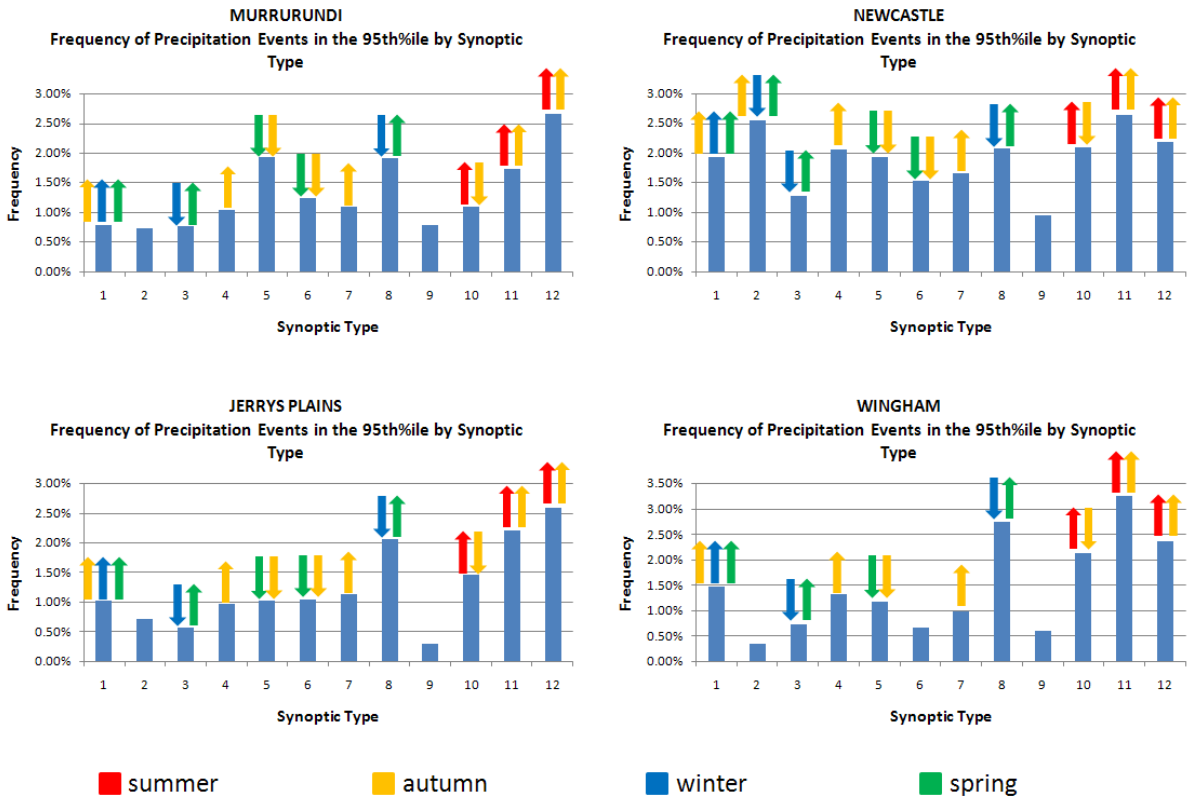


Figure 60 - Frequency of precipitation events in the 95%ile by ST for selected stations with arrows indicating seasonal shifts

### 4.11.2 Maximum Temperature (Extreme Heat Days)

A clear relationship between ST12 and extreme heat days (EHDs) exists for all stations (Figure 61). This relationship is strongest in the far west of the region (Murrurundi) where ~72% of all EHDs (daily temperature greater than or equal to 37°C) occur when ST12 is the dominant monthly type. Projected increases in this ST during summer and autumn are likely to result in increased frequency of EHDs in the region during the period from 2020-2080.

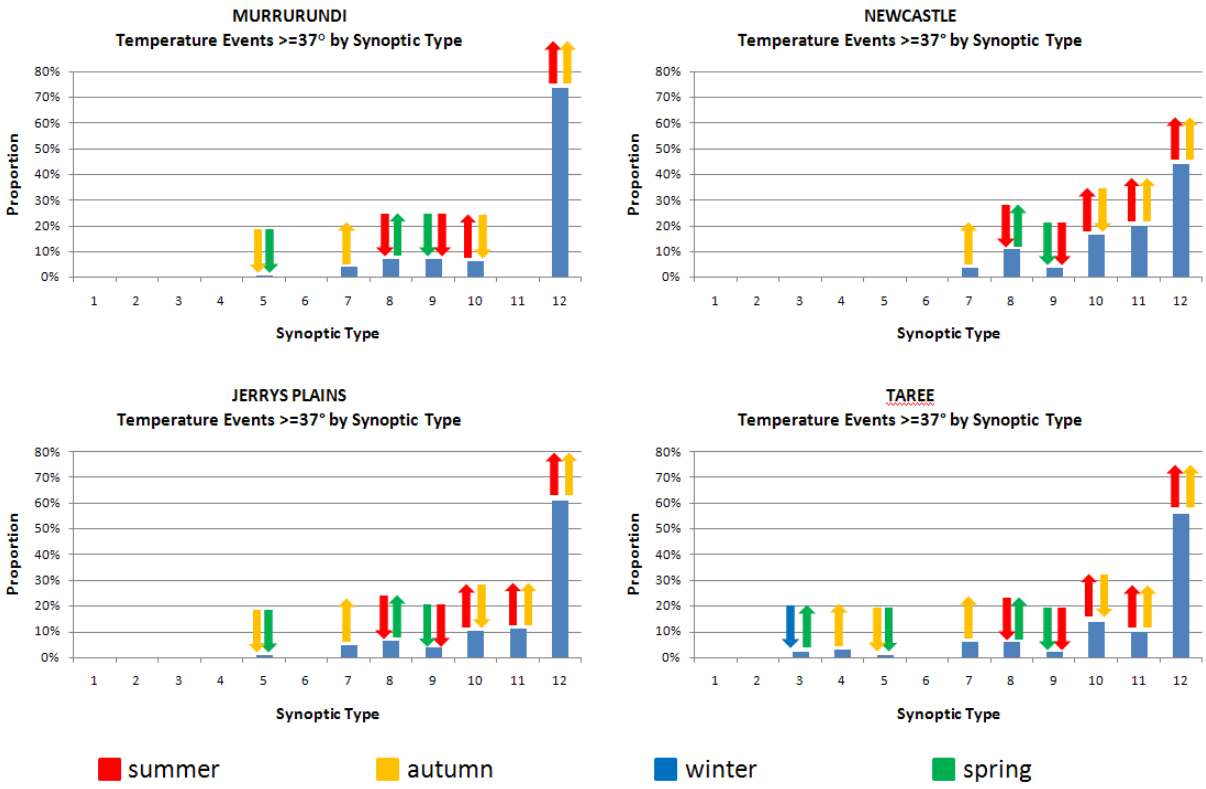


Figure 61 - Frequency of temperature events >=37°C by ST for selected stations with arrows indicating seasonal shifts

### 4.11.3 Minimum Temperature (Frosts)

Frost events (temperatures below or equal to 0°C) occur at each station in the western zone (Murrurundi and Jerrys Plains) and inland areas in the coastal zone (Taree) (Figure 62). It is reasonable to assume that these events also frequently occur within the central zone. No minimum temperature events less than or equal to 0°C were recorded during the period from January 1970 to December 2007 in Newcastle (Nobby's Head).

An association between minimum temperature events of less than or equal to 0°C and STs 1 and 3 are evident. Winter projections suggest increases in ST1 will be offset by decreases in STs 2 and 3, thus minimal change is expected during this season. However projected increases in the frequency of occurrence of STs 1, 2 and 3 during spring are likely to see an increase in the frequency of minimum temperature events (<=0°C) during this season. Increases in the frequency of occurrence of STs 1, 2 and 4 are also likely to produce an increase in minimum temperature events (<=0°C) in the projected period (2020-2080) during autumn.

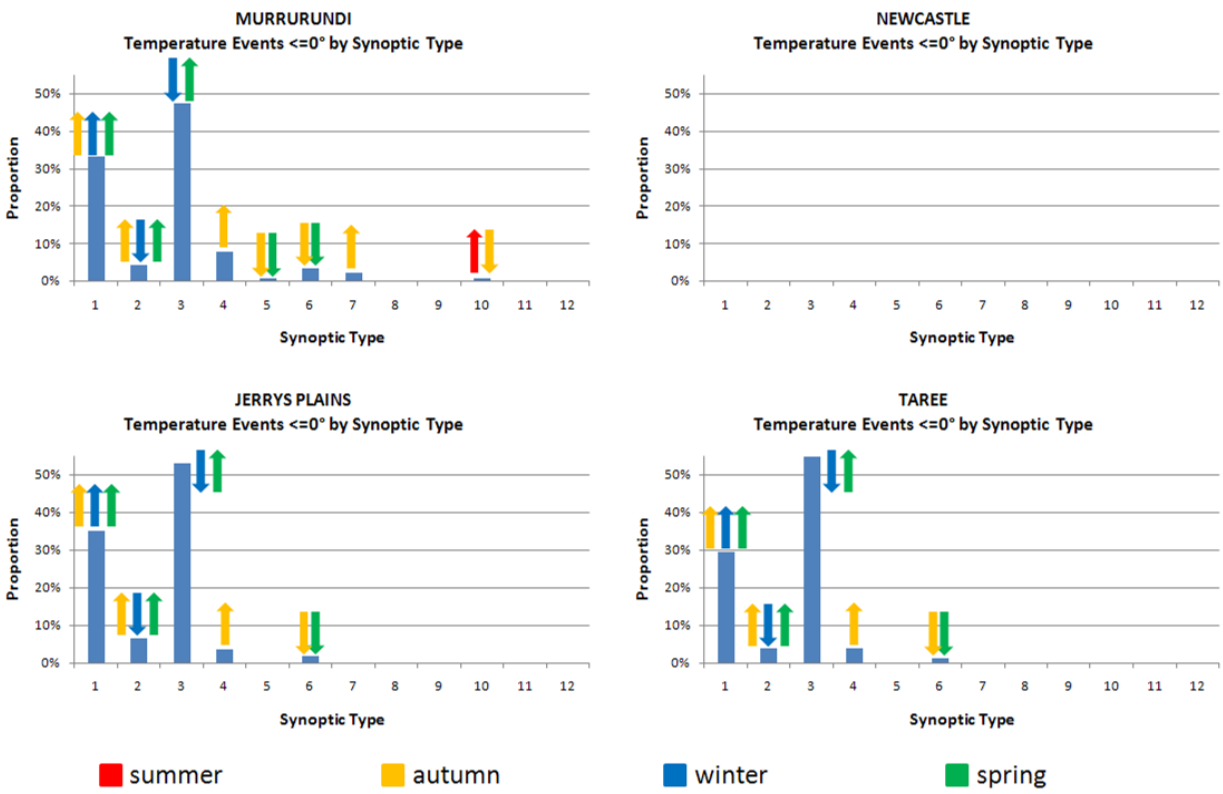


Figure 62 - Frequency of minimum temperature events <=0°C by ST for selected stations with arrows indicating seasonal shifts

### 4.11.4 Wind Gusts

Wind gusts recorded at only the Williamtown BOM recording station are analysed due to limited data availability in the region. In winter, gusts in the 95$^{th}$ percentile are most highly correlated with the dominant monthly STs of 1 and 3. Projected increases in the frequency of occurrence of ST1 in the period from 2020-2080 are offset by decreases in ST3 and thus no significant change is anticipated during this season. Increases in the frequency of these STs during spring are expected to produce more high wind gust events during this season. Overall increases in the frequency of STs associated with high wind gusts in autumn (i.e. STs 1, 4, 7 and 12) are expected to result in increases in autumn. An increase is also expected during summer due to increased frequency of occurrence of STs 10 and 12.

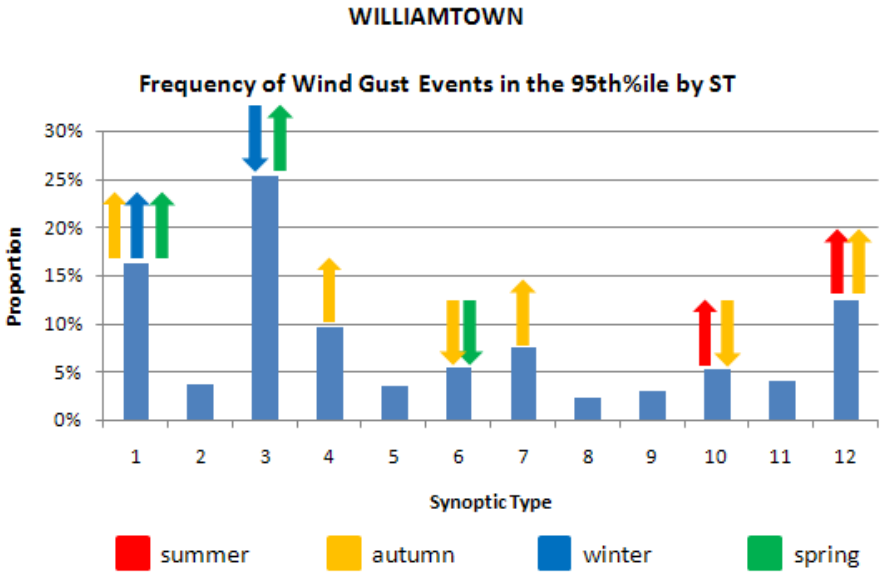


Figure 63 - Frequency of wind gust events in the 95th%ile by ST with arrows indicating seasonal shifts

# 5 Summary

HOW SHOULD STAKEHOLDERS AND READERS USE THE CLIMATE IMPACT PROJECTIONS FROM THIS STUDY?

Regional climate impacts have been resolved throughout this study using a statistical downscaling approach, based on CSIRO principally the projected monthly representation of the sea-level pressure field output from the CSIRO Mk3.5 GCM. The skill in projecting regional climate change impacts for the study area depends upon the model representation of the historical and future atmospheric circulation, together with the sensitivity of the Self Organised Mapping (SOM) approach to resolving change or shifts in the frequency of synoptic types.

We have approached the problem of sensitivity and predictive skill testing by training the methods on a calibration period from 1968 to 1990. This period spans a natural shift in the mean state of the climate, between a La Nina-like and an El Nino-like state, referred to as the Interdecadal Pacific Oscillation (IPO). The GCM's do not fully capture the range and shift in frequency of the key ST's determined from the analysis of the observed or instrumental sea-level pressure data (NCEP-NCAR Reanalysis data). Hence the GCM's do not fully capture the inherent interdecadal variability in the natural climate system that produces the climate shift and extremes that society, agriculture and the natural environment respond to.

Generally, the climate change projections for the 2020-2040, 2040-2060 and 2060-2080 are comparable, and do not display the interdecadal variability observed in the historical record. Hence, the projected climate variables should be interpreted as indicative of the shifts in climate relative to the specific historic period (i.e. +ve or –ve IPO phase). For example, if the shift is towards the interdecadal mean values experienced in the 1948-1976 period of persistent La Nina-like climate, then environmental management, planning and policy decisions should draw on the historical impacts during this period, when drafting responses to future climate change during this century. We interpret all statistically significant trends in this study as being of moderate to high confidence, and accordingly, all non statistically significant trends as being indicative of low confidence projections.

The climate change projections reported in this study provide the next order of detail and insight over the previous CSIRO (2007) projections for the region, and it is now possible to assess the sensitivity and associated climate change risks for the sub-regional zones: coastal; central; and, western. It is important to note that the science of climate change impact projection will advance with the next generation of GCM's.

OVERVIEW OF KEY CLIMATE CHANGE IMPACTS FOR THE HUNTER, CENTRAL AND LOWER NORTH COAST REGION

*Precipitation, Evaporation and Water Balance*

- Some seasonal and zonal changes in precipitation are projected. Although no overall increase in precipitation outside historical boundaries of natural variability is projected for the period from 2020-2080, a return to precipitation patterns similar to those experienced during the 1948-1977 IPO period (La Nina like –ve phase) is projected. Some seasonal shifts are also projected with moderate to high confidence, with decreases of approximately 12.5% for the coastal and central zones during winter and increases of approximately 13% in these zones during spring. A significant 33% increase in autumn rainfall in the western zone is also projected.

- A statistically significant decrease in water balance in the western zone is projected for the period from 2020-2080. Seasonal shifts in water balance in the coastal and central zones balance out to produce no change in annual projections. Projections (2020-2080) for summer are for increases in average daily water balance of ~1.3mm in the central zone and ~0.5mm in the western zone relative to the 1970-2007 period. Water balance in the coastal zone remains relatively unchanged. A significant decrease of ~1.9mm in average daily water balance for autumn is projected in the central zone. Decreases of ~0.9mm and ~0.3mm per day are expected in autumn in the coastal and western zones respectively. Increases in the coastal and western zones are projected for winter; ~0.7mm per day in the coastal zone and ~0.2mm per day in the western zone. A decrease of ~0.5mm per day is projected in the central zone during winter. Spring projections are for increased average daily water balance in all zones; ~1.8mm per day in the coastal zone, ~1.3mm per day in the central zone and ~1.4mm per day in the western zone.

*Air Temperature*

- Minimum temperatures will generally be warmer, particularly in the west of the region. Projections (2020-2080) in the coastal and central zones for summer are for decreases in average minimum temperature of ~0.8$^{o}$C relative to the 1970-2007 period. A significant increase of ~4.2$^{o}$C in average minimum temperature for summer is projected in the western zone. Increases in all three zones are projected for autumn; ~1.4$^{o}$C in the coastal and central zones and again a significant ~4.8$^{o}$C in the western zone. Winter projections are for warmer average minimum temperatures in the coastal and central zones (~1.3$^{o}$C and ~1.2$^{o}$C respectively) and lower temperatures in the western zone (~0.8$^{o}$C). The study region is likely to

experience lower average spring minimum temperatures with a decrease of ~0.2$^{o}$C projected for the coastal and central zones, and ~1.2$^{o}$C in the western zone.

- The most significant changes in average maximum temperatures are projected to occur during autumn and winter in the region. Projections (2020-2080) in the coastal and western zones for summer are for decreases in average maximum temperature of ~0.2$^{o}$C relative to the 1970-2007 period. No change for summer is projected in the central zone. Increases in all three zones are projected for autumn; ~1.2$^{o}$C in the coastal zone, ~1.8$^{o}$C in the central zone and ~2.0$^{o}$C in the western zone. Winter projections are for warmer average maximum temperatures, ~1.3$^{o}$C in the coastal zone, ~1.6$^{o}$C in the central zone and ~1.8$^{o}$C in the western zone. The study region is likely to experience lower spring average maximum temperatures with a decrease of ~0.7$^{o}$C projected for the coastal zone, and ~1.3$^{o}$C in the central and western zones.

*Extreme Events*

- The frequency of weather patterns responsible for extreme storm events along the NSW coast suggest an increase in the mean circulation pattern (ST1) during autumn/winter, and accordingly there is a higher probability of east coast low (ECL) formation.

- Projected changes in the frequency of occurrence of STs associated with high rainfall events are likely to impact the region. An increase in the frequency of occurrence of high rainfall events in summer and autumn are projected in all zones. A corresponding decrease in extreme rainfall events during winter and spring is also projected.

- Projected increases in ST12 during summer and autumn are likely to result in increased frequency of extreme heat days (EHDs) in the region during the period from 2020-2080.

- No change in winter frost events is projected, however increases in autumn and spring are projected for the western and central parts of the region.

# 6 Acknowledgements

The following acknowledgements are made in respect to assistance and/or data provided to compile this report:

- *NOAA_ERSST_V3 data provided by the NOAA/OAR/ESRL PSD, Boulder, Colorado, USA, from their web site at* http://www.cdc.noaa.gov/.
- *NCEP Reanalysis data provided by the NOAA/OAR/ESRL PSD, Boulder, Colorado, USA, from their web site at* http://www.cdc.noaa.gov/ .
- Bureau of Meteorology (BOM).

# 7 References

Church, J.A., N.J. White, R. Coleman, K. Lambeck and J.X. Mitrovica (2004), Estimates of the Regional Distribution of Sea Level Rise over the 1950 to 2000 Period. *Journal of Climate*, **17**, pp.2609-2625.

Church, J. A., and White, N.J. (2006). A 20th century acceleration in global sea-level rise. *Geophysical Research Letters*, 33, L01602, doi:10.1029/2005GL024826.

CSIRO (2007). *Climate change in Australia*. Technical Report 2007. Australian Government, 148 pp.

Goodwin, I. D. (2003). Unravelling climate influences on late Holocene sea-level and coastal evolution. In Mackay, A., Battarbee, R., Birks, J. and Oldfield, F. Global Change in the Holocene. Edward Arnold, London., pp.406-421.

Goodwin and Blackmore, in prep 2009.

Goodwin and Browning, in prep 2009.

HCCREMS, UofN (2007). Progress Report 1 to HCCREMS on Stage 1 of the Regional Climate Change Study. Hunter Councils, NSW.

HCCREMS, UofN (2008). Report 2: Climate Variability of the Hunter, Lower North Coast and Central Coast Region of NSW. Hunter Councils, NSW.

Hennessy, K., Lucas, C., Nicholls, N., Bathols, J., Suppiah, R., and Ricketts, J. (2005). *Climate change impacts on fire-weather in south-east Australia*. CSIRO Marine and Atmospheric Research, Aspendale, Victoria, 34 pp.

Hundecha, Y. and Bárdossy, A. (2008). Statistical downscaling of extremes of daily precipitation and temperature and construction of their future scenarios. *International Journal of Climatology*. **28**(5). pp.589-610.

IPCC Special Report on Emissions Scenarios. [online] http://www.grida.no/climate/ipcc/emission/. Accessed 29 September 2008.

IPCC (2007a). Summary for Policymakers. In: *Climate Change 2007: The Physical Science Basis: Contribution of Working Group I to the Fourth Assessment Report of the Intergovernmental Panel on Climate Change* Solomon, S., D. Qin, M. Manning, Z. Chen, M. Marquis, K.B. Averyt, M.Tignor and H.L. Miller, Eds., Cambridge University Press, Cambridge, United Kingdom and New York, NY, USA.

IPCC (2007b). *Climate Change 2007: Impacts, Adaptation and Vulnerability. Contribution of Working Group II to the Fourth Assessment Report of the Intergovernmental Panel on Climate Change,* M.L. Parry, O.F. Canziani, J.P. Palutikof, P.J. van der Linden and C.E. Hanson, Eds., Cambridge University Press, Cambridge, UK, p.976.

IPCC (2007c). *Scenario data for the atmospheric environment*. [online] http://www.ipcc-data.org/sres/ddc_sres_emissions.html. Accessed 29 September 2008.

Kalnay, E., Kanamitsu, M., Kistler, R., Collins, W., Deaven, D., Gandin, L., Iredell, M., Saha, S., White, G., Woolen, J., Zhu,Y., Chelliah, M., Ebisuzaki, W., Higgins, W., Janowiak, J., Mo, K. C., Ropelewski, C., Wang, J., Leetma, A., Reynolds, R., Jenne, R., & Joseph, D. (1996). The NCEP/NCAR 40-year reanalysis project. *Bulletin of American Meteorology Society*, *77*, pp.437-471.

Lord, D. and Kulmar, M. (2000). The 1974 storms revisited: 25 years experience in ocean wave measurement along the south-east Australian coast. In, *Proceedings of the 27th International Conference on Coastal Engineering*, ASCE, Sydney, pp.559-572.

Lucas, C., Hennessy, K., Mills, G. & Bathols, J. (2007). *Bushfire weather in southeast Australia: recent trends and projected climate change impacts*, Consultancy report prepared for The Climate Institute of Australia, Bushfire CRC and CSIRO, Melbourne.

Matlab Version 7.4.0.287 (R2007a). The Mathworks, Inc [Computer software].

McInnes, K.L. , Abbs, D., O'Farrell, S., Macadam, I., O'Grady, J., Ranasinghe, R. (2007). Projected changes in climatological forcing for coastal erosion in NSW. *CSIRO Marine and Atmospheric Research Report to the NSW Dept. Environment and Climate Change*, 38pp.

NSW Government (2008). *NSW Climate Change Action Plan*. [online] http://www.environment.nsw.gov.au/climatechange/actionplan.htm. Accessed 5 November 2008.

NSW Government (2009). Draft sea-level rise policy for NSW. NSW Department of Environment and Climate Change.

Perkins, SE and Pitman, AJ and Holbrook, NJ and McAneney, J (2007) *Evaluation of the AR4 Climate Models' Simulated Daily Maximum Temperature, Minimum Temperature, and Precipitation over Australia Using Probability Density Functions.* Journal of Climate, 20 (17). pp. 4356-4376.

Sturman, A. and Tapper, N. (2006).The weather and climate of Australia and New Zealand. Second Edition. Oxford University Press, Melbourne, 541pp.

Teng H, Buja LE, and Meehl GA, (2006). Twenty-first-century climate change commitment from a multi-model ensemble. *Geophysical Research Letters* 33(7).

Wilby, R.L. and T.M.L. Wigley. (1997). Downscaling general circulation model output: A review of methods and limitations. *Progress in Physical Geography* 21:530-548.

Wilby, R.L., T.M.L. Wigley, D. Conway, P.D. Jones, B.C. Hewitson, J. Main, and D.S. Wilks. (1998). Statistical downscaling of general circulation model output: A comparison of methods. *Water Resources Research* 34. pp.2995-3008.

Wilby, R.L., L.E. Hay, and G.H. Leavesley. (19990. A comparison of downscaled and raw GCM output: Implications for climate change scenarios in the San Juan river basin, Colorado. *Journal of Hydrology* 225. pp.67-91.

Wilby, R.L. and T.M.L. Wigley. (2000). Downscaling general circulation model output: A reappraisal of methods and limitations. In *Climate Prediction and Agriculture,* M.V.K. Sivakumar (ed.). Proceedings of the START/WMO International Workshop, 27-29 September 1999, Geneva. International START Secretariat, Washington, DC, pp.39-68.

Wilby, R.L., Charles, S.P., Zorita, E., Timbal, B., Whetton, P. and Mearns, L.O. (2004). *Guidelines for Use of Climate Scenarios Developed from Statistical Downscaling Methods*. 27 pp. [online] http://ipcc-ddc.cru.uea.ac.uk. Accessed 5 November 2008.

You Z.J., and Lord, D. (2008) Influence of the El Niño-Southern Oscillation on NSW Coastal Storm Severity. *Journal of Coastal Research,* Vol. 24, No. sp2. pp.203- 207.

## Appendix A – Synoptic Type Profiles

**Synoptic Type 1**

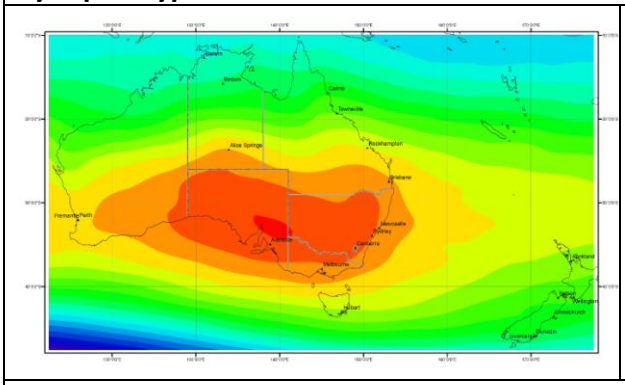

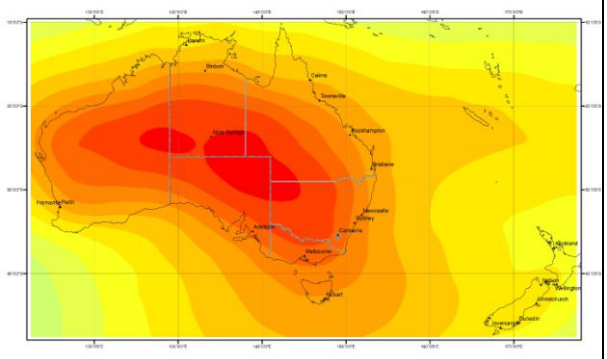

- High pressure over central and south eastern Australia, with a strong long wave ridge over south eastern Australian longitudes
- Most frequently occurring type (19.2% of time)
- Dominant winter and autumn type, also occurs to a lesser degree in spring
- Largest variation in annual average monthly precipitation, averaging 71mm, ranging from 1.4mm to 359mm
- Produces approximately 50% of temperature events where the minimum temperature is <=0°C in western parts of the region (i.e. Jerrys Plains and Murrurundi)
- Responsible for 23% of extreme precipitation events (i.e. in the 95$^{th}$ percentile) in Newcastle; 17% of events regionally

**Synoptic Type 2**

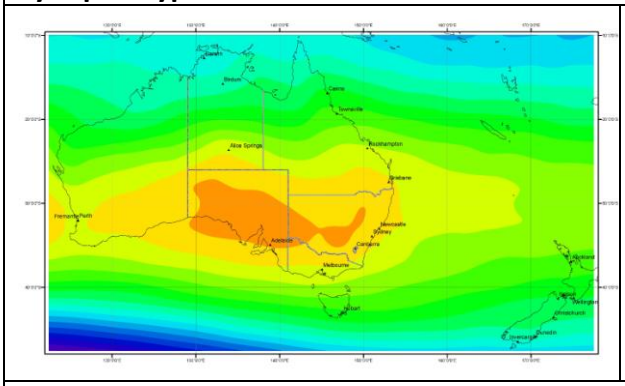

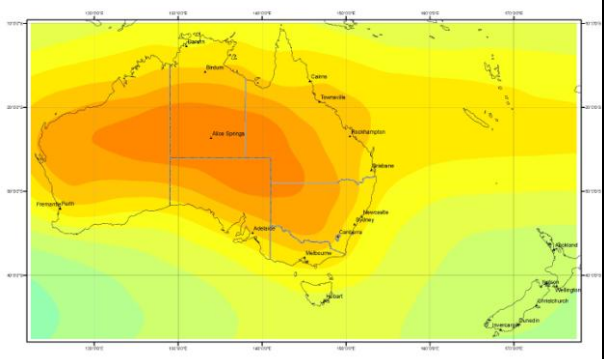

- High pressure over central and south eastern Australia, with a weak long wave ridge over south eastern Australian longitudes
- Occurs infrequently (3.3% of time)
- Predominantly occurs during winter, followed by spring and autumn
- Similar average monthly precipitation to ST1 (74mm) however less variable (i.e. ranging from 9mm to 226mm)

**Synoptic Type 3**

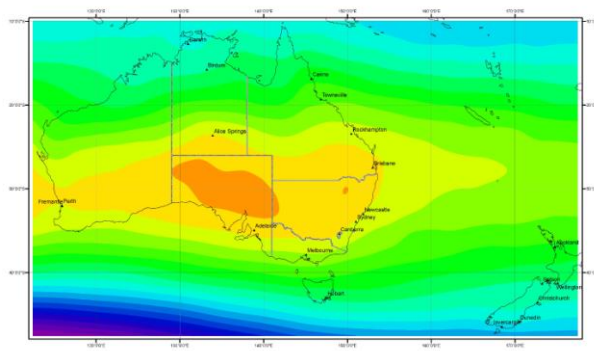
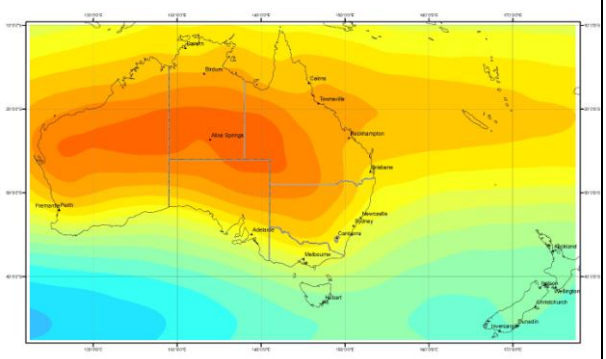

- High pressure over central and northern Australia
- Occurs 9.2% of time, predominantly in winter, followed by spring and autumn
- Comparatively low average monthly precipitation (45mm), ranging from 1.3mm to 132mm
- Produces almost 50% of temperature events where the minimum temperature is <=0°C in northern parts of the region (i.e. Taree)

**Synoptic Type 4**

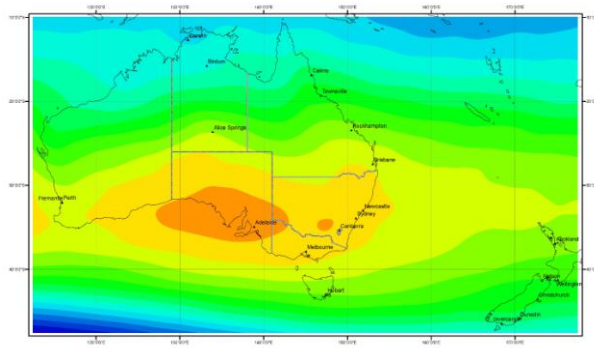
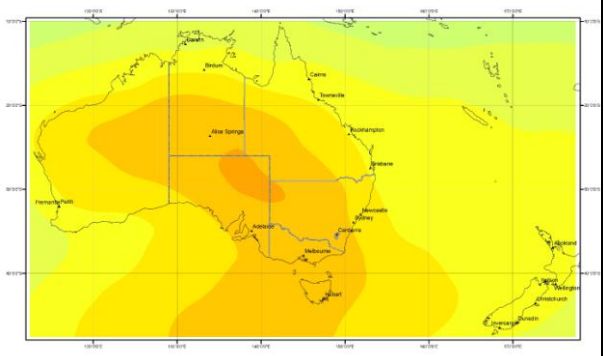

- High pressure through central and southern Australia with a strong long wave ridge over southern Australian longitudes
- Occurs 7.2% of time, predominantly in autumn, followed by spring and winter
- Relatively wet type with average monthly precipitation of 83mm, ranging from 10mm to 245mm

**Synoptic Type 5**

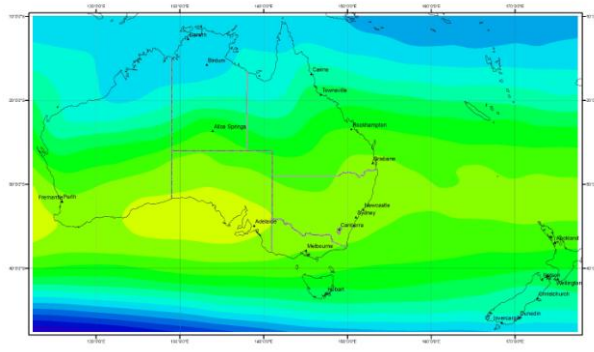
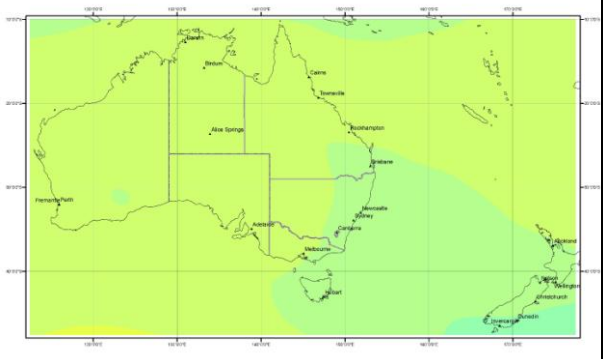

- Stable pressure over Australia
- Occurs infrequently (3.9% of time), predominantly in spring followed by autumn, and rarely in winter

- Associated with average monthly precipitation of 78mm, ranging from 10mm to 207mm

**Synoptic Type 6**

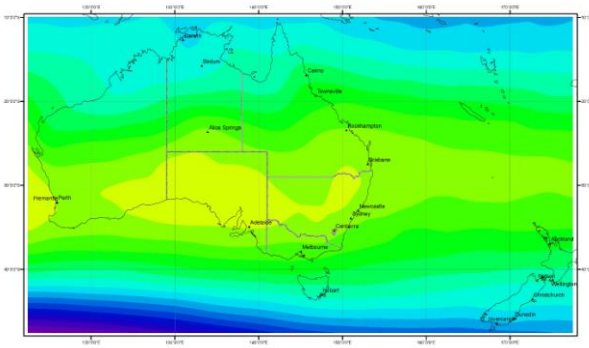
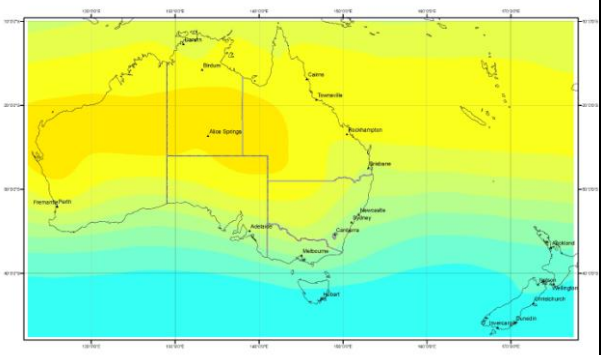

- High pressure over northern Australia with an equator-ward circumpolar trough
- Occurs 9.2% of time, predominantly in spring and winter, less frequently during autumn
- Relatively low average monthly precipitation (53mm), ranging from 2mm to 204mm

**Synoptic Type 7**

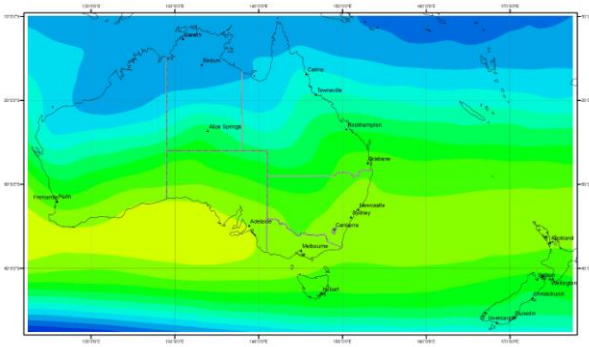
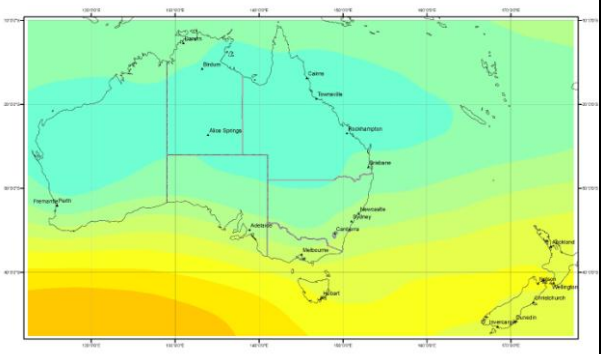

- High pressure band below southern Australia, low pressure over central and northern
- Occurs 7.9% of time, predominantly during spring, followed by autumn and rarely during summer
- ST associated with high average monthly precipitation (101mm), ranging from 11mm to 297mm

**Synoptic Type 8**

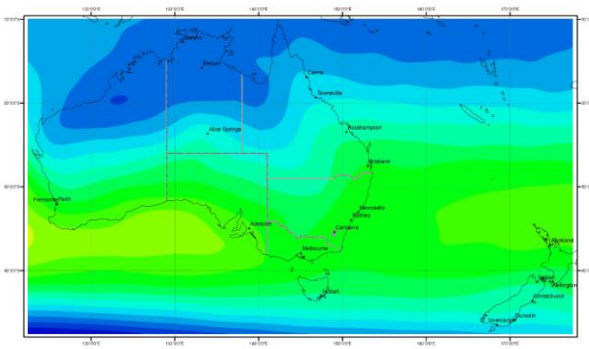
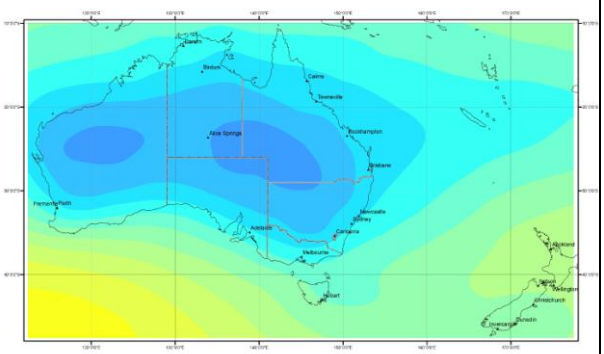

- Low pressure over central and eastern Australia, high pressure south-east of western Australia and a weak long-wave in south eastern Australian longitudes
- Most infrequently occurring type (2.8% of time), occurring predominantly during summer and spring, and rarely during autumn
- Associated with average monthly precipitation of 88mm, ranging from 16mm to 126mm

**Synoptic Type 9**

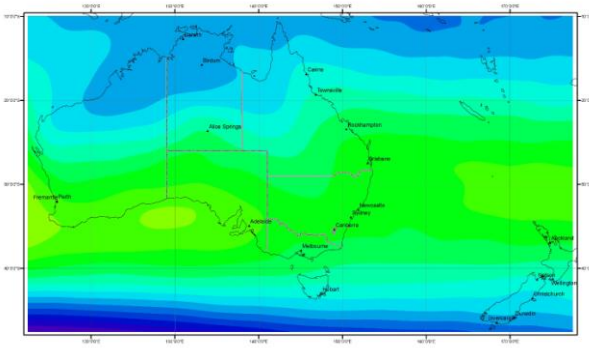

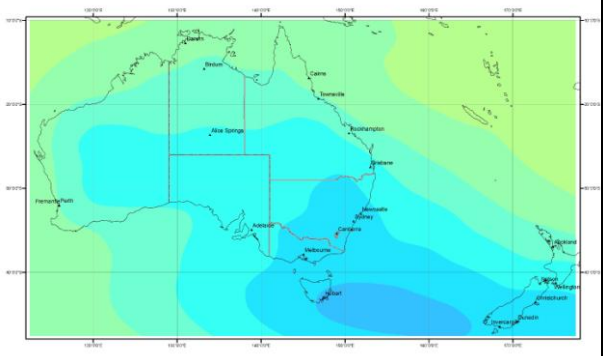

- Low pressure over central and south eastern Australia, southern Tasman Sea low and strong long-wave trough over Tasman Sea longitudes
- Occurs 5.8% of time, dominant spring type which can occur during autumn and very infrequently during summer and winter.
- Low average monthly precipitation (50mm) with the smallest range (i.e. 7mm to 114mm)

**Synoptic Type 10**

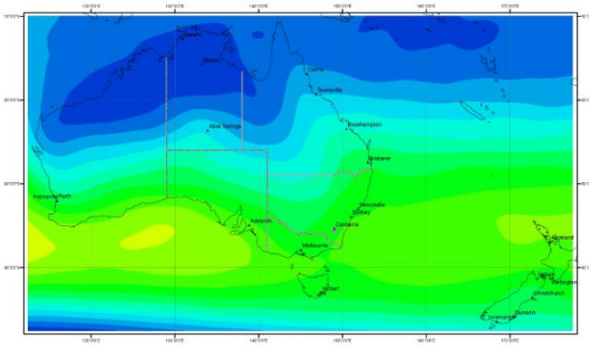

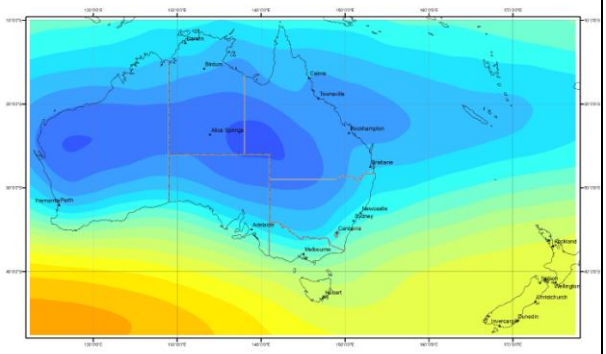

- Low pressure over central and eastern Australia, high pressure below southern Australia
- Occurs 11.2% of time, predominantly in summer, followed by autumn and less frequently in spring
- High average monthly precipitation (122mm) ranging from 14mm to 277mm
- Responsible for 17% of extreme precipitation events (i.e. in the 95$^{th}$ percentile) regionally and up to 23% in the northern parts of the region (i.e. Wingham)
- Produces 26% of extreme heat days (i.e. >=37°C) regionally and up to 31% in the most western parts of the region (i.e. Murrurundi)

**Synoptic Type 11**

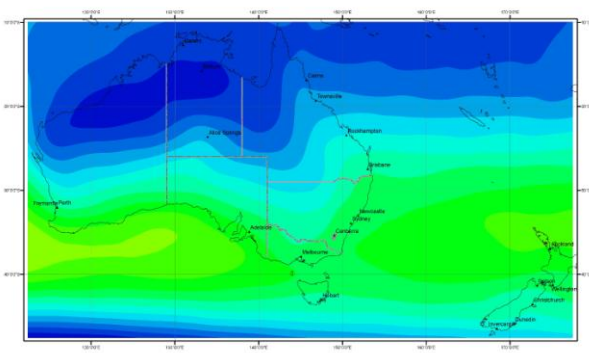

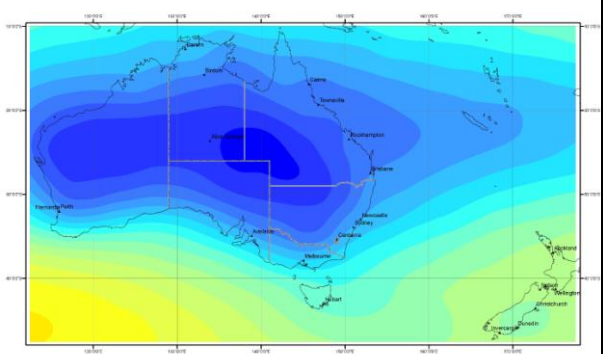

- Strong low pressure over Australia

- Occurs 10.4% of time, dominant summer type which occurs rarely during spring and autumn
- Highest average monthly precipitation of STs (122mm), ranging from 24mm to 343mm
- Responsible for the highest number (20%) of extreme precipitation events (i.e. in the 95$^{th}$ percentile) regionally and up to 24% in the western parts of the region (i.e. Jerrys Plains and Murrurundi)
- Produces 33% of extreme heat days (i.e. >=37°C) regionally and up to 35% in coastal areas (i.e. Newcastle)

**Synoptic Type 12**

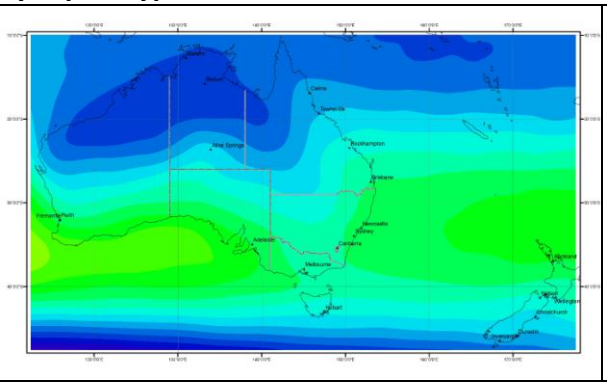

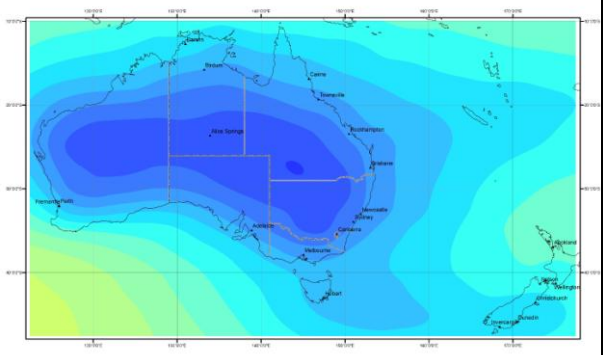

- Strong low pressure over Australia with a moderate long-wave trough in south-eastern Australia and Tasman Sea longitudes
- Occurs 9.9% of time, predominantly in summer, followed by spring and infrequently in autumn
- Produces average monthly precipitation of 70mm with a range of 6mm to 220mm
- Produces 23% of extreme heat days (i.e. >=37°C) regionally and up to 26% in northern areas (i.e. Taree)

## APPENDIX B – Seasonal Layout of Grids from the SOM Process

### NCEP/NCAR

| Summer Types Hits - ALL | | | |
|---|---|---|---|
| 0 | 0 | 5 | 46 |
| 0 | 0 | 9 | 71 |
| 0 | 0 | 1 | 48 |

| Autumn Types Hits - ALL | | | |
|---|---|---|---|
| 38 | 34 | 36 | 29 |
| 4 | 11 | 3 | 1 |
| 6 | 9 | 6 | 3 |

| Winter Types Hits - ALL | | | |
|---|---|---|---|
| 87 | 2 | 0 | 0 |
| 13 | 1 | 0 | 0 |
| 49 | 27 | 1 | 0 |

| Spring Types Hits - ALL | | | |
|---|---|---|---|
| 13 | 16 | 16 | 6 |
| 7 | 16 | 8 | 3 |
| 11 | 30 | 34 | 20 |

### CSIRO

| Summer Types Hits - ALL | | | |
|---|---|---|---|
| 0 | 0 | 0 | 4 |
| 0 | 0 | 8 | 28 |
| 0 | 0 | 8 | 132 |

| Autumn Types Hits - ALL | | | |
|---|---|---|---|
| 8 | 32 | 45 | 51 |
| 2 | 8 | 1 | 19 |
| 3 | 8 | 1 | 2 |

| Winter Types Hits - ALL | | | |
|---|---|---|---|
| 56 | 7 | 0 | 0 |
| 13 | 0 | 0 | 0 |
| 101 | 3 | 0 | 0 |

| Spring Types Hits - ALL | | | |
|---|---|---|---|
| 25 | 24 | 25 | 14 |
| 3 | 14 | 10 | 1 |
| 29 | 23 | 12 | 0 |

### ECHO

| Summer Types Hits - ALL | | | |
|---|---|---|---|
| 0 | 0 | 0 | 0 |
| 0 | 0 | 0 | 0 |
| 34 | 54 | 58 | 34 |

| Autumn Types Hits - ALL | | | |
|---|---|---|---|
| 86 | 19 | 7 | 3 |
| 10 | 3 | 2 | 1 |
| 31 | 11 | 4 | 3 |

| Winter Types Hits – ALL | | | |
|---|---|---|---|
| 15 | 28 | 42 | 52 |
| 0 | 1 | 2 | 40 |
| 0 | 0 | 0 | 0 |

| Spring Types Hits – ALL | | | |
|---|---|---|---|
| 15 | 25 | 19 | 23 |
| 10 | 10 | 8 | 27 |
| 14 | 9 | 12 | 8 |

### IPSL

| Summer Types Hits - ALL | | | |
|---|---|---|---|
| 11 | 25 | 41 | 103 |
| 0 | 0 | 0 | 0 |
| 0 | 0 | 0 | 0 |

| Autumn Types Hits - ALL | | | |
|---|---|---|---|
| 35 | 24 | 9 | 8 |
| 15 | 10 | 5 | 0 |
| 45 | 14 | 13 | 2 |

| Winter Types Hits - ALL | | | |
|---|---|---|---|
| 0 | 0 | 0 | 0 |
| 3 | 0 | 1 | 0 |
| 51 | 36 | 39 | 50 |

| Spring Types Hits - ALL | | | |
|---|---|---|---|
| 12 | 19 | 11 | 7 |
| 3 | 5 | 7 | 30 |
| 13 | 9 | 19 | 45 |

### MIROC

| Summer Types Hits - ALL | | | |
|---|---|---|---|
| 63 | 42 | 48 | 27 |
| 0 | 0 | 0 | 0 |
| 0 | 0 | 0 | 0 |

| Autumn Types Hits - ALL | | | |
|---|---|---|---|
| 55 | 11 | 2 | 0 |
| 17 | 2 | 1 | 0 |
| 61 | 19 | 10 | 2 |

| Winter Types Hits - ALL | | | |
|---|---|---|---|
| 0 | 0 | 0 | 0 |
| 0 | 0 | 2 | 27 |
| 41 | 34 | 43 | 33 |

| Spring Types Hits - ALL | | | |
|---|---|---|---|
| 4 | 9 | 11 | 31 |
| 9 | 6 | 7 | 37 |
| 11 | 17 | 18 | 20 |

### MRI

| Summer Types Hits – ALL | | | |
|---|---|---|---|
| 145 | 13 | 2 | 0 |
| 10 | 0 | 0 | 0 |
| 10 | 0 | 0 | 0 |

| Autumn Types Hits – ALL | | | |
|---|---|---|---|
| 4 | 2 | 0 | 2 |
| 5 | 8 | 2 | 6 |
| 45 | 51 | 44 | 11 |

| Winter Types Hits - ALL | | | |
|---|---|---|---|
| 0 | 0 | 0 | 68 |
| 0 | 0 | 4 | 40 |
| 0 | 0 | 21 | 47 |

| Spring Types Hits - ALL | | | |
|---|---|---|---|
| 3 | 17 | 22 | 33 |
| 14 | 23 | 7 | 6 |
| 10 | 19 | 18 | 8 |

**APPENDIX C – Comparison of NNR and MRI and NNR and CSIRO/MRI Ensemble Anomaly Types (1948-2007)**

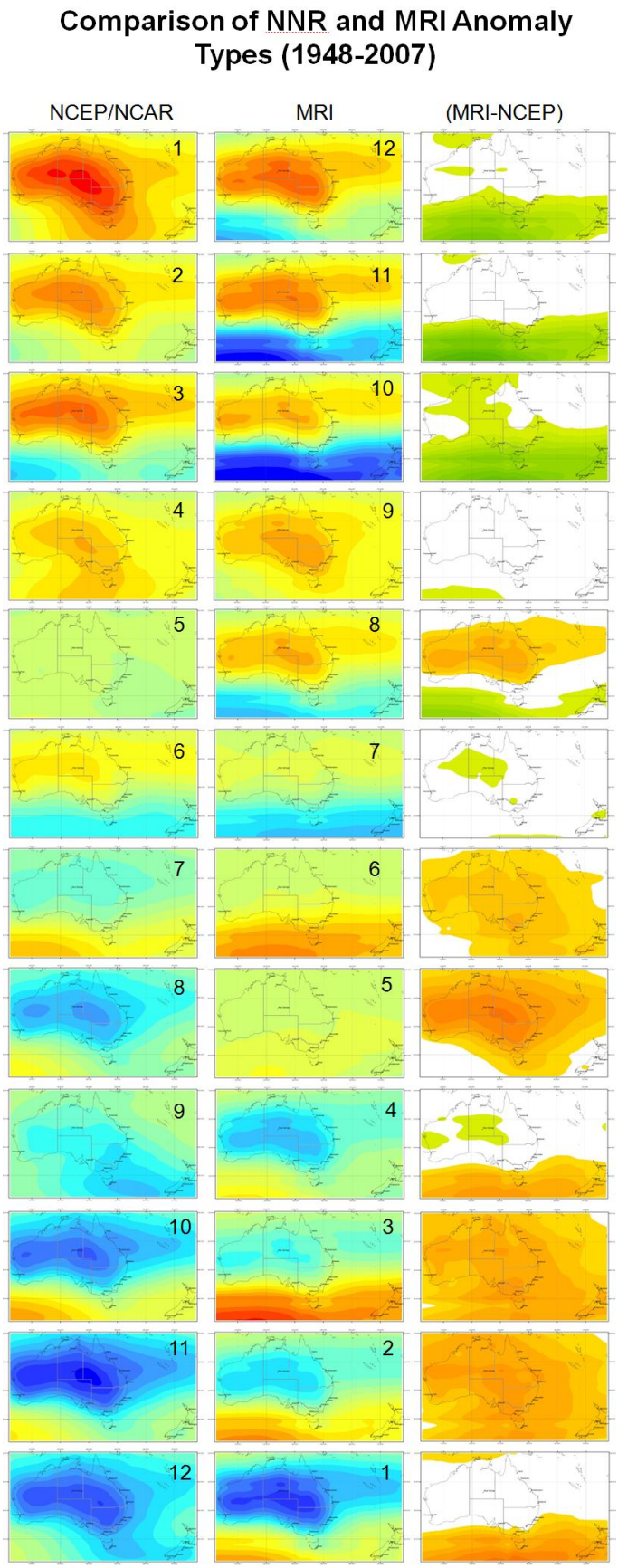

## Comparison of NNR and MRI Anomaly Types (1948-2007)

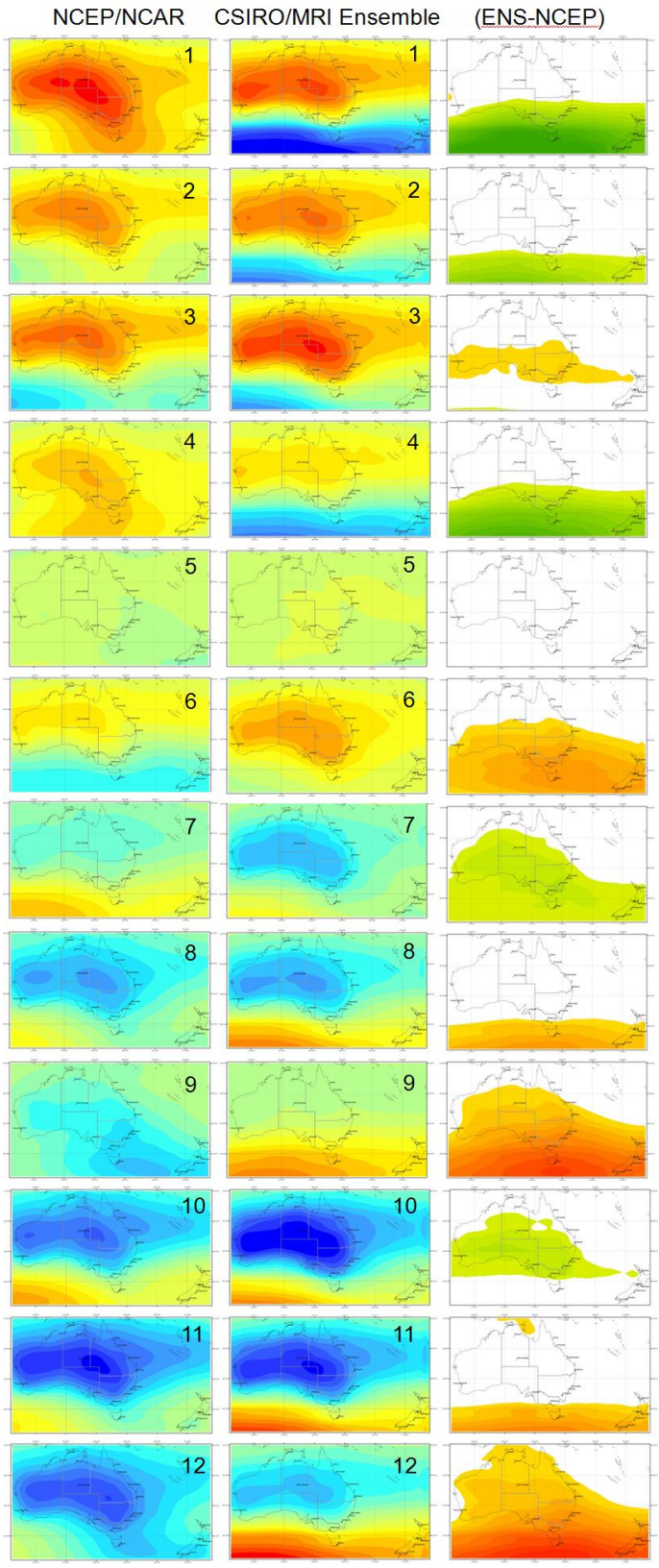

HCCREMS (the Hunter and Central Coast Regional Environmental Management Strategy) is a partnership initiative of the 14 local councils of the Hunter, Central and Mid North Coast regions of NSW.

Established in 1996, the HCCREMS team works with urban, rural and costal councils to facilitate a collaborative approach to sustainable planning, development and natural resource management. Our activities include:

- Facilitating local government input to a range of natural resource management and planning processes.
- Providing specialist support and services to member councils on environmental management and planning issues.
- Developing and maintaining a repository of the region's natural resource management data and maps.
- Designing and managing a range of regional environmental projects through the Hunter and Central Coast Regional Environmental Management Strategy (HCCREMS) framework.

At the time of publishing our project areas include:

- Biodiversity
- Aquatic and terrestrial weeds
- Roadside environmental management
- Climate change adaptation
- The urban water cycle
- Environmental compliance
- Sustainability
- Community education, including rural residential living
- Natural resource data management and mapping

For more information visit **www.huntercouncils.com.au/environment/hccrems**

With thanks to our partners:

and our member councils:

An initiative of the Hunter and Central Coast Regional Environmental Management Strategy.